Fakultät für Medizin

Institut für Neurowissenschaften

In Vivo Two-Photon Calcium Imaging of Hippocampal Neurons in a Mouse Model of Alzheimer´s Disease

Marc Aurel Busche

Vollständiger Abdruck der von der Fakultät für Medizin der Technischen Universität München zur Erlangung des akademischen Grades eines

Doctor of Philosophy (Ph.D.)

genehmigten Dissertation.

Vorsitzender: Univ.-Prof. Dr. Roland M. Schmid

Prüfer der Dissertation:

1. apl. Prof. Dr. Helmuth K. H. Adelsberger

2. Univ.-Prof. Dr. Thomas Misgeld

3. Univ.-Prof. Dr. Martin Kerschensteiner,

   Ludwig-Maximilians-Universität München

Betreuer: Univ.-Prof. Dr. Arthur Konnerth

Die Dissertation wurde am 17.04.2013 bei der Fakultät für Medizin der Technischen Universität München eingereicht und durch die Fakultät für Medizin am 21.08.2013 angenommen.

The hippocampus is a prime target of Alzheimer´s disease (AD), yet little is known about how the disease affects neuronal activity patterns in the hippocampus *in vivo*. This information has been difficult to obtain because of the inaccessibility of the hippocampus for cellular-level functional imaging. Here, we advanced two-photon microscopy towards calcium imaging of neurons in the CA1 region of the hippocampus *in vivo*. By using this method, we studied the functional alterations of hippocampal neurons in AD transgenic mice. We found that plaque-laden transgenic mice exhibited greater proportions of silent and hyperactive neurons in the hippocampus than wild type mice, consistent with previous findings from cortex. Surprisingly, already before the deposition of amyloid-ß (Aß) into plaques, there was a massive increase of hippocampal neuronal activity with many neurons being abnormally hyperactive. Our finding that neuronal hyperactivity occurred independent of plaque formation suggested that soluble species of Aß, and not plaques themselves, might underlie this dysfunction. To test this hypothesis, we treated plaque-free transgenic mice with the γ-secretase inhibitor LY-411575 and found that a single oral dose reduced soluble Aß levels and restored hippocampal neuronal function within few hours. Furthermore, we demonstrated that the direct application of soluble Aß induced hippocampal hyperactivity. Taken together, this thesis advances two-photon microscopy to enable optical studies of hippocampal neuronal activity *in vivo*. By using this method, we revealed that neuronal function was profoundly impaired in the hippocampus of AD transgenic mice already before plaque formation. Remarkably, the early hippocampal dysfunction was fully reversed by a single dose of a γ-secretase inhibitor indicating that it was causally related to the action of soluble Aß. This work has resulted in a publication in the *Proceedings of the National Academy of Sciences of the United States of America* in 2012. The title of this publication was *"Critical role of soluble amyloid-β for early hippocampal hyperactivity in a mouse model of Alzheimer's disease"*.

Contents

Acronyms

Aß	amyloid-ß
AAV	adeno-associated virus
ACSF	artificial cerebrospinal fluid
AD	Alzheimer´s disease
AM	acetoxymethyl
AP	action potential
APD	avalanche photo diode
APO	apolipoprotein
APP	amyloid precursor protein
APV	D,L-2-amino-5-phosphonovaleric acid
CAA	cerebral amyloid angiopathy
CA	cornu ammonis
CNQX	6-cyano-7-nitroquinoxaline-2,3-dione
CT	computed tomography
DAB	diaminobenzidine

DMSO	dimethyl sulfoxide
EEG	electroencephalogram
FDG	fluorodeoxyglucose
fMRI	functional magnetic resonance imaging
GFP	green fluorescent protein
LIA	large irregular amplitude
LTP	long-term potentiation
MRI	magnetic resonance imaging
NA	numerical aperture
NPY	neuropeptide Y
CA	cornu ammonis
OGB-1	Oregon Green BAPTA-1
PBS	phosphate-buffered sulfate
PET	positron emission tomography
PFA	paraformaldehyde
PiB	Pittsburgh compound B
PMT	photomultiplier tube
PS	presenilin
ROI	region of interest
SDS	sodium dodecyl sulfate

SIA	small irregular amplitude
SNR	signal-to-noise-ratio
SPECT	single-photon emission computed tomography
TBS	Tris-buffered saline
TGA	transient global amnesia
Tg	transgenic
TTX	tetrodotoxin
Wt	wild type

1 Introduction

As the aim of this thesis was to advance two-photon microscopy towards high resolution imaging of neuronal activity patterns in the hippocampus *in vivo*, and in parallel to apply this method to a transgenic mouse model of Alzheimer´s disease (AD), this chapter is subdivided into three introductory sections which provide the physical and biological fundamentals required to comprehend the results presented in chapter 3. Section 1.1 introduces the basic anatomy and functional organization of the hippocampus. Section 1.2 gives a short overview of basic principles underlying two-photon microscopy, followed by a brief review on state of the art fluorescence labeling techniques used to visualize biological structure and function *in vivo*. Finally, section 1.3 describes imaging techniques used in the study of AD. In particular, it focuses on own previously published research investigating the effects of the disease at the level of neurons and their networks *in vivo*.

1.1 The hippocampus

1.1.1 Anatomy

The hippocampus proper is subdivided in three parts: CA3, CA2 and CA1 (CA comes from cornu ammonis). The other regions of the hippocampal formation include the dentate gyrus, subiculum, presubiculum, parasubiculum, and enthorinal cortex. Dentate gyrus, hippocampus proper and subiculum have a single cell layer with less-cellular or acellular layers above and below it, whereas the other regions have several cellular layers [Shepherd 2004; Andersen 2007].

Basic circuits. Much of the neocortical input reaches the hippocampus through the enthorinal

cortex, which can be considered as the starting point of the intrinsic hippocampal circuit. The enthorinal cortex receives most of the sensory information via the adjacent perirhinal and postrhinal cortices (also termed parahippocampal cortex). Neurons in layer II of the enthorinal cortex project to the dentate gyrus and the CA3 region via the perforant path. The granule cells of the dentate gyrus project to the CA3 region via the mossy fiber projections. The pyramidal cells of CA3 are the source of major input to the CA1 region (via axons that form the Schaffer collaterals). In addition, CA3 pyramidal cells are highly interconnected. CA1 pyramidal cells project to the subiculum. Both CA1 and the subiculum project back to the deep layers of the enthorinal cortex. The basic hippocampal circuitry seems to be similar in humans, monkeys and rodents, however some species differences, such as the commissural connections of the dentate gyrus, are especially relevant for this thesis. In rodents, there is a massive commissural system that provides nearly one-sixth of the excitatory input to the dentate gyrus [Gottlieb and Cowan 1973], whereas those connections are absent in humans and monkeys [Amaral et al. 1984]. Furthermore, the CA1 pyramidal cell layer becomes thicker and more heterogeneous in humans and monkeys as compared to rats. In rats, the pyramidal cell layer is about 5 cells thick, whereas it can be more than 30 cells thick in humans.

Cellular elements. The principal cell layer in the hippocampus is the pyramidal cell layer, which is tightly packed in CA1 but loosely packed in CA2 and CA3. Deep to the pyramidal cell layer lies the stratum oriens, which mainly contains the basal dendrites of the pyramidal cells and several classes of interneurons. Within stratum oriens some of the CA3 to CA3 associational connections and the CA3 to CA1 Schaffer collaterals are located. Below the stratum oriens the fiber containing alveus is located. It contains axons from pyramidal neurons that project to the fimbria/fornix, one of the major outputs of the hippocampus. In CA3, but not in CA2 and CA1, there is a narrow acellular zone, the stratum lucidum, which is located above the pyramidal cell layer and which contains the mossy fibers. The stratum radiatum is located above the stratum lucidum in CA3 and immediately above the pyramidal cell layer in CA2 and CA1. It contains CA3 to CA3 associational connections as well as the CA3 to CA1 Schaffer collaterals.

Finally, the stratum lacunosum-moleculare is the most superficial layer containing fibers from the enthorinal cortex. The principal neurons in the dentate gyrus are the granule cells, whereas in the hippocampus they are the pyramidal cells. Pyramidal cells exhibit a basal dendritic tree that extends into the stratum oriens and an apical dendritic tree that extends to the hippocampal fissure. The length and organization of CA3 pyramidal cells are variable, whereas CA1 cells exhibit a remarkable homogeneity of their dendritic tree. Additionally, CA1 pyramidal cells are on average smaller than CA3 cells (CA1: around 15 μm in diameter, CA3: around 20 – 30 μm in diameter). The dendrites of pyramidal neurons are covered with spines onto which most excitatory synapses terminate. Although pyramidal neurons are the most abundant cell type in the hippocampus, there is a heterogeneous group of interneurons scattered through all cell layers [Freund and Buzsáki 1996]. Most interneurons in the hippocampus have locally restricted target regions, lack spines, and are GABAergic. Hippocampal interneurons are classified on the basis of their synaptic targets as axo-axonic cells, basket cells, and bistratified cells. Axo-axonic cells synapse onto the initial segments of pyramidal neurons and regulate action potential (AP) initiation. Basket cells synapse onto the soma of pyramidal neurons and bistratified cells contact the apical or basal dendrites of pyramidal neurons.

1.1.2 Functional organization

The hippocampal formation plays a key role in learning and memory. Damage to the hippocampal formation produces an enduring impairment in the ability to encode new information into long-term-memory. This anterograde amnestic syndrome was initially observed in the patient H.M., who underwent bilateral hippocampal removal for the treatment of intractable epilepsy [Scoville and Milner 1957; Corkin et al. 1997]. In recent years a number of reports about other patients with bilateral damage to the hippocampus have been published [Andersen 2007]. It is important to note that damage to the hippocampal formation also leads to severe memory impairments in rodents, measured for example by performance in the Morris water maze, contextual fear conditioning, delay non-match to sample test or spatial alternation T-maze. Studies

in animals have tried to explore the functional neuronal changes that underlie the observed learning and memory impairments. In particular, single-cell electrical recordings in rodents have shown that neurons in the hippocampus code for the spatial position of the animal [Ranck 1973; O'Keefe 1976; Henze et al. 2000]. Those place cells are active whenever the animal is in a certain place within the local environment and neighboring place cells fire at different locations, suggesting that the hippocampus forms a cognitive map of the outside world [O'Keefe and Nadel 1978]. In the following years more classes of cells with spatial correlates have been found in the hippocampal formation such as the head direction cells in the dorsal presubiculum [Taube et al. 1990; Chen et al. 1994] and the grid cells in the medial enthorinal cortex [Hafting et al. 2005]. Place cells code for the animal´s location, head direction cells represent the animal´s direction of heading and the grid cells provide information about distances moved in particular directions. Importantly, hippocampal neurons also code for events and stimuli that occur in particular places, thus laying the basis for the more general episodic memory system in the human hippocampus. In humans, putative place cells have been identified during recordings of pre-surgical epilepsy patients [Bird and Burgess 2008]. Furthermore, patients with transient global amnesia (TGA) were found to have an impairment of spatial memory with the degree of impairment correlating with the lesion size within the hippocampal CA1 region and the duration of TGA [Bartsch et al. 2010]. As such, this finding lend strong support to the notion that the human hippocampus is critically involved in spatial memory, consistent with studies of hippocampal function in lower mammals. Finally, studies in rodents demonstrated that hippocampal cells can respond to non-spatial stimuli (e.g., odors, auditory stimuli), suggesting a broader function for the hippocampus than just spatial, which would be in line with the hippocampus being an episodic and narrative memory system as well as a spatial one.

The hippocampus displays very characteristic electroencephalographic (EEG) patterns hat may be associated with learning and memory [Andersen 2007]. Six EEG patterns have been reported in freely behaving rodents, including four rhythmical and two non-rhythmical. Rhythmical patterns are the theta (6 – 12 Hz), beta (12 – 30 Hz), gamma (30 – 100 Hz), and ripple

(100 – 200 Hz) oscillations. The non-rhythmical patterns are the large irregular amplitude (LIA) and the small irregular amplitude (SIA) states. In rodents theta occurs primarily during translational movements such as walking, running, swimming, jumping, exploratory head movements and struggling [Vanderwolf 1969; McFarland et al. 1975; Buzsáki 2002]. Theta activity organizes the temporal organization of pyramidal neurons in the hippocampus. Interestingly, theta-related activity is also found in other brain regions such as prefrontal cortex [Hyman et al. 2005], amygdala [Collins et al. 1999] or supramammillary nucleus [Kocsis and Vertes 1994]. Therefore, it has been hypothesized that theta activity coordinates neuronal activity in those different parts of the nervous system [Bland 1986; O'Keefe and Burgess 2005]. LIA activity occurs during behaviors that do not change the animal´s location such as sitting quietly, eating, drinking, grooming, and during slow wave sleep [Buzsáki 1986]. During LIA highly synchronized bursts of activity in CA3 neurons (sharp waves; 50 – 100 ms in duration) are followed by the generation of a very fast (about 200 Hz) oscillation in CA1 (ripples) [Buzsáki et al. 1992]. Sharp wave-ripples have been reported to be involved in reactivation, a process in which hippocampal neurons activated during specific learning tasks exhibit elevated activity patterns once again during sleep [Pavlides and Winson 1989; Wilson and McNaughton 1994; Nádasdy et al. 1999]. Reactivation is hypothesized to facilitate the consolidation of information in the form of long-term memories elsewhere in the cortex [Sutherland and McNaughton 2000; Rasch and Born 2007; Cheng and Frank 2008] and may involve sustained changes in synaptic strength such as those observed during long-term potentiation (LTP). Little is known about the behavioral correlates of beta and gamma activity, but both have been shown to be associated with olfaction [Andersen 2007].

1.2 *In vivo* two-photon calcium imaging

The functional analysis of neurons and their networks requires the simultaneous measurements of many individual neurons in the context of their spatial locations. By using two-photon microscopy in combination with fluorescent calcium indicators, it has become possible to stain

entire local populations of neurons and to image their activity patterns *in vivo*. Two-photon calcium imaging has thus opened the opportunity to image deep in intact biological tissue with outstanding spatial resolution and signal contrast. Electrical recordings, which previously have been most commonly used for studying neuronal activity in living brains, have several important limitations when compared with two-photon calcium imaging. In particular, electrical measurements are usually obtained from spatially dispersed sets of neurons, whereas imaging can resolve the activity patterns of a population of nearby neurons. Other limitations of electrical recordings are poorly defined identity of recorded cells (for example with regard to neuronal subtype or laminar position) and blindness for hypoactive and silent neurons.

1.2.1 Two-photon microscopy

The major advantage of two-photon microscopy is its lower sensitivity to light scattering as compared to other fluorescence techniques such as confocal microscopy (which is based on one-photon excitation). Scattering leads to a degradation of resolution and contrast in biological tissue. Therefore, traditional fluorescence techniques, including confocal microscopy, cannot provide high-resolution deep imaging within tissue. Two-photon microscopy overcomes this limitation due to the unique properties of two-photon excitation. It is based on the quasi-simultaneous absorption (typically within less than 10^{-15} s) of two near-infrared photons promoting an electronic transition that would otherwise require a single photon of approximately twice the energy [Helmchen and Denk 2005; Svoboda and Yasuda 2006]. The probability for such a two-photon absorption is extremely low at ambient light intensities and occurs at appreciable rates only at very high intensities (in general $> 10^{17}\ \frac{W}{m^2}$) [Denk and Svoboda 1997]. Those high light intensities can only be achieved by using a pulsed laser source and spatially focusing the laser beam through a high numerical aperture (NA) microscope lens. Usually, lasers used for two-photon microscopy provide laser pulses of about 100 fs width and repetition rates of approximately 100 MHz (and thus matching the nanosecond fluorescence lifetime of many fluorophores). Most widely used is the Ti:sapphire laser with 700 – 1100 nm tunable output

and high average power capability of about 1 W. Besides the longer wavelength, which makes the excitation light less susceptible to scattering, a major advantage of two-photon excitation is its quadratic dependence on the average laser power due to which fluorescence generation is confined to the focal region and out-of-focus fluorescence is negligible. Two-photon microscopy provides inherent optical sectioning without the use of a spatial filter, because the exact place of origin of fluorescence photons is well-defined at each point in time. Consequently, all fluorescence photons (also scattered photons) that enter the objective and are passed by the detection filter are collected. Both the detection of scattered fluorescence and the longer excitation wavelength (700 – 1100 nm) contribute to the capability of two-photon microscopy to provide high resolution images from deep (several hundred micrometers) within living tissue. Moreover, confining excitation to the focal region not only allows for a significant increase in detection efficiency but also reduces photobleaching and damage in the out-of-focus volume.

1.2.2 Two-photon microscope setup

The main components of a two-photon microscope are an infrared ultra-short pulses emitting laser as excitation light source (Ti:sapphire laser is used in this thesis), scanning mirrors and optics (resonant galvanometric mirrors are used in this thesis), a fluorescence detector and a data acquisition system [Denk et al. 1990]. Images are generated by scanning the laser beam across the x-y plane of a specimen. The microscope objective focuses the laser beam into the specimen. Fluorescence is collected by the same objective, then separated by a dichroic mirror from the excitation light and guided onto a detector, which can be either a photomultiplier tube (PMT) or an avalanche photo diode (APD). Since all emitted photons are generated in the focal region, even scattered photons carry useful information. Therefore, whole-field detection is the preferred modality that enables the detection system to collect as many fluorescence photons emerging from the specimen as possible. A commonly used acquisition mode for two-photon imaging is raster-like frame scanning. However, this mode is not optimized for fast measurements of many neurons. In this thesis, we used resonant galvanometric mirrors for the fast scan axis [Sanderson

and Parker 2003]. Typical resonance frequencies range from 1 - 12 kHz and thus allow frame rates of about 60 Hz (for 128 - 256 lines). The fast scanning is advantageous because the brief dwell time of the laser focus on each cell (about 5 - 10 µs per crossing) reduces fluorophore exhaustion by preventing molecular transition into non-fluorescent dark states.

1.2.3 Fluorescence labeling

Two-photon calcium imaging relies on the use of calcium-sensitive activity-dependent fluorescent indicators. Calcium imaging takes advantage of the properties of calcium homeostasis inside neurons. In resting conditions the concentration of calcium is very low inside the cells (typically 50 - 100 nM), whereas the calcium ions concentration outside cells is several orders of magnitude higher than inside, several millimolar in the bloodstream or cerebrospinal fluid [Berridge et al. 2000; Grienberger and Konnerth 2012]. Neuronal membranes contain voltage-gated calcium channels that open when a cell produces an AP. This leads to a brief influx of calcium ions and a transient rise in the intracellular calcium concentration. Those AP-evoked calcium transients are reported by fluorescent calcium indicators as they change their fluorescence properties upon calcium binding. Because increases in the intracellular calcium concentration are tightly coupled to AP firing in most neurons, fluorescence changes of indicators are a good measure of suprathreshold activity [Yuste et al. 2011]. Following the rapid rise after an AP the intracellular calcium concentration decays back to resting level on a longer time scale of hundreds of milliseconds as calcium is buffered within the cytosol and removed via various extrusion mechanisms.

Small molecule calcium indicators. Many fluorescent calcium indicators are based on the calcium specific chelator 1,2-bis-[2-aminophenoxy]ethane-N,N,N´,N´-tetraaacetic acid (BAPTA) [Tsien 1989]. Those small molecule calcium indicators exhibit large calcium-induced fluorescence changes and a high specificity for calcium as opposed to other ions such as magnesium as well as rapid kinetics. Most small molecule indicators are also available in membrane-permeable acetoxymethyl (AM) ester form to allow bolus loading of a population

of cells in the intact brain [Stosiek et al. 2003]. Among the indicators that have been used for *in vivo* imaging of neural network dynamics are Oregon Green BAPTA-1 (OGB-1) AM [Stosiek et al. 2003; Kerr et al. 2005], Fura-2 AM [Sohya et al. 2007], Fluo-4 AM [Sato et al. 2007], and various others. The most common method for delivering small molecule calcium indicators to a neuronal population *in vivo* involves the targeted pressure ejection of a solution of the AM, membrane-permeant, form of small molecule calcium indicator directly into the brain region of interest via a pipette inserted into the brain through a small skull craniotomy [Stosiek et al. 2003; Garaschuk et al. 2006]. This bolus loading procedure (originally termed multi-cell bolus loading) can be used for a large spectrum of indicator dyes and enables the homogeneous staining of hundred of cells present in a brain region with a diameter of several hundred micrometers. For example, bolus loading has been successfully applied in different cortical regions in different species, such as mice, rats, ferrets and cats, and in rodent cerebellum and spinal cord [Garaschuk et al. 2006; Grienberger and Konnerth 2012]. So far, the bolus loading technique has not been successfully applied to the hippocampus *in vivo*.

Genetically encoded calcium indicators. Genetically encoded calcium indicators offer an alternative to the chemical small molecule indicators. A key advantage of genetically encoded compared to small molecule indicators is the possibility of performing long-term calcium imaging *in vivo*, not only at the cellular level but also in specific sub-cellular compartments [Holtmaat and Svoboda 2009; Holtmaat et al. 2012]. Genetically encoded indicators use autofluorescent proteins such as the green fluorescent protein (GFP) in combination with calcium-sensitive proteins such as calmodulin or Troponin C [Mank and Griesbeck 2008]. In contrast to the small molecule indicators genetically encoded calcium indicators are not always directly applied to the tissue of interest. Instead, the genetic information (usually in the form of DNA) that codes for the indicator is inserted to the cells and the cell-intrinsic transcription and translation machinery is used to produce the final protein. For example, DNA plasmids can be directly electroporated (commonly performed *in utero*) into cells by application of brief electric pulses [Mank et al. 2008; Hires et al. 2008]. An alternative method that achieves

much higher transfection rates is viral vector mediated delivery of genes [Lütcke et al. 2010]. In a recent study viral transfection by adeno-associated virus (AAV) was used to deliver the genetically encoded calcium indicator GCaMP3 into the mouse hippocampus [Dombeck et al. 2010]. Finally, transgenic expression of indicators has been tried for various genetically encoded calcium indicators.

1.3 Alzheimer´s disease

AD is the most common cause of dementia worldwide, affecting an estimated 0.8 million people in Germany and 35 million worldwide [Prince et al. 2009; Wimo et al. 2010; Reitz et al. 2011; Förstl et al. 2012; Mayeux and Stern 2012]. The annual incidence increases from 1 % between the ages of 60 and 70 years to 6 - 8 % at the age of 85 years or older. In countries in which survival to the age of 80 years or older is not uncommon the proportion of persons in this age group with AD approaches 30 % and is expected to continue to increase substantially.

Memory loss is the predominant feature of AD [Andersen 2007; Budson and Solomon 2011; Tarawneh and Holtzman 2012; Weintraub et al. 2012]. Typically, an inability to retain recently acquired information is one of the first symptoms, whereas memory for remote events is relatively spared until later. Disorders of speech and language also occur in early stages of the disease with word-finding difficulty being very often the first problem that becomes manifest. Another typical early symptom of AD is topographical disorientation. Patients complain of "getting lost" initially in unfamiliar environments and later also in familiar places. Progressive dysfunction of other cognitive domains (e.g., word comprehension, abstract reasoning, and executive function or decision making) becomes increasingly prominent with disease progression.

At autopsy, the key pathological features in the brains of patients with AD are extracellular amyloid-ß (Aß) plaques and intracellular deposits of hyperphosphorylated tau protein in the form of neurofibrillary tangles. Of the hippocampal subfields, plaques and tangles are most abundant in CA1 and the subiculum [Andersen 2007; Serrano-Pozo et al. 2011]. The CA1 pyramidal cells are the first hippocampal neurons that show AD-related changes, and, after

the stellate cells in the enthorinal cortex, they represent the second neuronal population to be affected in AD. Over time, there is widespread loss of pyramidal cells in the hippocampus with the greatest loss occurring in CA1.

Most AD cases occur in sporadic form, with familial AD accounting for less than 5 % of all cases [Mayeux and Stern 2012]. There are rare cases of families with autosomal dominant inheritance of AD that develop between the ages of 30 and 50 years. Approximately half of those cases result from mutations in genes encoding amyloid precursor protein (APP), presenilin (PS) 1, or PS 2. Mutations in those genes lead to an increased generation and aggregation of Aß, which predisposes to the formation of plaques. The genetic variant encoding apolipoprotein (APO) ε4 is the only well-established mutation associated with the late-onset form of AD (between 60 and 80 years of age). Recently, whole-genome data from almost 1800 Icelanders revealed a coding mutation (A673T) in the APP gene that protects against AD as well as cognitive decline in the elderly without AD [Jonsson et al. 2012].

1.3.1 *In vivo* imaging

In vivo imaging has become an indispensable tool in AD research, clinical trials and medical practice [Johnson et al. 2012]. In recent years imaging has fundamentally increased our understanding of the morphological and functional changes in AD. Generally, imaging technologies can be grouped by the energy used to derive visual information (X-rays, positrons, photons or sound waves), the spatial resolution that is achieved (macroscopic, mesoscopic or microscopic) or the type of information that is obtained (structural, functional, cellular or molecular) [Linden 2012]. Macroscopic imaging technologies, including computed tomography (CT), magnetic resonance imaging (MRI) and positron emission tomography (PET), are now in routine clinical and preclinical use. Microscopic imaging is used to examine the structure and function of biological tissue in more detail with cellular or even sub-cellular resolution. The traditional microscopy techniques that use one-photon absorption processes for contrast generation are restricted to use near the tissue surface for high-resolution imaging because at greater depths strong and

multiple light scattering blurs the images [Helmchen and Denk 2005; Kerr and Denk 2008; Lichtman and Denk 2011]. With the development of two-photon microscopy in combination with fluorescence labeling techniques it has become possible, for the first time, to use *in vivo* imaging several hundreds of micrometer deep in intact tissue with spatial resolution sufficient to discern individual neurons, dendrites, and synapses. Combined with the generation of transgenic animal models, two-photon imaging offers numerous advantages in the investigation of the development, progression and potential treatment of AD and other brain diseases.

Macroscopic *in vivo* imaging. The medial temporal lobe is the prime target of AD neuropathology [Thal et al. 2002; Braak et al. 2006; Serrano-Pozo et al. 2011] and several studies using volumetric MRI analyses have consistently shown that AD is associated with significant hippocampal volume loss [Andersen 2007; Johnson et al. 2012; Carmichael et al. 2012]. Moreover, selective hippocampal atrophy has also been found in very mild and even pre-symptomatic stages of AD [Chételat et al. 2005; Smith et al. 2007; Whitwell et al. 2007; Jack et al. 2008; Johnson et al. 2012]. Importantly, the hippocampal volume, which is usually assessed on high resolution T1-weighted magnetic resonance images, correlates with neuronal numbers in the hippocampus in AD [Bobinski et al. 2000; Gosche et al. 2002]. The brain atrophy is accompanied by a profound loss of dendritic, axonal and myelin structures [Frisoni et al. 2010], as can be revealed by magnetic resonance spectroscopy [Adalsteinsson et al. 2000], diffusion weight imaging [Kantarci et al. 2005], fiber tracking [Taoka et al. 2006] and magnetization transfer imaging [Ridha et al. 2007]. It is important to note that hippocampal atrophy can reliably differentiate between AD and age-matched controls, however it lacks the specificity to confidently exclude other dementias such as dementia with Lewy bodies, frontotemporal dementia or vascular dementia [Andersen 2007]. The fact that hippocampal atrophy alone does not sufficiently discriminate between different dementias indicates that other disease biomarkers are needed to reliably diagnose AD in the clinical setting.

Functional imaging methods, including single-photon emission computed tomography (SPECT), PET and functional MRI (fMRI), can provide a means of detecting the regional changes in

blood flow and metabolism that are associated with AD. Studies using various functional imaging techniques have consistently demonstrated a reduced cerebral blood flow and metabolism, primarily in the temporo-parietal and posterior cingulate regions, as a prominent feature of AD [Andersen 2007; Small et al. 2011; Johnson et al. 2012]. Moreover, previous fMRI studies showed hypoactivation in medial temporal lobe structures during episodic encoding tasks in AD patients as compared to healthy control subjects [Sperling et al. 2010]. Surprisingly, some brain areas exhibit increased fMRI activation in humans with AD performing memory tasks [Sperling et al. 2003; Grady et al. 2003]. Particular attention has been paid to the functional activation patterns in the hippocampus and related medial temporal lobe regions in the earliest stages of AD. Recent evidence has indicated that there is a period of hippocampal hyperactivation in the earliest stages of prodromal AD [Dickerson et al. 2005]. However, this period is followed by a significant decrease in hippocampal activation as cognition declines and subjects start meeting the clinical criteria for dementia [O'Brien et al. 2010]. Interestingly, even asymptomatic individuals with genetic risk factors for AD, such as APO ε4 carriers, exhibit hippocampal hyperactivation as compared to non-carriers [Bookheimer et al. 2000]. Other risk factors for AD, including PS1 mutations [Mondadori et al. 2006], trisomy 21 [Haier et al. 2003] or a family history of AD [Bassett et al. 2006], are also linked to increased activation of medial temporal lobe structures. In recent years, fMRI has been increasingly used to study the interregional correlations between spontaneous fMRI signals. Those studies have shown that various brain regions are organized into functional networks, which persist during sleep and anesthesia, and support sensory and motor systems, as well as higher integrative cognitive networks such as default mode and control networks [Greicius et al. 2004; Buckner et al. 2009]. Changes in the functional connectivity of those networks have been reported in humans with AD, such as a decreased bilateral hippocampal connectivity [Li et al. 2002] and decreased connectivity between the hippocampus and other regions within the default mode network, particularly the medial prefrontal cortex and the posterior cingulate cortex [Wang et al. 2006; Allen et al. 2007]. Recently, radiological-contrast compounds have been developed that specifically bind

the pathological lesions of AD, particularly Aß plaques [Perrin et al. 2009; Johnson et al. 2012]. Among those tracers most extensively studied and applied in research has been 11C-Pittsburgh compound B (PiB). In humans with AD, PET scans have revealed an increased uptake of PiB in cortical regions that are known to contain significant numbers of Aß plaques [Klunk et al. 2004]. Now, PiB-imaging has also become feasible in AD transgenic mice [Manook et al. 2012]. Amyloid imaging raises the possibility to detect the key pathological changes in the earliest stages of AD and thus it may allow earlier diagnosis of the disease and accurate differential diagnosis of the dementias [Johnson et al. 2012].

Microscopic *in vivo* imaging. Two-photon microscopy in combination with Aß specific fluorescent markers (e.g., methoxy-X04 [Klunk et al. 2002; Meyer-Luehmann et al. 2008], thioflavin-S [Bacskai et al. 2001; Christie et al. 2001; Eichhoff et al. 2008; Busche et al. 2008; Grienberger et al. 2012], PiB [Bacskai et al. 2003], fluorescent antibody 10D5 [Bacskai et al. 2001]) has been increasingly used to visualize and characterize plaque formation in AD mouse models *in vivo*. The fluorescent markers were administered either by direct application to the pial surface or systemic injection. A key advantage of two-photon microscopy is that it allows simultaneous imaging of multiple fluorescent markers by separating the different colors using filters on the detection side. For example, viral transfer of GFP into cortical neurons in APP transgenic mice enabled to image the detrimental effects of plaques, which were labeled by methoxy-XO4, on adjacent dendrites and spines [Spires et al. 2005]. A different approach to study the relation between plaque formation and the alterations in local neuritic architecture has been to cross AD transgenic mice with mouse lines containing fluorescent markers [Brendza et al. 2003; Tsai et al. 2004; Meyer-Luehmann et al. 2008]. Surprisingly, it has been shown that anti-Aß antibody treatment leads to a decrease in the amount of plaques and a rapid reduction in the number and size of dystrophic neurites in AD transgenic mice [Brendza et al. 2005; Rozkalne et al. 2009; Jones et al. 2009]. Furthermore, the dynamic interaction between plaques and microglia has been imaged *in vivo* by crossing transgenic Iba1-GFP [Bolmont et al. 2008] or CX3CR1-GFP mice [Davalos et al. 2005; Koenigsknecht-Talboo et al. 2008] with AD transgenic

mice. Apart from plaque formation, the aggregation of Aß results in widespread cerebral amyloid angiopathy (CAA). CAA is based on the aggregation of Aß in cerebral vessel walls, which can lead to a loss of smooth muscle cells [Mandybur 1975; Vinters 1987], disruption of vessels [Greenberg 2002], and even parenchymal hemorrhage [Kalyan-Raman and Kalyan-Raman 1984; Gilles et al. 1984; Mott and Hulette 2005]. With the use of two-photon microscopy the initiation and progression of methoxy-X04 labeled CAA in APP transgenic mice was studied for the first time *in vivo* [Robbins et al. 2006]. Traditional methods that have previously examined histological sections from animals and humans at single time points were not able to monitor those sequential events during the formation of CAA. All those studies focused mainly on the structural dynamics of Aß aggregation and plaque-associated alterations of spines, dendrites and microglia.

Recently, we and others have begun to use two-photon microscopy in combination with calcium sensitive fluorescent indicators to explore neuronal and astrocytic function in AD transgenic mouse models *in vivo*. Those studies have revealed, for the first time, that neuronal and astrocytic populations are functionally impaired in plaque-depositing AD transgenic mice. For instance, cortical circuits show increased fractions of abnormally hypoactive and hyperactive neurons [Busche et al. 2008], neurites near plaques exhibit calcium dyshomeostasis [Kuchibhotla et al. 2008] and astrocytes are synchronously hyperactive [Kuchibhotla et al. 2009]. In the following, a more detailed review of those and other studies is given together with a brief overview about current research on neural dysfunction in AD.

1.3.2 Neuronal dysfunction

Alzheimer's disease (AD) is associated with functional impairments of brain neurons that are responsible for the storage and processing of information [Mattson 2004]. Early studies revealed a massive decrease in the activity of central neurons [Silverman et al. 2001; Prvulovic et al. 2005] and the idea of a generalized silencing of brain circuits found strong support in the synaptic failure hypothesis [Selkoe 2002]. However, recent studies both in humans and in

animal models of AD revealed a more complex picture of the functional neuronal changes in AD, demonstrating a mix of both hypoactivity and hyperactivity at the level of neurons, circuits and wider networks [Palop and Mucke 2010].

In a previous study, we have used two-photon microscopy in combination with bolus loading of the calcium indicator OGB-1 AM to image neuronal activity patterns of cortical layer 2/3 neurons in a mouse model of AD [Busche et al. 2008]. We used the APP23xPS45 double transgenic mouse model which overexpresses both mutant APP with the Swedish (670/671) mutation [Sturchler-Pierrat et al. 1997] and the human G384A-mutated PS1 [Herzig et al. 2004]. The transgenic animals replicate several key aspects of AD pathogenesis, including plaque formation and memory loss. In the transgenic mice, we found that half of the neurons in layer 2/3 of the cortex were functionally impaired, with a decrease in neuronal activity in 29 % of the neurons (termed silent neurons) and a profound increase in more than 20 % of neurons (termed hyperactive neurons) (Figs. 1 and 2). Surprisingly, hyperactive neurons were exclusively found in the direct vicinity of plaques (Fig. 3). This was initially unexpected because several lines of evidence have suggested that structural neuronal alterations, including loss of dendritic spines and axonal dystrophies, are most prominent in the local environment of plaques [Meyer-Luehmann et al. 2008]. The alterations of cortical activity were not observed in younger, plaque-free transgenic or in wild type mice (Figs. 4 and 5), suggesting that the functional neuronal alterations were correlated temporally with plaque formation.

Consistent with our findings, a study using an adenoviral-based expression of the genetically-encoded calcium indicator Yellow Cameleon 3.6 in combination with two-photon microscopy showed that resting calcium levels in cortical dendrites of APP/PS1 transgenic mice were abnormally increased in the area surrounding plaques [Kuchibhotla et al. 2008]. This calcium overload was associated with morphological neuritic alterations mediated, at least in part, by activation of the calcium/calmodulin-dependent phosphatase calcineurin. Furthermore, chronic video-EEG monitoring revealed that APP transgenic mice exhibited aberrant excitatory nonconvulsive seizure activity in cortex and hippocampus that was counteracted by a compensatory

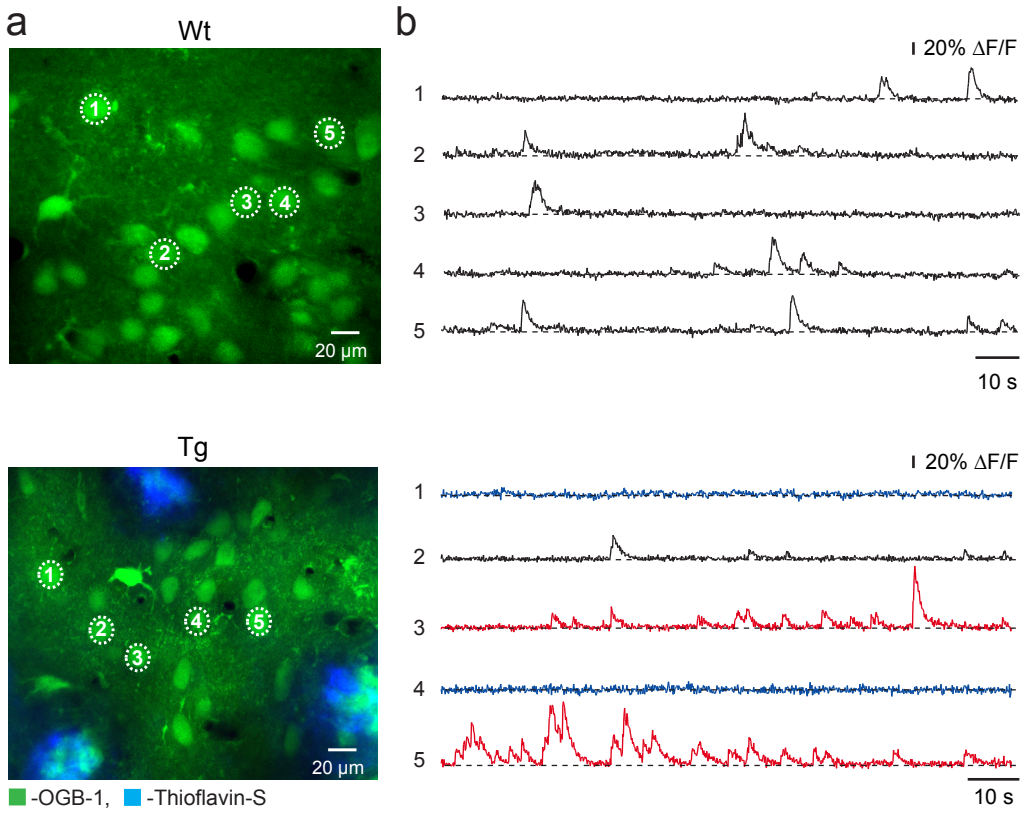

Figure 1: (**a**) Cortical layer 2/3 neurons imaged *in vivo* in a wild type (wt, upper) and a transgenic (tg, lower) mouse with thioflavin-S positive plaques (light blue). (**b**) Spontaneous calcium transients of the corresponding neurons marked in (a). Traces in (b) were color-coded to mark neurons that were either inactive during the recording period (blue) or showed an increased frequency of calcium transients (red).

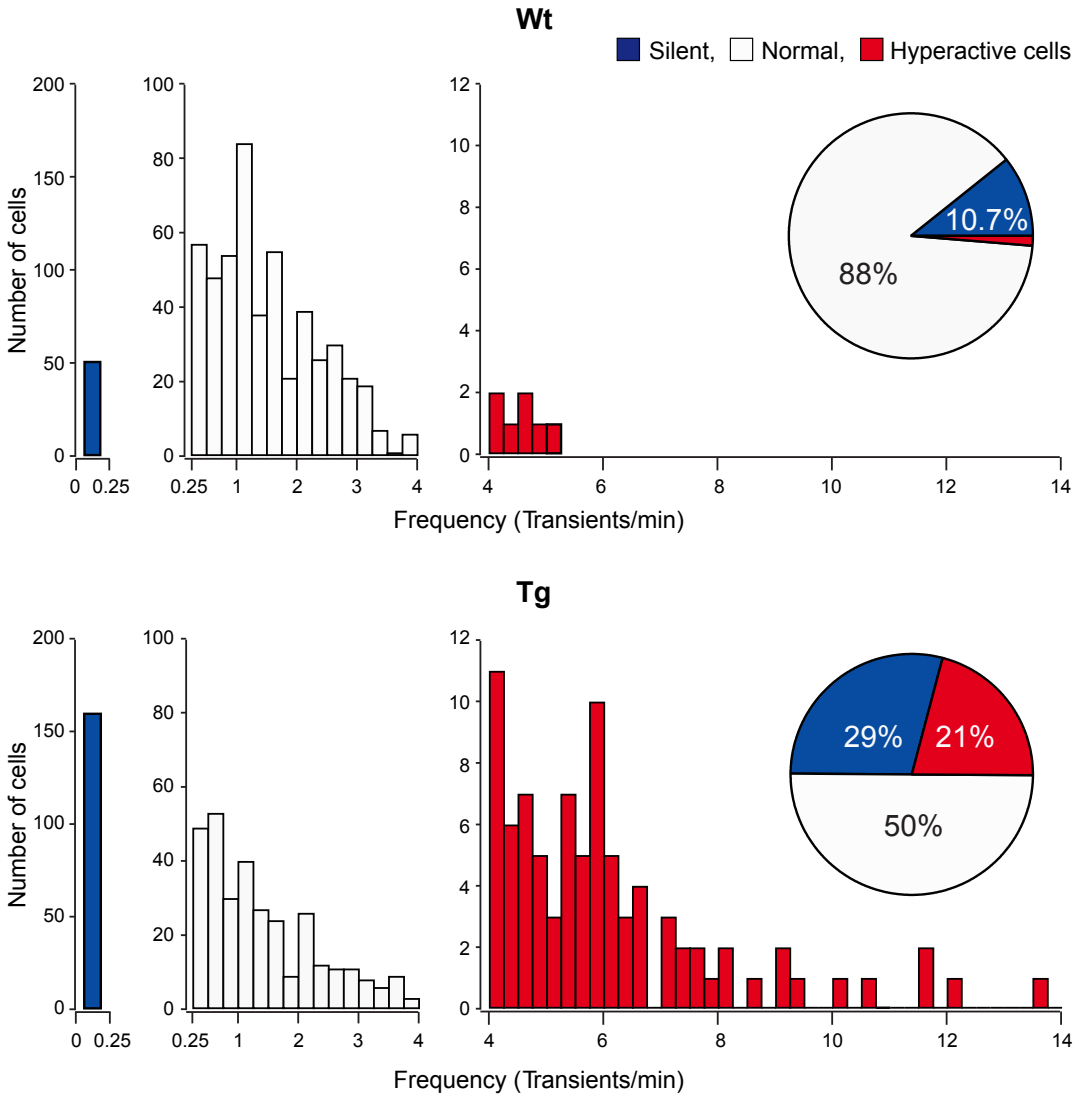

Figure 2: Histograms showing the frequency distribution of calcium transients in wild type (wt, upper) and plaque-laden transgenic (tg, lower) mice (in both cases n = 564 cells). There was a profound increase in the amount of silent and hyperactive neurons in tg mice. Pie charts showing the relative proportions of silent, normal, and hyperactive neurons in wt (n = 10) and tg (n = 20) mice.

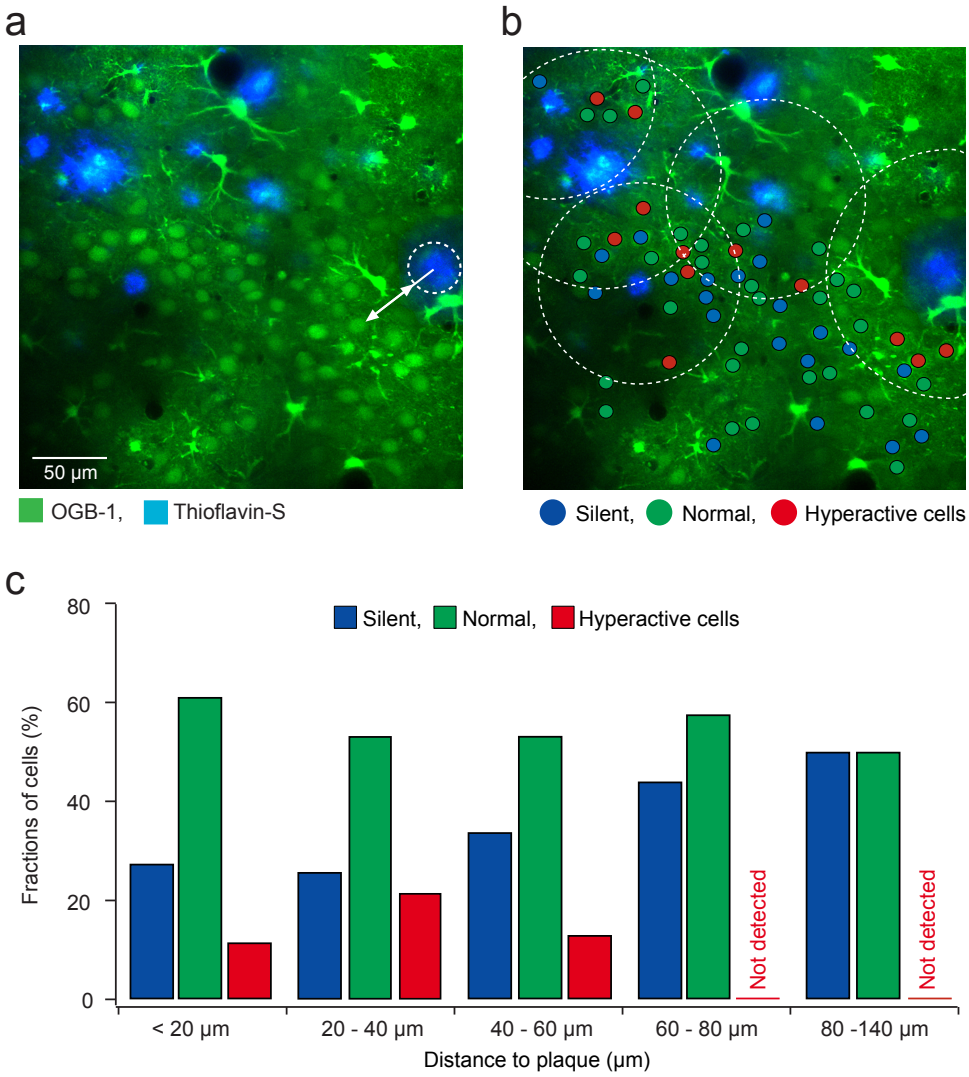

Figure 3: (**a**) Maximal projection image (100 - 130 µm depth) of layer 2/3 in the cortex of a plaque-laden transgenic (tg) mouse. To measure the distance from the plaque to the recorded cell, we fitted the plaque with a circle and measured the distance (arrow) between the plaque border and the middle of the cell. The cortical area located above and below the imaged plane (55 - 175 µm depth) was also scanned to assure that plaques shown were nearest to the recorded neurons. (**b**) Activity map of this region with neurons color-coded according to the frequency of their calcium transients. The broken line circles were centered at the respective plaques and delineate the area located less than 60 µm from the plaque border. (**c**) Bar graph showing the abundance of silent, normal, and hyperactive neurons at different distances from the border of the nearest plaque (n = 422 cells).

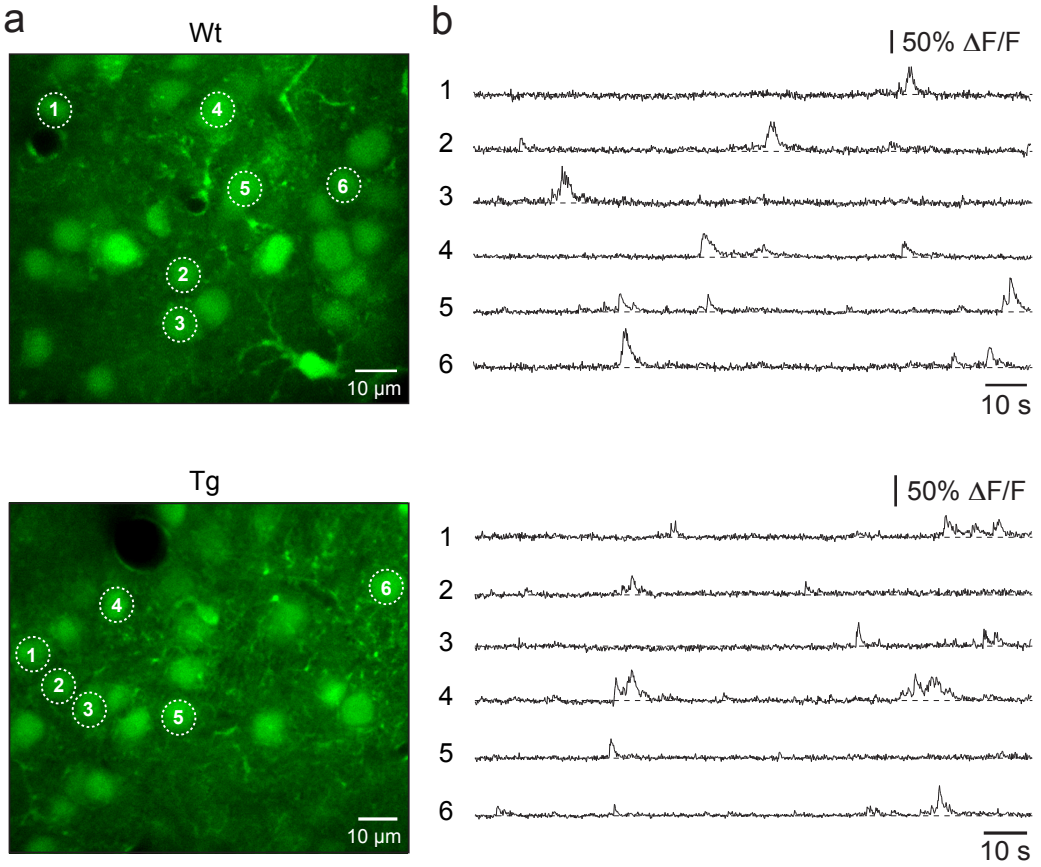

Figure 4: (**a**) Cortical layer 2/3 neurons imaged *in vivo* in a young wild type (wt, upper) and a young, plaque-free transgenic (tg, lower) mouse. (**b**) Spontaneous calcium transients of the corresponding neurons marked in (a).

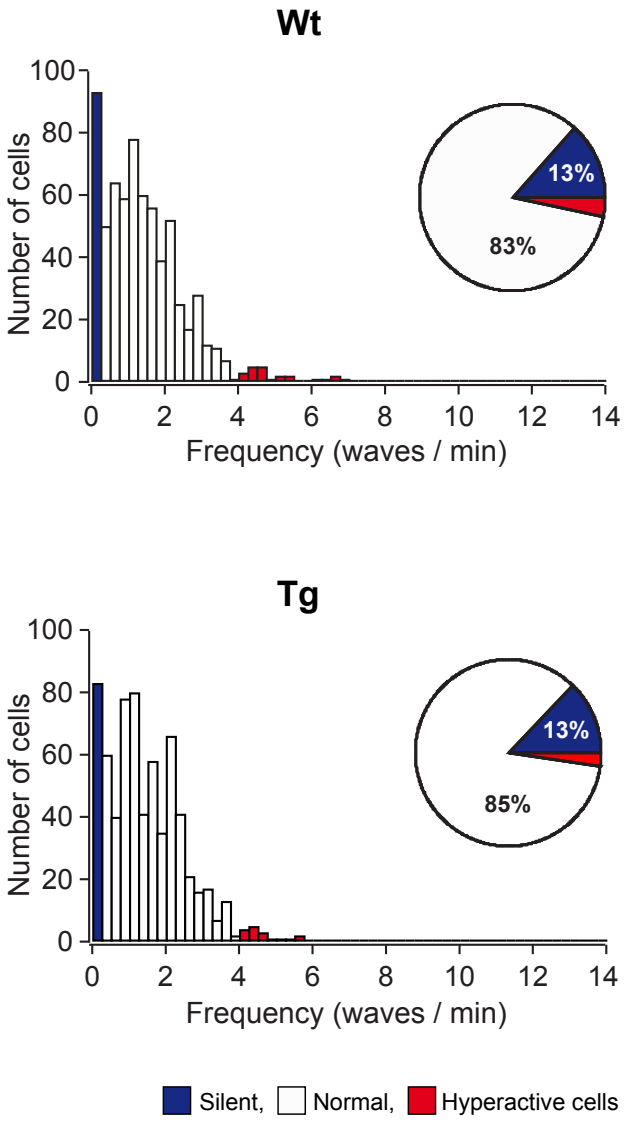

Figure 5: Histograms showing the frequency distributions of calcium transients in young, plaque-free transgenic (tg, lower) and age-matched wild type (wt, upper) mice. Both groups were 1.5- to 2-months-old (n= 675 cells in both cases). Pie charts showing the relative proportions of silent, normal and hyperactive neurons in wt and tg mice.

inhibitory response in the hippocampus, including altered levels of neuropeptide Y (NPY) receptors, ectopic NPY expression, GABAergic sprouting, and increased synaptic inhibition [Palop et al. 2007; Minkeviciene et al. 2009]. Those compensatory inhibitory mechanisms interfered with normal neuronal and synaptic functions required for learning and memory.

In humans with AD, plaques in temporo-parietal cortices, as detected *in vivo* on PiB imaging, were associated with aberrant increases in fMRI activation during memory encoding, yet these regions typically demonstrate hypometabolism in PET recordings using F-18-fluorodeoxyglucose (FDG) [Sperling et al. 2009]. Moreover, recent fMRI studies showed that humans with prodromal AD exhibit increased medial temporal lobe activation during an associative memory paradigm early in the course of the disease followed by a subsequent decrease as the disease progresses and cognition declined [Dickerson et al. 2005; O'Brien et al. 2010].

Taken together, there is converging evidence that synaptic depression and excess neuronal activity appear to coexist in an unknown manner in AD transgenic mice as well as in humans with AD [Palop and Mucke 2010]. It is entirely unclear what comes first, neuronal silencing or hyperactivity, and whether plaques are directly involved in the initiation of neuronal dysfunction. The basis of synaptic depression in AD has been examined in many studies [Chapman et al. 1999; Kamenetz et al. 2003; Hsieh et al. 2006; Shankar et al. 2007]. In particular, several studies have shown that Aß reduces glutamatergic synaptic transmission strength and plasticity and attenuates excitatory synaptic transmission by decreasing the number of surface α-amino-3-hydroxy-5-methyl-4-isoxazolepropionic acid (AMPA) and N-methyl-D-aspartate (NMDA) receptors, associated with a collapse of glutamatergic dendritic spines. However, the mechanisms underlying neuronal hyperactivity remain a major unresolved issue. Plaques and hyperactive neurons occur together in the cortex of transgenic mice [Busche et al. 2008], but whether plaques are directly responsible for the increase in activity is unclear. In fact, there is experimental evidence suggesting that soluble species of Aß, particularly oligomers, may be the disease-causing entity in AD [Shankar et al. 2008]. This raises the question whether soluble Aß, rather than plaques themselves, may be causally related to the functional alterations of neurons and

circuits. A promising strategy to address this question might be to examine early stages of the disease, when the AD pathology is still mild. The hippocampal CA1 pyramidal cell circuit represents a particularly good model system to address this question because the hippocampus is known to be a very early target in AD. First, impaired learning and memory, which is believed to involve hippocampal dysfunction [Squire and Zola-Morgan 1991], is typically among the first symptoms of the disease both in animal models and humans [Hyman et al. 1984; Moran et al. 1995]. Second, previous *in vitro* studies provided clear evidence that structural hippocampal abnormalities can occur at very early stages of the disease, long before the emergence of plaques [Hsia et al. 1999; Moechars et al. 1999; Mucke et al. 2000].

2 Material & Methods

This chapter provides detailed information on all methodological aspects of the thesis. The experiments were done in anesthetized animals. All experimental procedures were in compliance with institutional animal welfare guidelines and were approved by the state government of Bavaria, Germany.

2.1 Animals

APP23xPS45 mice were used as the AD transgenic mouse model in this thesis. Those mice overexpress the human APP with the Swedish (670/671) mutation [Sturchler-Pierrat et al. 1997] and the human G384A-mutated PS1 [Herzig et al. 2004]. Both transgenes are driven by a Thy-1 promoter. The mutations are known to induce a rapid increase in soluble brain Aß levels, followed by the formation of plaques beginning at an age of about 3 months. Two different age groups were used (1- to 2-month-old mice without plaques and 6- to 7-month-old mice with plaques) and compared to age-matched nontransgenic wild type mice.

2.2 Surgery and labeling procedure for hippocampal imaging

For surgery, mice were anesthetized by inhalation of 1 - 1.5 % isoflurane in pure oxygen and placed onto a warming plate (38 °C). The skin was removed and a custom-made recording chamber was glued to the skull with cyanoacrylic glue (UHU, Buhl-Baden, Germany). The stereotactic coordinates of the hippocampus were located using a mouse brain atlas [Paxinos and Franklin 2001] and a dental drill was used to open a 1 - 2 mm wide cranial window in

the skull centered 2.5 mm posterior to bregma and 2.2 mm lateral to the midline. The dura was dissected with fine forceps and the cortical tissue above the hippocampus was carefully removed by aspiration. Then the dorsal surface of the hippocampus was thoroughly irrigated with warm (37 °C) external saline and the mouse was transferred into the recording set-up. Mice were continuously supplied with 0.5 - 0.8 % isoflurane in pure oxygen through a face mask. The core body temperature was maintained at 37 – 38 °C, and both respiratory and pulse rate were continuously monitored. The recording chamber was perfused with warm (37°C) artificial cerebrospinal fluid (ACSF; 125 mM NaCl, 4.5 mM KCl, 26 mM $NaHCO_3$, 1.25 mM NaH_2PO_4, 2 mM $CaCl_2$, 1 mM $MgCl_2$, 20 mM glucose, pH 7.4, when bubbled with 95 % O_2 and 5 % CO_2). For calcium imaging, the fluorescent calcium indicators OGB-1 AM (Molecular Probes, Eugene, USA) or Fluo-8 AM (AAT Bioquest, California, USA) were used. Briefly, the fluorescent calcium indicator dye was dissolved in dimethyl sulfoxide (DMSO) plus 20 % Pluronic F-127 and the solution was diluted with a standard pipette solution to a final concentration of 0.5 to 1 mM. Then, the solution was pressure-ejected (2 - 4 min, 0.5 - 0.6 bar) to the pyramidal cell layer of CA1 using a glass micropipette. 30 - 60 min were allowed for loading of the cells. Plaques were stained in a similar way, by pressure-ejecting thioflavin-S (0.001 % (w/v)). To reduce brain motion during *in vivo* recordings, the craniotomy was filled with agarose (1 - 2 %) and stabilized with a cover glass. For calcium imaging of cortical neurons animals were prepared similarly, but of course, with the difference that cortical tissue was not removed [Garaschuk et al. 2006; Busche et al. 2008].

2.3 Two-photon imaging

In vivo two-photon recordings were made using a custom-built two-photon microscope based on a Ti:sapphire excitation laser (Chameleon; Coherent, California, USA) operating at 925 nm and a resonant galvo-mirror system (8 kHz; GSI) for x-y-scanning [Sanderson and Parker 2003]. The laser intensity was modulated with a Pockel´s cell. The laser scanning unit was mounted on an upright microscope equipped with a water-immersion objective (Nikon 40 x, 0.8

NA; Japan) and the fluorescence was detected using a GaAsP photomultiplier tube (H7422-40; Hamamatsu Photonics, Herrsching, Germany). Full-frame images were acquired at 30 Hz using a custom-written software based on LabVIEW (National Instruments, Austin, USA). At each focal plane, spontaneous calcium transients of CA1 neurons were recorded for at least 5 minutes. For simultaneous visualization of Fluo-8 labeled neurons and thioflavin-S labeled plaques the emitted fluorescence was split at 515 nm.

2.4 Image analysis

The image analysis was performed off-line using ImageJ (`http://rsb.info.nih.gov/ij/`) and Igor Pro (Wavemetrics, Lake Oswego, USA). First, regions of interest (ROI) were drawn around individual somata and then relative fluorescence change (ΔF/F) versus time traces were generated for each ROI. Calcium transients were identified as changes in ΔF/F that were three times larger than the standard deviation of the noise band. Astrocytes were excluded from the analysis based on their selective staining by sulforhodamine 101 and their specific morphology [Nimmerjahn et al. 2004; Garaschuk et al. 2006; Nimmerjahn and Helmchen 2012].

2.5 Cell-attached recordings

Somatic cell-attached recordings of Fluo-8 labeled CA1 neurons were obtained using an EPC10 amplifier (USB Quadro Amplifier, HEKA Elektronik, Lambrecht, Germany) by the "shadow-patching" procedure under two-photon imaging guidance [Kitamura et al. 2008]. The patch pipette solution contained ACSF with 50 μM Alexa Fluor 594 (Invitrogen, Karlsruhe, Germany) for pipette visualization. The pipette had a tip resistance of 5 - 7 MΩ. Electrophysiological data were filtered at 10 kHz and sampled at 20 kHz using Patchmaster software (HEKA Elektronik, Lambrecht, Germany).

2.6 Treatment with γ-secretase inhibitor

The γ-secretase inhibitor LY-411575 (gift of Novartis, Basel, Switzerland) was suspended in 0.5 % methylcellulose at a concentration of 10 mg/kg [Abramowski et al. 2008]. Mice received a single dose of inhibitor by oral gavage at 10 mg/kg. Control animals received a single dose of vehicle (0.5 % methylcellulose in water) instead of γ-secretase inhibitor treatment.

2.7 Dimer application

Synthetic Aß-40 S26C dimers [Shankar et al. 2008; Hu et al. 2008; O'Nuallain et al. 2010] were purchased from Anaspec (San Jose, USA) and dissolved in DMSO. The dimer preparation was diluted to 100 nM in ACSF, filled into a micropipette and locally pressure-applied to the cells of interest (30 sec, 0.15 bar).

2.8 Quantification of Aß

Frozen hippocampus samples were weighed and homogenized in 9 volumes (w/v) of ice-cold Tris-buffered saline (TBS) Complete (20 mM Tris-HCl pH 7.4, 137 mM NaCl, 1x Complete [Protease Inhibitor Cocktail Tablets: 1 836 145, Roche, Penzberg, Germany]) using douncing with micropistills (#0030 120.973, Eppendorf, Schonenbuch, Switzerland). To extract TBS-soluble Aß-40 and Aß-42 samples were incubated for 15 min on ice, ultracentrifuged (100 000xg, 4 °C, 15 min) and the clear supernatants analyzed for Aß. To extract sodium dodecyl sulfate (SDS)-soluble Aß-40 and Aß-42 the pellets from the TBS extraction were dissolved in 0.5 % SDS, incubated for 15 min at 4 °C, ultracentrifuged (100 000xg, 4 °C, 15 min) and the clear supernatants analyzed for Aß. To prepare standards for the calibration curves, non-transgenic forebrain was extracted with TBS and the pellet with SDS as described above and spiked with Aß1-40 or Aß1-42 standard dilutions. Aß-40 and Aß-42 were determined with the Meso Scale Discovery (MSD) 96-well MULTI-ARRAY Human (6E10) Aß-40 Ultra-Sensitive Kit and the MSD 96-well MULTI-ARRAY Human (6E10) Aß-42 Ultra-Sensitive Kit (Cat# K111FTE-3

and K111FUE-3, MSD, Gaithersburg, USA). The means from duplicate wells were used in SOFTmax PRO 4.0 for calculation of standard curves and quantification of samples.

2.9 Detection of Aß plaques

For immunohistological and thioflavin-S staining of plaques, mice were perfused with phosphate-buffered sulfate (PBS) followed by 4 % paraformaldehyde (PFA) under deep isoflurane anesthesia. Brains were removed and postfixed in 4 % PFA for 24 h. Fixed brains were immersed in 30 % sucrose, frozen in 2-methylbutane and sliced in 25 µm thick coronal cryosections. All sections were cut along the rostrocaudal axis. Sections were washed in PBS and heat induced antigen retrieval with a microwave at 90 °C for 5 minutes in 0.1 M citric acid buffer (pH 5.8) was performed. For immunohistological detection of the plaques, slices were treated according to standard procedures. Primary mouse anti-human Aß antibody 4G8 (Covance, New Jersey, USA) with a dilution of 1:1000 and a secondary biotinylated horse anti mouse IgG antibody (BA2000, Vector Laboratories) diluted 1:200 was used. The slices were further processed using the Vectorstain Elite ABC Kit (Vector Laboratories, California, USA). After the reaction with diaminobenzidine (DAB) (Roche, Penzberg, Germany, Code 17118096), slices were counterstained with hemalum solution, dehydrated and coverslipped. Thioflavin-S stainings of plaques were done after a protocol previously described [Sun et al. 2002]. Briefly, slices were incubated in thioflavin-S solution (0.05 % w/v in 50 % ethanol) for 8 min in darkness followed by two differentiation steps in 80 % ethanol. Subsequently, slices were rinsed three times with distilled water and incubated in high concentration of phosphate buffer for 30 min at 4 °C. Finally, sections were washed with distilled water, dried and coverslipped. Fluorescence and transmitted light images were taken with a camera (XC10, Olympus) mounted on a microscope (MVX10, Olympus). Images were acquired using a 2x objective with a 6.3x magnification. Plaques with a diameter of only about 7 µm can be detected.

2.10 Statistical analysis

Statistical analysis was performed using SPSS (SPSS 16.0 for Windows). The statistical methods used were the Student´s t-test and the Kolmogorov-Smirnov test. $P < 0.05$ was considered statistically significant.

3 Results

The main objective of this thesis was to advance two-photon microscopy towards high-resolution imaging of neuronal activity patterns in the hippocampus *in vivo* to allow the study of hippocampal neuronal network function in AD transgenic mice.

3.1 Imaging neuronal activity in the hippocampus

The hippocampus is located beneath over a millimeter of neocortical tissue and so far has been inaccessible to cellular-level functional imaging *in vivo*. To achieve hippocampal imaging at cellular level, we adapted a protocol previously used to expose the surface of the dorsal hippocampus [Kandel et al. 1961; Mizrahi et al. 2004; Dombeck et al. 2010; Kuga et al. 2011; Sasaki et al. 2011]. We very carefully suctioned away a small piece of overlying neocortex and used bolus loading of fluorescent calcium indicators to label neurons in the CA1 region of the hippocampus for *in vivo* calcium imaging. Our experimental approach is illustrated in Fig. 6. The bolus loading procedure is based on the pressure-ejection of a solution containing the membrane-permeant, AM-ester form of a fluorescent calcium indicator into a brain region of interest [Stosiek et al. 2003; Garaschuk et al. 2006; Garaschuk and Konnerth 2010]. Initially, we used bolus loading of the small-molecule calcium indicator OGB-1, which is commonly used for two-photon imaging of neuronal activity in cortical layer 2/3 neurons *in vivo* [Stosiek et al. 2003; Kerr et al. 2005; Ohki et al. 2006; Greenberg et al. 2008; Busche et al. 2008; Rochefort et al. 2009; Grienberger et al. 2012]. Two-photon imaging of the labeled CA1 region at a depth of 110 – 180 µm below the surface revealed the densely packed neurons of the CA1 pyramidal cell

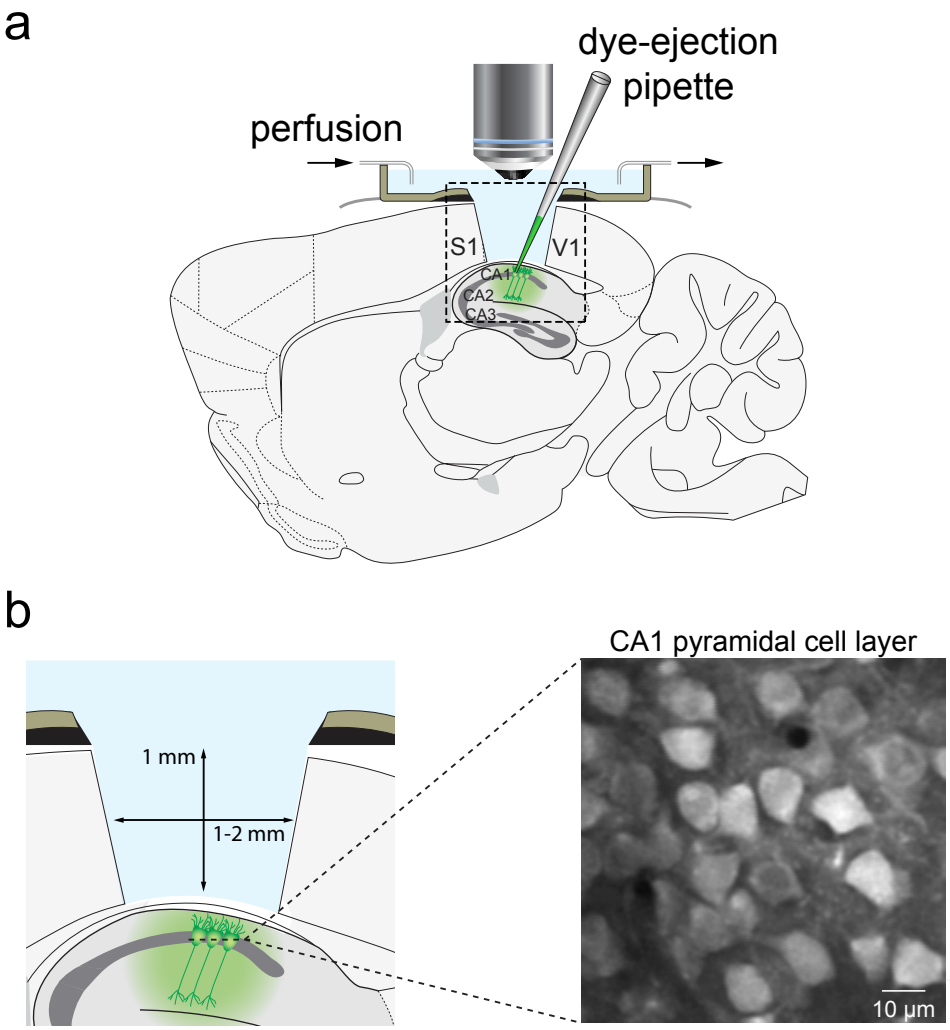

Figure 6: (**a**) Side view schematic showing the location of the hippocampal imaging window. (**b**) Left, detailed view of the boxed region in (a). Right, *in vivo* image of CA1 pyramidal cell layer.

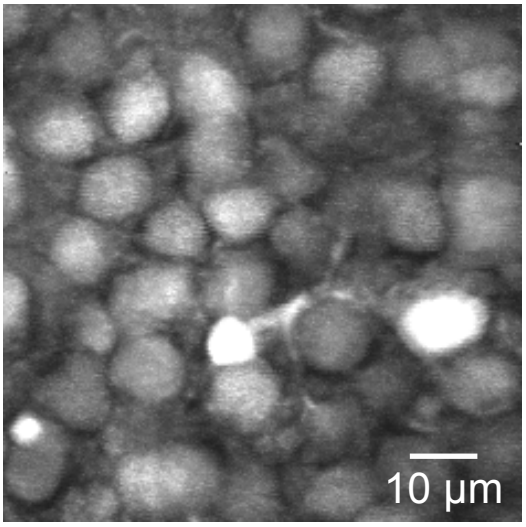

Figure 7: *In vivo* image of Oregon Green BAPTA-1 labeled CA1 pyramidal cell layer.

layer (Fig. 7). Voids of fluorescence indicative of unlabeled cells were not seen suggesting near ubiquitous local labeling. The CA1 neurons displayed spontaneous transient increases in the fluorescence signal (see Fig. 8 for one of the first recordings *in vivo*). Those transients were characterized by a fast rise and slow decay. The time course of the transients suggested that they were caused by APs. AP firing leads to a brief influx of calcium ions and transient increases in the intracellular calcium concentration, which are reported by the fluorescent calcium indicators [Kerr et al. 2005; Yuste et al. 2011]. The decay time constant of the transients likely reflects clearance of calcium from the neuronal cytoplasm [Markram et al. 1995; Scheuss et al. 2006]. In the cortex, OGB-1 is known to be a very sensitive reporter of neuronal activity allowing optical detection of single APs in identified neurons *in vivo* [Kerr et al. 2005; Rochefort et al. 2008; Garaschuk and Konnerth 2010]. To test whether this is the case also in hippocampal neurons, we combined cell-attached recordings with calcium imaging. Calcium transients and APs were clearly correlated and transients were only found after APs. However, single APs were not resolved in OGB-1-labeled hippocampal neurons and only spike trains with more than 3 APs were reliably detected (Fig. 9).

The calcium indicator dyes Fluo-3 and Fluo-4 are known to provide larger fluorescence

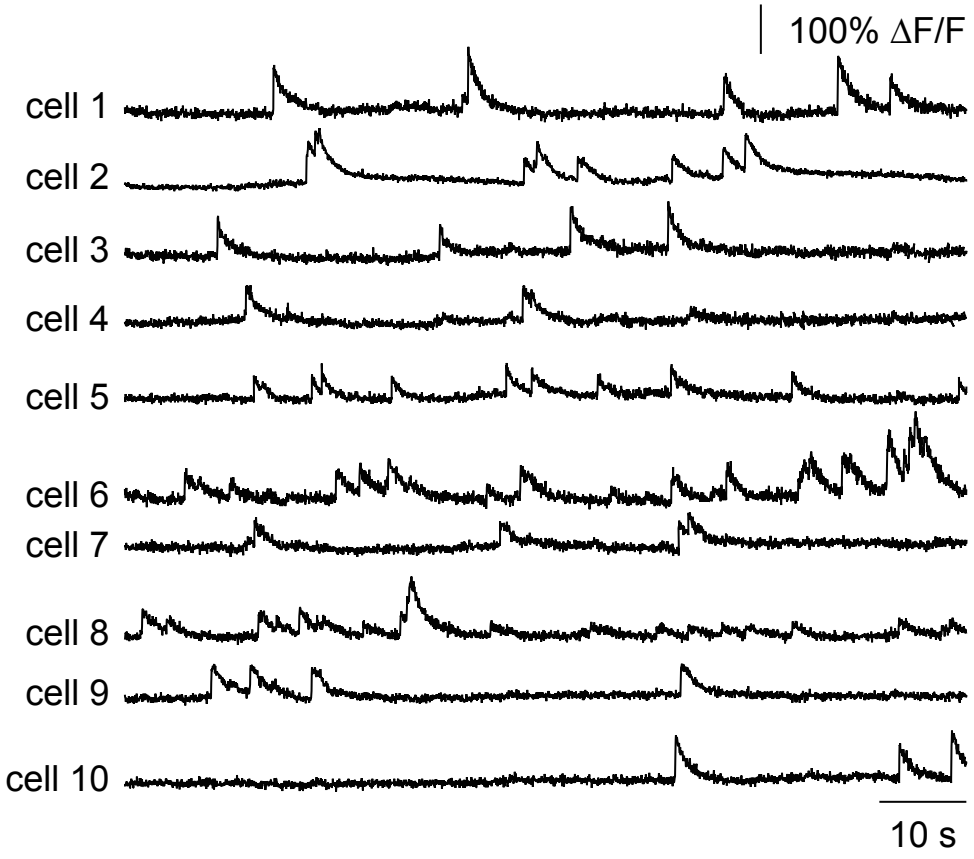

Figure 8: One of the first *in vivo* recordings of spontaneous calcium transients in Oregon Green BAPTA-1 labeled CA1 pyramidal neurons.

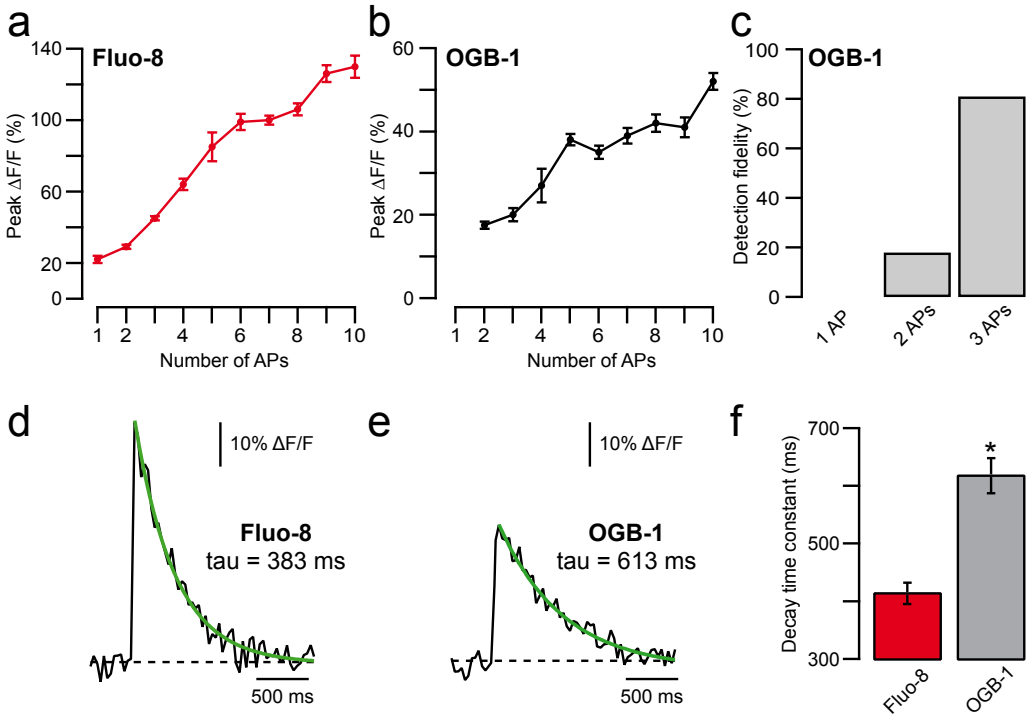

Figure 9: (**a and b**) Peak amplitudes of calcium transients (ΔF/F) in CA1 neurons as a function of the number of action potentials (APs) as detected from simultaneous cell-attached recordings (n = 15 cells for Fluo-8 and n = 8 cells for OGB-1). (**c**) Fractions of single APs and trains of APs optically detected in OGB-1 labeled CA1 neurons (n = 8 cells). (**d and e**) Decay time constants of exponential fits from calcium transients (average of 6 calcium transients evoked by 4 AP train). (**f**) Mean decay time constants of calcium transients evoked by 4 AP trains (n = 12).

changes upon calcium binding than OGB-1 [Thomas et al. 2000; Yasuda et al. 2004]. Thus, we next used the recently developed Fluo-8 dye, an improved version of Fluo-3 and Fluo-4. Fluo-8 is suggested to be more readily loaded into cells and even brighter than Fluo-3 and Fluo-4 (AAT Bioquest Product Technical Information Sheet). As described above, cells in the hippocampal CA1 region were stained with Fluo-8 using bolus loading (Fig. 6). Similar to the OGB-1 labeled neurons, Fluo-8 labeled cells displayed spontaneous transient increases in the fluorescence signal. Those fluorescence transients had a similar onset but decayed faster compared to transients in OGB-1 loaded cells (Fig. 9). To characterize the relationship between calcium transients and the electrical cellular activity, we combined cell-attached recordings with calcium imaging (Fig. 10). Fluorescence transients and APs were highly correlated and transients directly reported the firing of APs. 73% of all single APs and 100% of all AP trains were reliably detected in the recorded cells (Fig. 10). Importantly, Fluo-8 also performed better than OGB-1 in terms of absolute response and signal-to-noise ratio (SNR) (Figs. 9 and 10).

Together, the labeling of hippocampal neurons with Fluo-8 provides substantially better SNR and AP detection efficiency as compared to OGB-1. In addition, Fluo-8 shows much greater photostability and faster kinetics than OGB-1. All these factors translate into improved detection and measurement of physiologically relevant calcium signals.

3.2 Patterns of neuronal activity in hippocampus and cortex

Two-photon microscopy in combination with bolus loading of fluorescent calcium indicators has been widely used to study neuronal activity in the cerebral cortex [Stosiek et al. 2003; Kerr et al. 2005; Ohki et al. 2006; Greenberg et al. 2008; Busche et al. 2008; Rochefort et al. 2009; Grienberger et al. 2012]. Those studies have revealed that individual neurons and populations of cortical layer 2/3 neurons exhibit sparse spontaneous activity [Kerr et al. 2005; Busche et al. 2008; Rochefort et al. 2009]. So far, the precise patterns of neuronal activity within the hippocampus have been unknown. To address this issue, we compared spontaneous activity of layer 2/3 with that of CA1 neurons in wild type mice. Fig. 11 illustrates that CA1 neurons

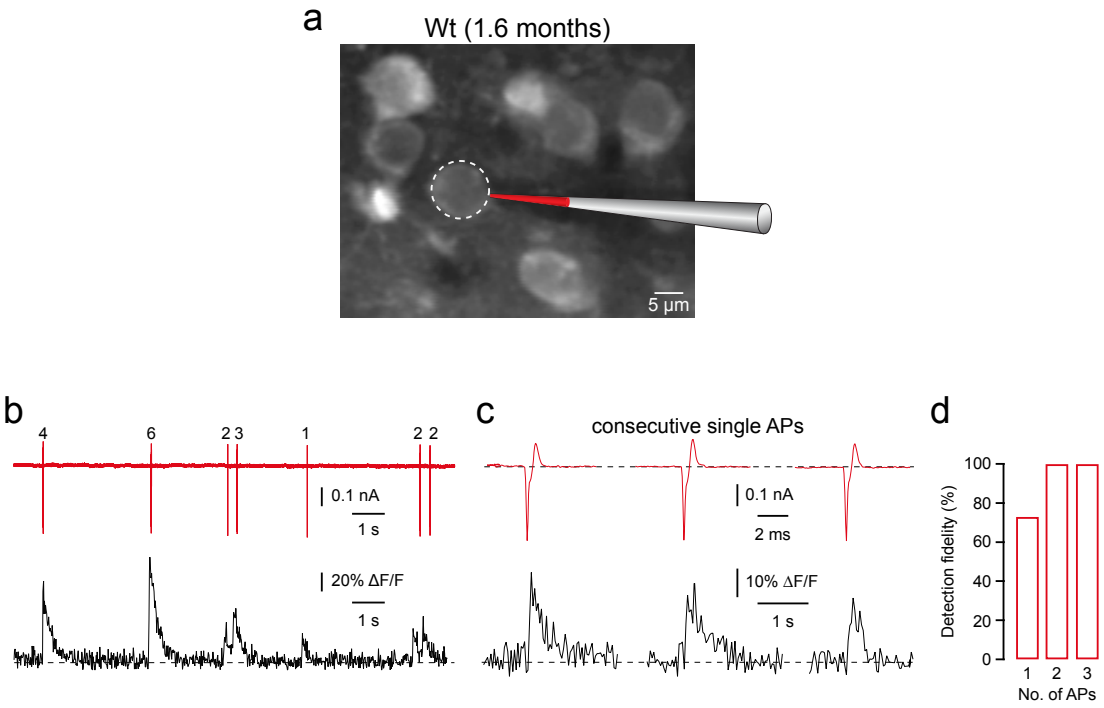

Figure 10: (**a**) CA1 neurons imaged *in vivo* in a wild type (wt) mouse. A neuron in the middle of the image was patched with a pipette containing Alexa Fluor 594. (**b**) Simultaneous *in vivo* recordings of spontaneous calcium transients (black trace) and underlying action potential (AP) firing (red trace, number of APs indicated) in cell-attached configuration from neuron in (a). (**c**) Examples of spontaneous calcium transients (black trace) evoked from three consecutive single APs (red trace) in a wt mouse. (**d**) Fractions of single APs and trains of APs optically detected in CA1 neurons of wt mice (n = 15 cells in 3 mice).

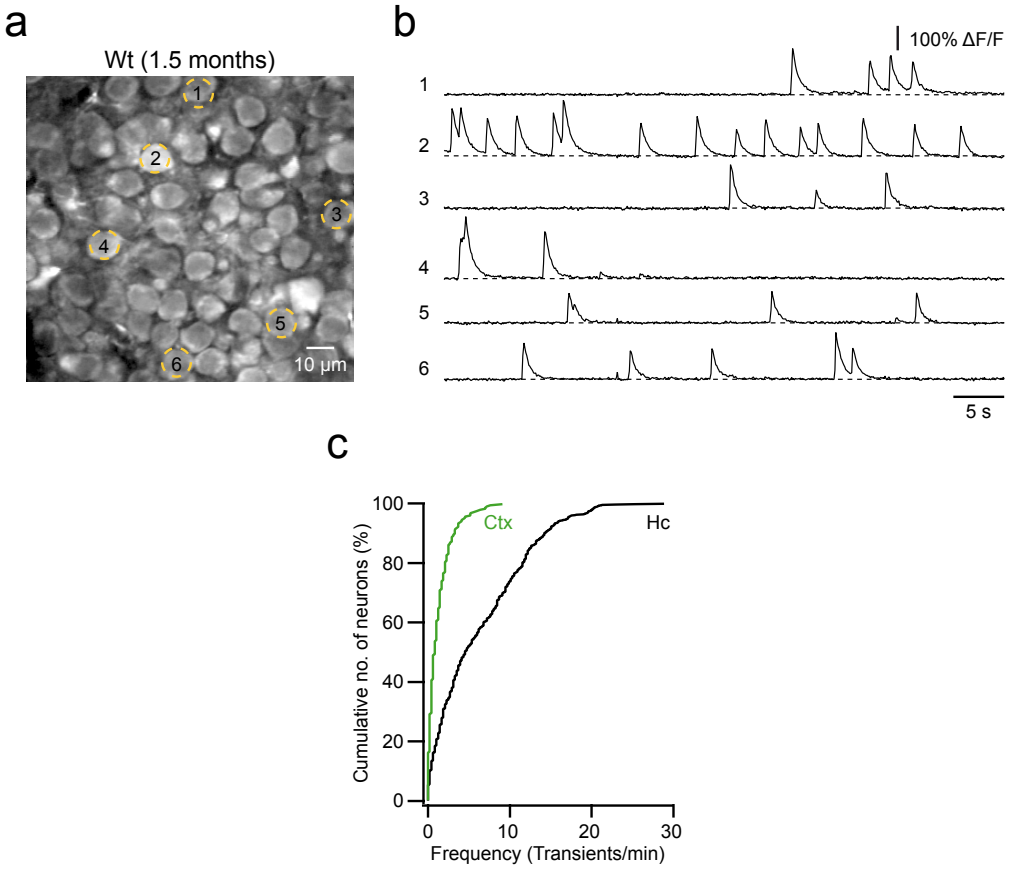

Figure 11: (**a**) CA1 neurons imaged *in vivo* in a wild type (wt) mouse. (**b**) Spontaneous calcium transients of the corresponding neurons marked in (a). (**c**) Cumulative distribution showing higher rates of spontaneous calcium transients in CA1 (Hc, n = 693 cells in 6 mice) than cortical layer 2/3 neurons (Ctx, n = 262 cells in 7 mice, $P < 0.001$, Kolmogorov-Smirnov test).

exhibited much higher rates of spontaneous calcium transients than layer 2/3 neurons. This indicates that hippocampal neurons display dense activity patterns as compared to the sparse activity in the upper layer cortical neurons. Furthermore, we found that groups of hippocampal neurons tended to be co-active repeatedly over the course of many minutes. This is illustrated in a short segment of data during which six cells were co-active at different times (Fig. 12). The observation of a co-activation of neuronal ensembles in the hippocampus may suggest that functionally related cells are organized into distinct subnetworks.

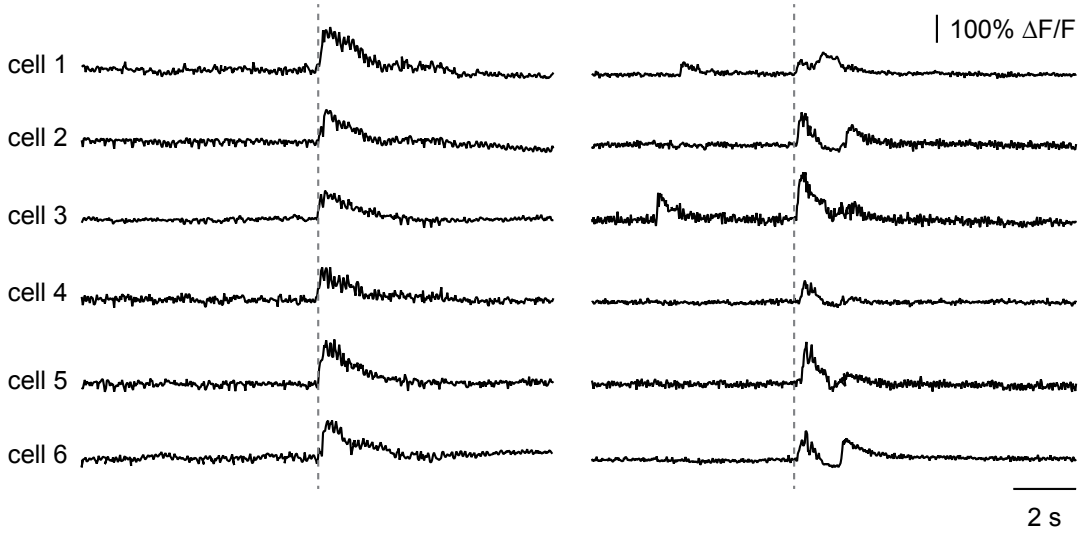

Figure 12: Example of six CA1 neurons labeled with Oregon Green BAPTA-1 that were repeatedly co-active during spontaneous activity.

3.3 Imaging neuronal activity in the hippocampus of Alzheimer transgenic mice

In the next step, we used our novel method to study hippocampal function in the APP23xPS45 mouse model of AD [Busche et al. 2008; Grienberger et al. 2012]. Those mice overexpress the human APP with the Swedish (670/671) mutation [Sturchler-Pierrat et al. 1997] and the human G384A-mutated PS1 [Herzig et al. 2004] under control of the Thy-1 promoter. The mutations are known to induce a rapid increase in soluble brain Aß levels, followed by the formation of plaques beginning at an age of about 3 months [Busche et al. 2008; Grienberger et al. 2012]. Fig. 13 shows sections from transgenic mice stained with the classic amyloid-staining dye thioflavin-S [Kurucz et al. 1981; Khachaturian 1985] as well as with the 4G8 antibody against Aß [Wisniewski et al. 1989]. Thioflavin-S stains primarily ß-pleated sheets characteristic of more mature amyloid deposits, whereas 4G8 also labels more diffuse Aß deposits. As expected, we detected no plaques in mice 1- to 2-months of age, however we found many plaques in mice 6- to 7-months of age. In the following, we studied neuronal activity in the hippocampus of

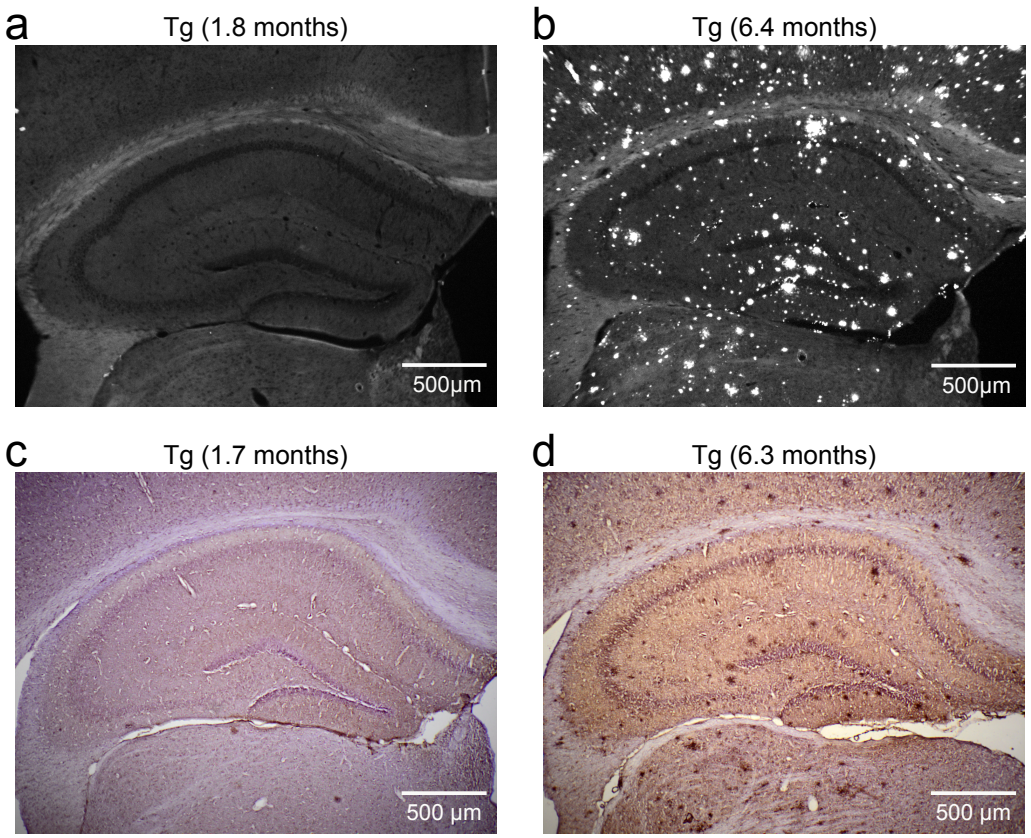

Figure 13: (**a and b**) Hippocampal sections from transgenic (tg) mice were stained with thioflavin-S and imaged by means of light microscopy. No plaques were detected in the hippocampus of 1- to 2-month-old tg mice (n = 5 mice, 10 – 34 sections per mouse were analyzed), while 6- to 7-month-old tg mice displayed multiple thioflavin-S positive plaques (n = 5 mice, 10 – 34 sections per mouse were analyzed). (**c and d**) Hippocampal sections from tg mice were immunoperoxidase stained for Aß with the 4G8 antibody and imaged by light microscopy. Note the absence of plaques in 1- to 2-month- old tg (n = 3 mice, 34 sections per mouse were analyzed) compared to 6- to 7-month-old tg mice (n = 3 mice, 34 sections per mouse were analyzed).

mice at both of these ages.

3.3.1 Altered activity of CA1 neurons in plaque-bearing mice

We first imaged spontaneous activity of CA1 neurons in the hippocampus of 6- to 7-months-old transgenic mice that were depositing plaques. As described above, cells were labeled with Fluo-8 by bolus loading and imaged by two-photon microscopy. Fig. 14 illustrates that the pattern of hippocampal activity was markedly altered in transgenic as compared to age-matched wild type mice. In older transgenic mice (in which many plaques had already developed) silent and excessively active neurons were more abundant than in wild type mice. For a detailed analysis, all recorded neurons were classified based on their individual activity rates as "silent" (0 – 0.2 transients/min), "normal" (0.2 - 20 transients/min) or "hyperactive" ($\geq$ 20 transients/min), similar to previous assessment of neurons in cortex [Busche et al. 2008; Grienberger et al. 2012]. The fraction of neurons that were silent was significantly larger in transgenic (11.72 ± 0.65 %, n = 5 mice) as compared to wild type mice (4.76 ± 0.31 %, n = 5 mice, $P < 0.001$, Student´s *t*-test, Fig. 15). In addition, the fraction of hyperactive neurons was significantly larger in transgenic (9.51 ± 1.75 %, n = 5 mice) as compared to wild type mice (2.86 ± 0.63 %, n = 5 mice, $P <$ 0.001, Student´s *t*-test, Fig. 15). We next mapped the distribution of the three types of neurons in relation to the three-dimensionally nearest plaque. Hyperactive neurons were only found in the vicinity of the plaque border (< 60 μm), whereas silent cells and cells with regular frequencies of calcium transients were distributed throughout the hippocampal CA1 region (Fig. 16). Thus, the alterations of hippocampal activity in plaque-laden transgenic mice were qualitatively identical to those previously observed in cortex [Busche et al. 2008; Grienberger et al. 2012].

3.3.2 Early hyperactivity of CA1 neurons in plaque-free mice

To address the question whether alterations of neuronal activity occur also in the absence of plaques, we studied 1- to 2-months old transgenic mice before plaque formation (Fig. 13). Surprisingly, the majority of CA1 neurons in the transgenic mice exhibited markedly elevated

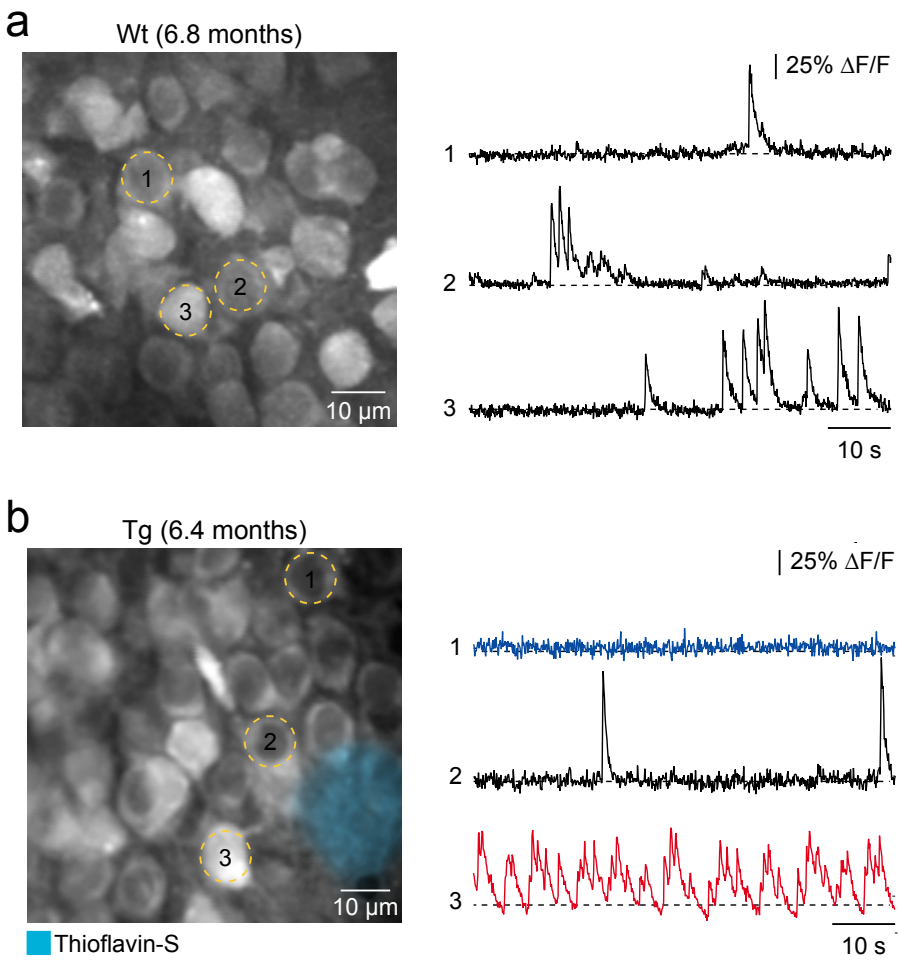

Figure 14: (**a**) Left, CA1 neurons imaged *in vivo* in a wild type (wt) mouse. Right, spontaneous calcium transients of the corresponding neurons marked in left panel. (**b**) Left, CA1 neurons imaged *in vivo* in a transgenic (tg) mouse with thioflavin-S positive plaque (light blue). Right, spontaneous calcium transients of the corresponding neurons marked in left panel. Traces were color-coded to mark neurons that were either silent (blue) or hyperactive (red) during the recording period.

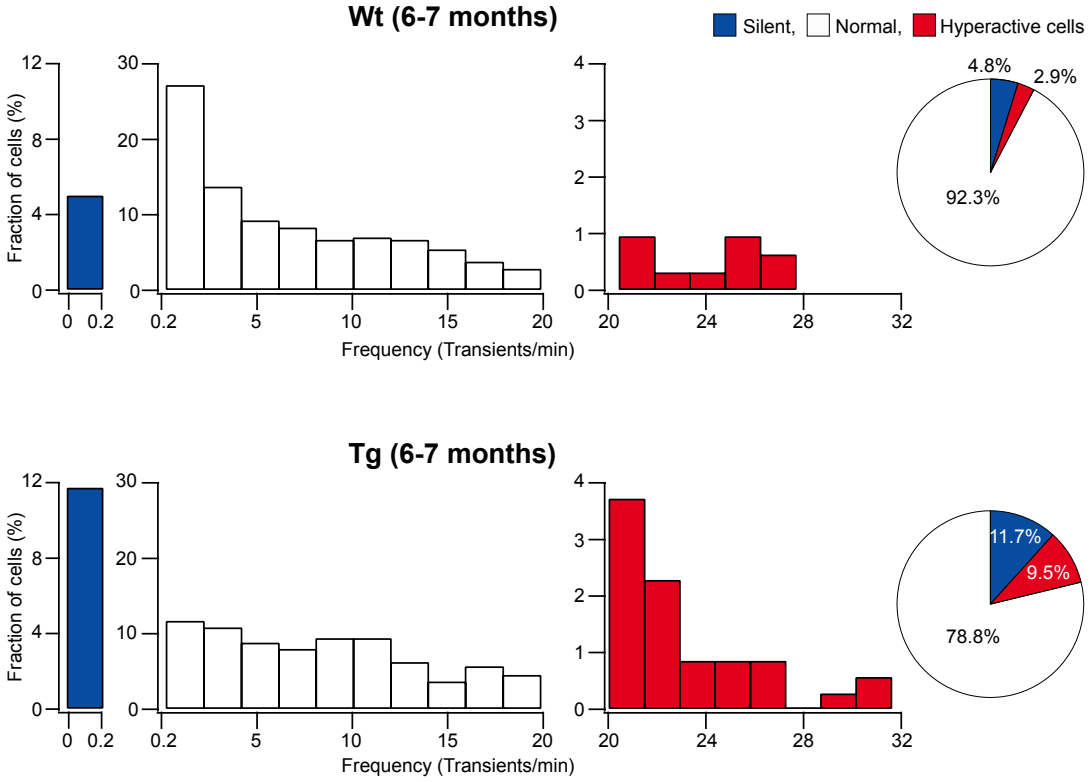

Figure 15: Histograms showing the frequency distributions of calcium transients in wild type (wt, upper, n = 312 cells in 5 mice) and transgenic (tg, lower, n = 349 cells in 5 mice) mice. Note increased fractions of silent and hyperactive neurons in tg mice. Pie charts showing the relative proportions of silent, normal and hyperactive neurons.

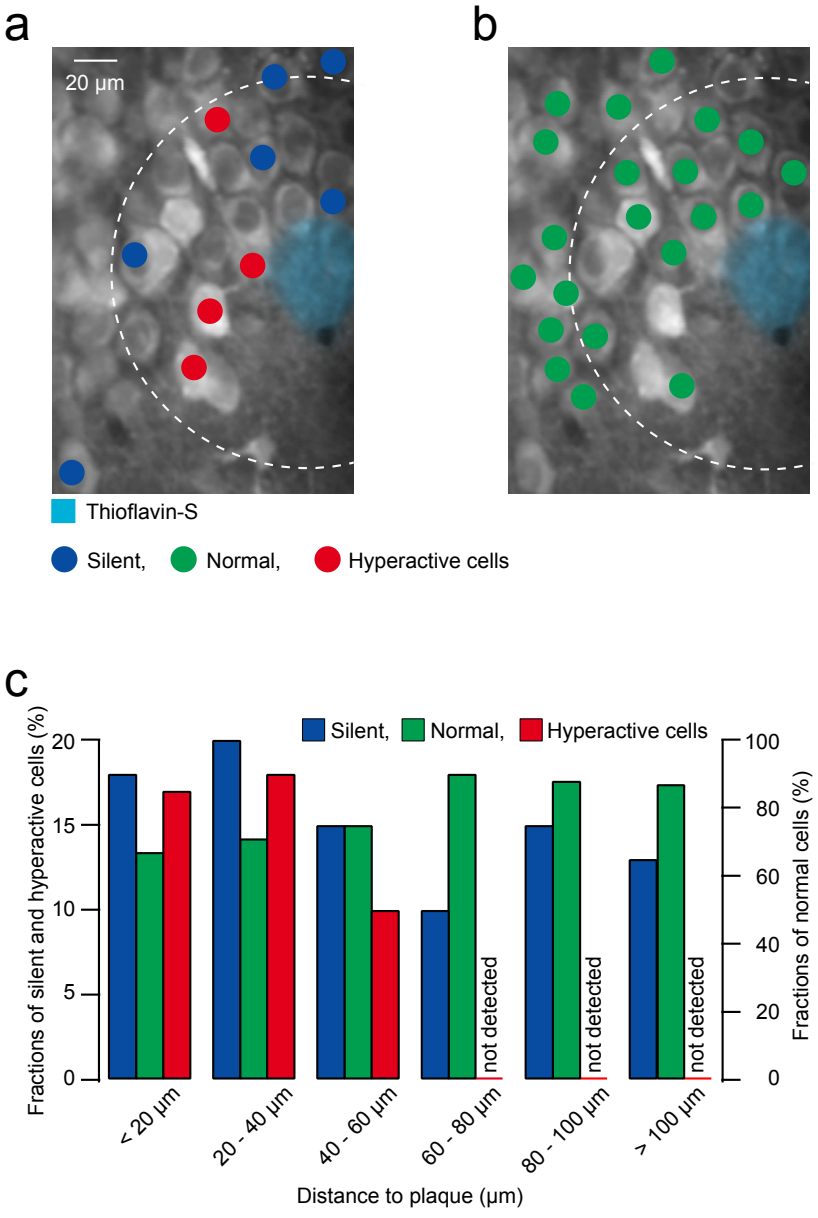

Figure 16: (**a and b**) Distribution of silent (blue) and hyperactive (red) as wells as normal (green) neurons in a 6.4 months old transgenic (tg) mouse with plaques. The broken line circle is centered at the nearest plaque and delineates the area located less than 60 µm from the plaque border. (**c**) Bar graph showing the abundance of silent, normal and hyperactive neurons at different distances from the border of the nearest plaque (n = 301 cells).

rates of spontaneous calcium transients when compared with age-matched wild type mice (Fig. 17). Detailed analyses showed that the frequency distribution of spontaneous calcium transients was generally shifted toward higher values in transgenic as compared to wild type mice (Figs. 19 and 20). This resulted in a strong increase in the median frequency of calcium transients (4.54 transients/min in wild type versus 12.37 transients/min in transgenic mice, $P < 0.001$, Kolmogorov-Smirnov test). As in 6- to 7-months-old transgenic mice, all recorded neurons were classified based on their individual activity rates as "silent" (0 – 0.2 transients/min), "normal" (0.2 - 20 transients/min) or "hyperactive" ($\geq$ 20 transients/min). We found that the fraction of hyperactive neurons was significantly larger in transgenic (25.85 ± 3.59 %, n = 7 mice) as compared to wild type mice (1.85 ± 0.86 %, n = 6 mice, $P < 0.001$, Student´s *t*-test, Fig. 19). Notably, there was a trend towards a smaller proportion of silent cells in transgenic (1.81 ± 0.57 %, n = 7 mice) as compared to wild type mice (5.44 ± 1.47 %, n = 6 mice, $P = 0.057$, Student´s *t*-test, Fig. 19), suggesting an overall increase in excitatory drive in the plaque-free transgenic mice.

To compare hippocampus and cortex more directly at this age, we imaged cortical and hippocampal neuronal activity in individual transgenic animals (Fig. 21). We first recorded spontaneous neuronal activity in layer 2/3 of the cortex of a transgenic mouse (n = 287 cells in seven mice) and found that it was indistinguishable from that in wild type mice (n = 262 cells in 7 mice, $P > 0.05$, Kolmogorov–Smirnov test), consistent with previous findings [Busche et al. 2008]. We then removed a small portion of the neocortex in the same mouse and recorded spontaneous activity of hippocampal neurons. We found an abnormal increase of hippocampal activity in transgenic (n = 731 cells in 5 mice) as compared to wild type mice (n = 817 cells in 6 mice, $P < 0.001$, Kolmogorov–Smirnov test), confirming our previous observation that the function of hippocampal neurons is altered long before that of cortical neurons.

Together, the results indicate that the earliest functional deficits of neurons occur in the hippocampus, progressing with age to the cortex. As a control, we analyzed the frequencies of spontaneous activity in the hippocampus of 1- to 2-months-old and 6- to 7-months-old wild

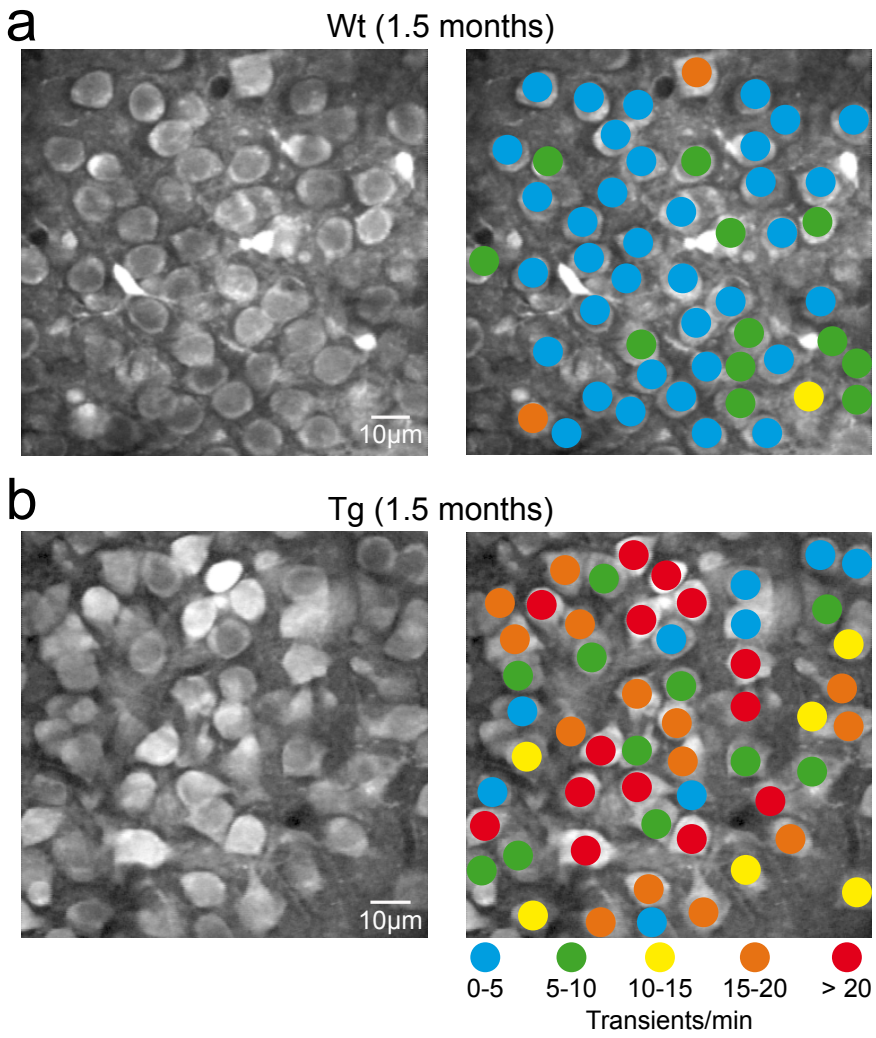

Figure 17: (**a and b**) Left, CA1 neurons imaged *in vivo* in a wild type (wt) and a transgenic (tg) mouse, respectively. Right, activity maps, in which hue is determined by the frequency of spontaneous calcium transients, overlaid with the anatomical image in left panel.

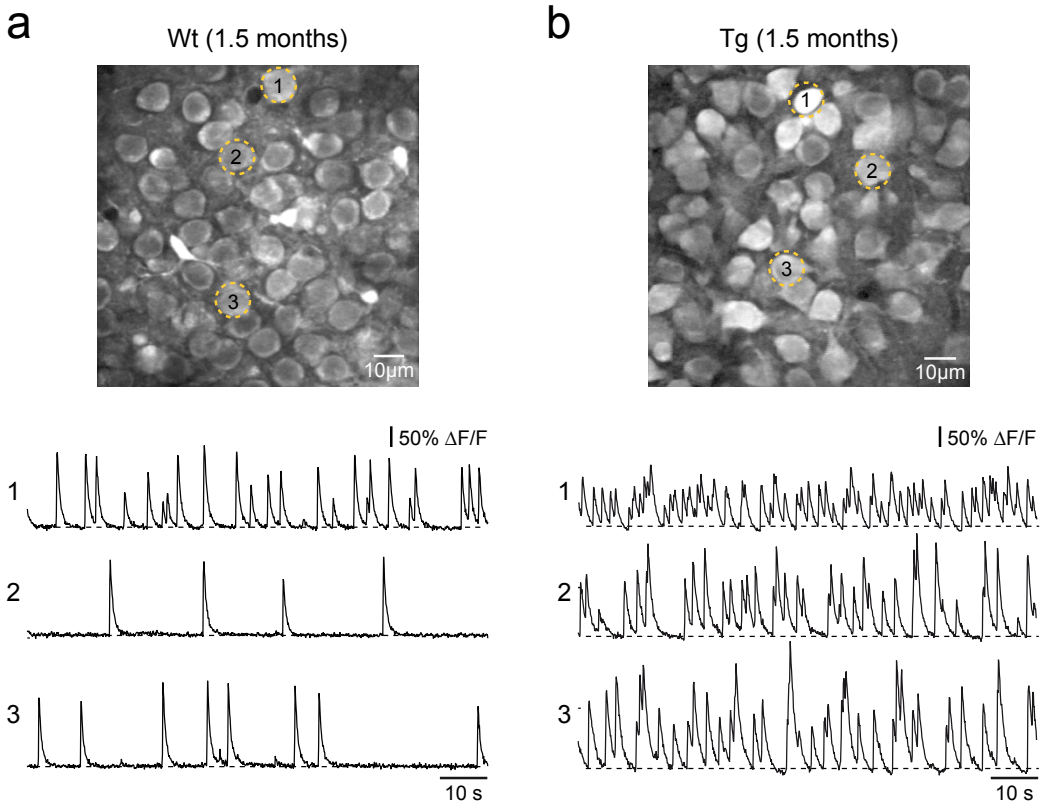

Figure 18: (**a and b**) Upper, CA1 neurons imaged *in vivo* in a wild type (wt) and a transgenic (tg) mouse, respectively. Lower, spontaneous calcium transients of the corresponding neurons marked above.

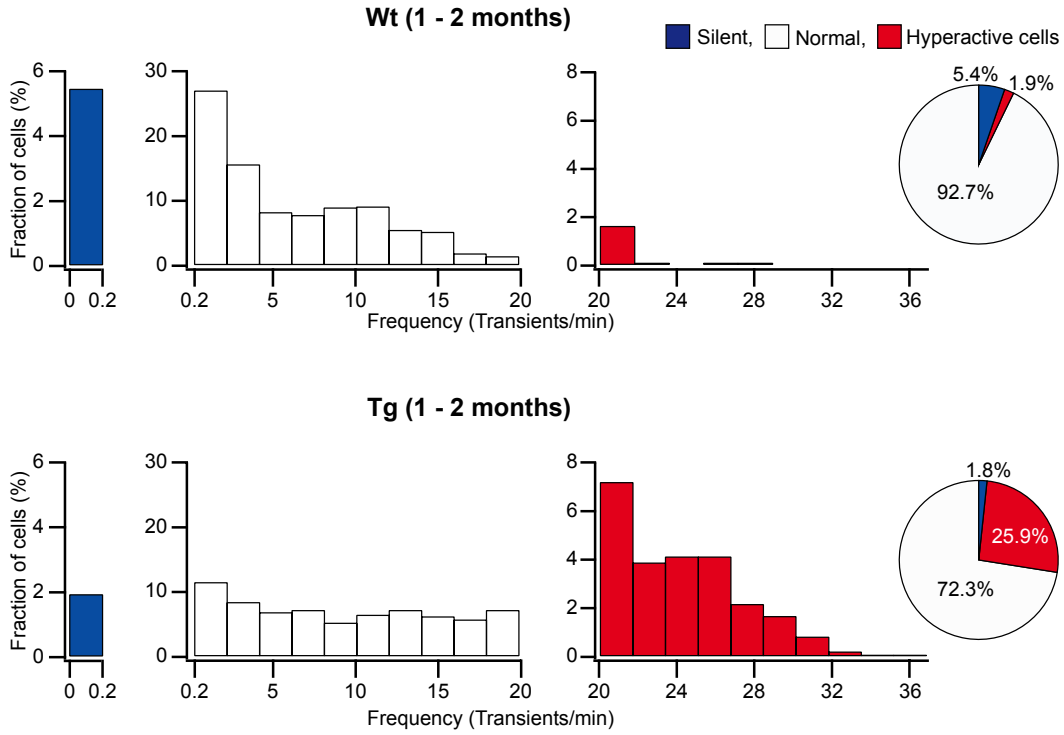

Figure 19: The frequency distribution of spontaneous calcium transients was shifted toward higher frequencies in transgenic (tg, lower, n = 818 cells in 7 mice) as compared to wild type mice (wt, upper, n = 693 cells in 6 mice). Pie charts showing the relative proportions of silent, normal and hyperactive neurons.

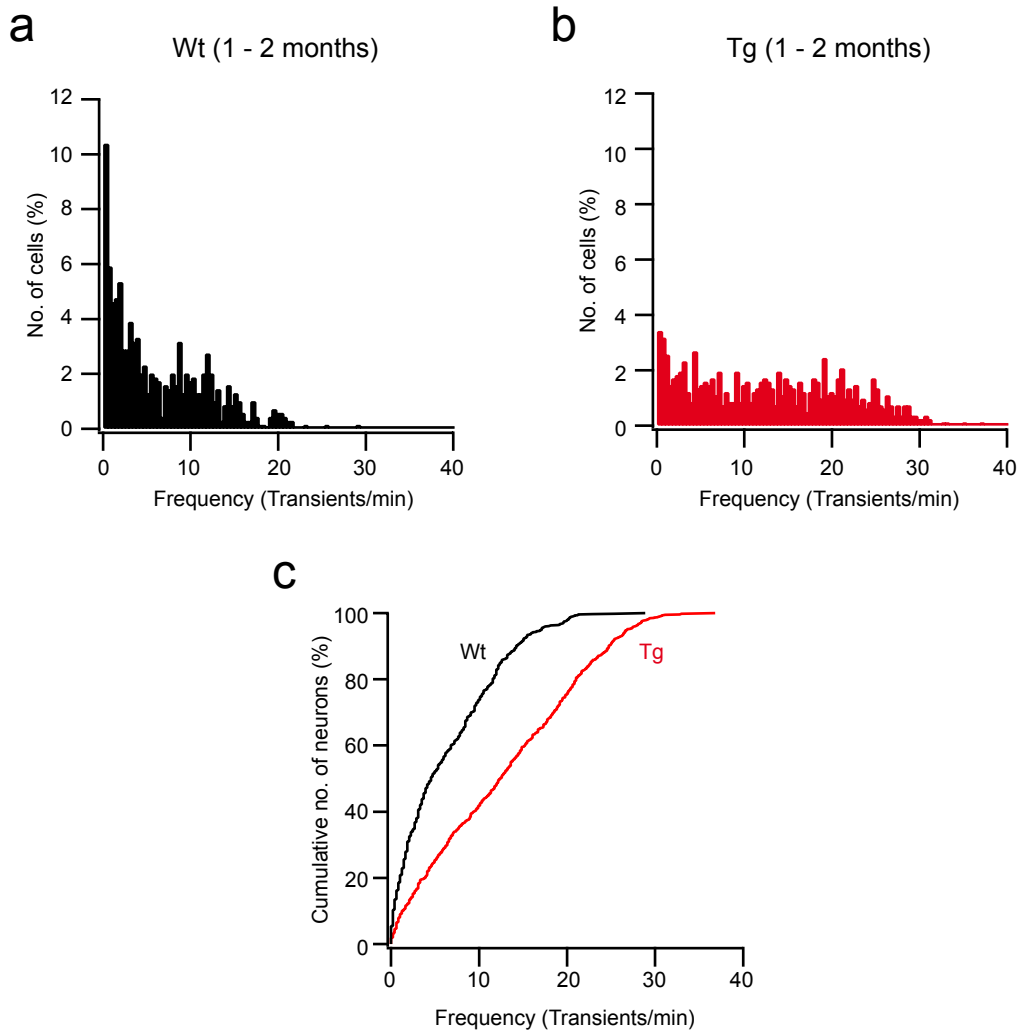

Figure 20: (**a and b**) Histograms showing the frequency distributions of spontaneous calcium transients in wild type (wt, n = 693 cells in 6 mice) and transgenic mice (tg, n = 818 cells in 7 mice). (**c**) Cumulative distribution of spontaneous calcium transients in wt (n = 693 cells) was significantly different from tg mice (n = 818 cells, $P < 0.001$, Kolmogorov-Smirnov test).

type mice (Fig. 22). Fig. 23 shows that the rates of spontaneous calcium transients were similar in younger and older mice. Thus, the results clearly indicate that, in contrast to transgenic mice, activity patterns of hippocampal neurons remain unaltered with age in wild type mice.

While we had shown that calcium transients in hippocampal neurons of wild type mice were evoked through AP firing (Fig. 10), the mechanisms underlying calcium signaling of hippocampal neurons in transgenic mice have remained unclear. This issue is particularly important, because several lines of evidence suggest that the intracellular calcium homeostasis may be disturbed in AD transgenic mice [Green and LaFerla 2008; Bezprozvanny and Mattson 2008; Kuchibhotla et al. 2008; Goussakov et al. 2010]. For example, the increased frequency of calcium transients may be caused by spontaneous calcium release from overfilled intracellular calcium stores. Indeed, the G384A mutation was shown to abolish the PS-mediated calcium leak from intracellular calcium stores [Ito et al. 1994; Nelson et al. 2007; Ho and Shen 2011]. The calcium leak is important to maintain the physiological filling state of the stores. We found that the sodium channel blocker tetrodotoxin (TTX) completely and reversibly blocked all calcium transients in hyperactive neurons (n = 3 mice), indicating that they were exclusively triggered by AP firing. Furthermore, we applied the ionotropic glutamate receptor blockers 6-cyano-7-nitroquinoxaline-2,3-dione (CNQX) and D,L-2-amino-5-phosphonovaleric acid (APV) and found that the spontaneous calcium transients were completely abolished (n = 3 mice, Fig. 24), indicating that calcium transients were exclusively evoked by synaptic activity. Finally, we combined cell-attached recordings with calcium imaging and demonstrated that calcium transients were exclusively triggered by APs (Fig. 25), consistent with the results from wild type mice (Fig. 10). These findings establish that calcium transients in hippocampal neurons of AD transgenic mice reflect exclusively synaptically-mediated APs but not calcium release signals from intracellular stores. In the next step, we examined what causes the overexcitation in plaque-free transgenic mice.

3.3.3 Rescue of neuronal hyperactivity by acute γ-secretase inhibition

The finding that hyperactivity of hippocampal neurons occurred independent of plaque formation has indicated an important role of soluble Aß. Indeed, soluble Aß levels were already elevated in younger transgenic mice (Fig. 26), consistent with previous reports by others [Hsiao et al. 1996; Mucke et al. 2000]. To test this hypothesis more directly, we treated 1- to 2-month-old transgenic mice with the γ-secretase inhibitor LY-411575. This compound has been shown to rapidly block central nervous system Aß production [Cirrito et al. 2003]. After oral administration LY-411575 crosses the blood-brain barrier and, by inhibiting γ-secretase activity within minutes, it reduces brain Aß levels [Lanz et al. 2004; Abramowski et al. 2008]. We found that administration of a single oral dose of 10 mg/kg LY-411575 significantly reduced hippocampal levels of aequously soluble (TBS-soluble, traditionally viewed as the soluble Aß fraction) and detergent-soluble (SDS-soluble, traditionally viewed as aggregated and membrane-associated Aß) Aß-40 and Aß-42 as compared to vehicle ($P < 0.001$ for Aß-40 and $P < 0.05$ for Aß-42, Student´s *t*-test, Fig. 26) in transgenic mice. Aß-40 and Aß-42 reached a low point about 4 to 6 hours after treatment, consistent with previous findings [Abramowski et al. 2008]. We next examined the effects of γ-secretase inhibition on spontaneous neuronal activity at 4 to 6 hours after oral administration, when soluble Aß levels were lowest. We found that activity levels of CA1 neurons in LY-411575-treated transgenic mice were almost completely restored to the control levels recorded in wild type mice (Fig. 27). The fraction of hyperactive neurons in LY-411575-treated transgenic mice was similar to that in the control wild type mice ($P > 0.05$, Student´s *t*-test, Figs. 28 and 29). The fraction of silent neurons was also similar in LY-411575-treated transgenic (5.29 ± 2.31 %, n = 5 mice) and wild type mice (5.44 ± 1.47 %, n = 6 mice, $P > 0.05$, Student´s *t*-test, Fig. 29). Importantly, LY-511575 treatment had no effect on hippocampal activity levels in wild type mice ($P > 0.05$, Kolmogorov-Smirnov test, Fig. 28).

Together, these results show that acute γ-secretase inhibition not only reduces soluble Aß levels but also effectively restores neuronal function in the hippocampus of transgenic mice. This suggests that soluble Aß is causally related to abnormal neuronal hyperactivity.

3.3.4 Soluble Aß induces neuronal hyperactivity

The soluble fraction of Aß includes monomers and oligomers that vary in size and shape from dimers to multimers and protofibrils [Haass 2010]. Converging evidence suggest that oligomers, rather than monomers, are the primary bioactive form of Aß in AD and that dimers are not only the most abundant form of oligomers in the human brain but also the principal mediators of neurotoxicity in AD [Shankar et al. 2008; Hu et al. 2008; Li et al. 2009, 2010; Mc Donald et al. 2010]. Therefore, we used previously characterized crosslinked Aß-40 dimers [Shankar et al. 2008; Hu et al. 2008; O'Nuallain et al. 2010; Jin et al. 2011] to test whether they can directly alter neuronal activity. The dimers were locally applied to the cells of interest in the hippocampal CA1 region by inserting a pipette through the craniotomy and releasing the dimer solution by pressure-ejection. The local application allowed a better control of drug effect in the treated area, the effect being restricted only to the cells situated in the close vicinity of the application pipette. We applied nanomolar concentrations of crosslinked dimers to CA1 neurons in wild type mice while monitoring their ongoing spontaneous activity. Figure 30 shows an experiment demonstrating the rapid excitatory effect of dimers on CA1 neurons *in vivo*. The dimers immediately elevated the rates of calcium transients in CA1 neurons (Fig. 31) indicating increased AP firing. As a control, heat-denatured dimers (dimers were boiled for 15 min, cooled to room temperature and then locally applied) did not alter neuronal activity (n = 158 cells in 3 mice, Fig. 31). In addition, the local application of the peptide vehicle (0.001 % DMSO in ACSF) alone did not alter neuronal activity (n = 60 neurons in 2 mice).

These results support and extend previous *in vitro* observations that soluble Aß can acutely induce inward currents in hippocampal neurons leading to increased AP firing and intracellular calcium elevations [Brorson et al. 1995; Snyder et al. 2005; Sanchez-Mejia et al. 2008; Alberdi et al. 2010]. They provide further evidence that soluble Aß directly induces neuronal hyperactivity, which underlies early hippocampal dysfunction in transgenic mice. We did not test different types of oligomeric species, thus we cannot exclude the possibility that oligomers other than dimers have similar or different effects on neurons.

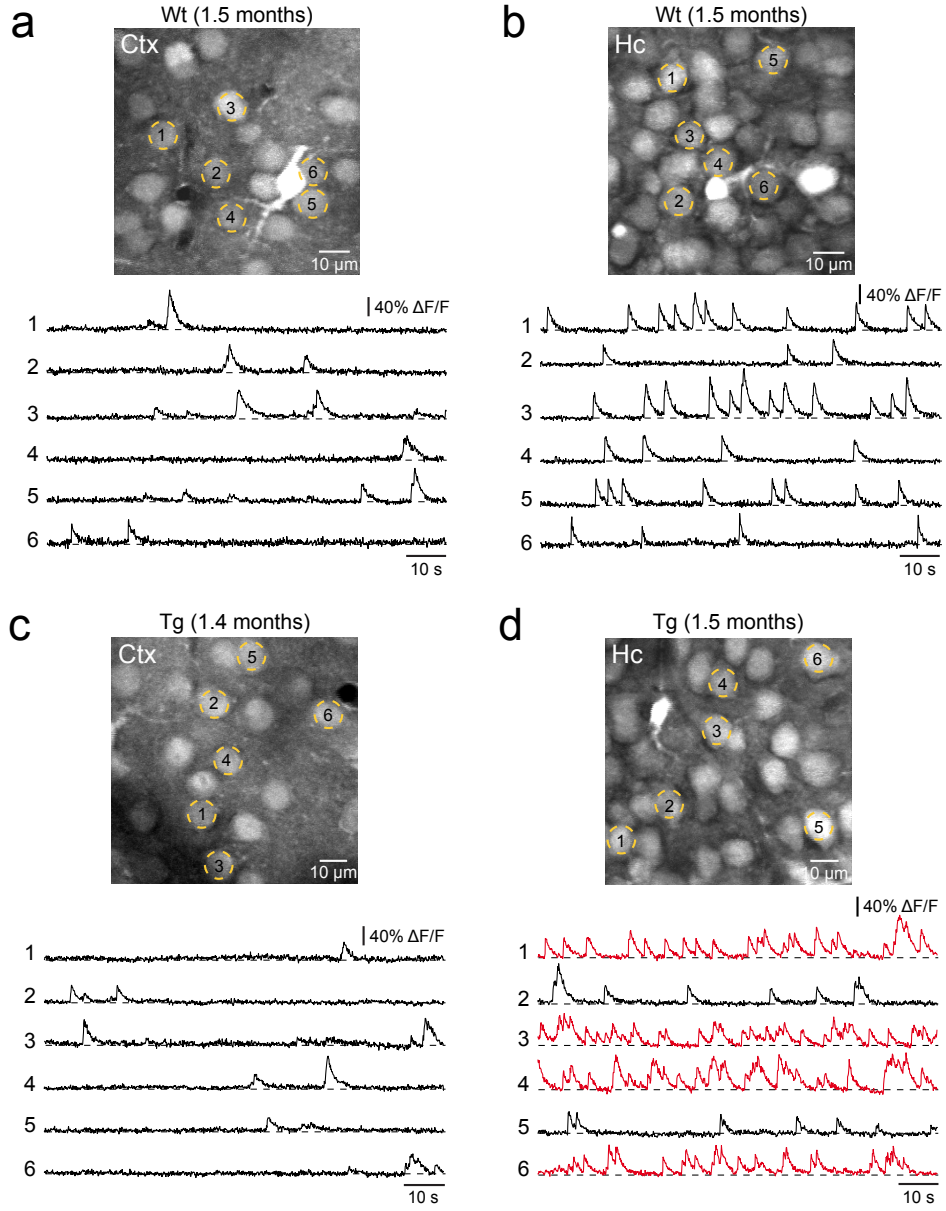

Figure 21: (**a and c**) Upper, cortical layer 2/3 neurons imaged *in vivo* in a wild type (wt) and a transgenic (tg) mouse, respectively. Lower, spontaneous calcium transients of the corresponding neurons marked in upper panel. (**b and d**) Upper, hippocampal CA1 neurons imaged *in vivo* in a wt and a tg mouse, respectively. Lower, spontaneous calcium transients of the corresponding neurons marked in upper panel. Traces were color-coded red to mark neurons that were hyperactive during the recording period. For a better comparison, the calcium indicator Oregon Green BAPTA-1 AM was used both for cortical and hippocampal recordings.

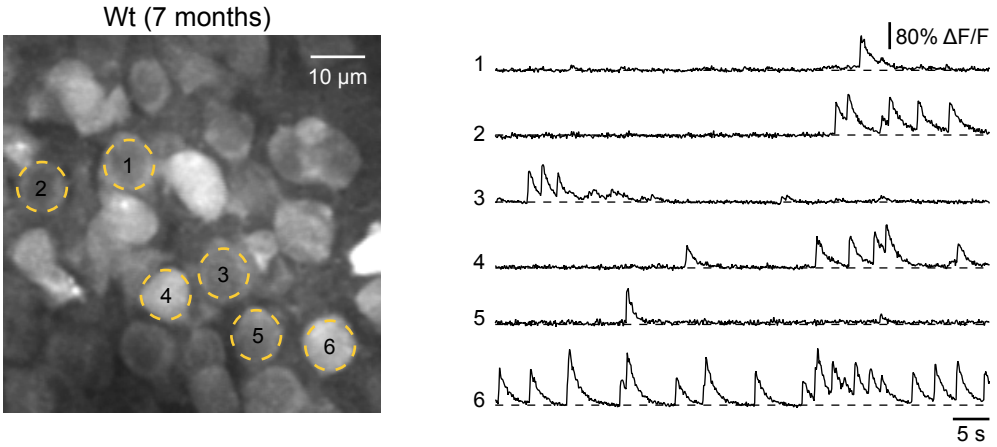

Figure 22: Left, CA1 neurons imaged *in vivo* in an older wild type (wt) mouse. Right, spontaneous calcium transients of the corresponding neurons marked in left panel.

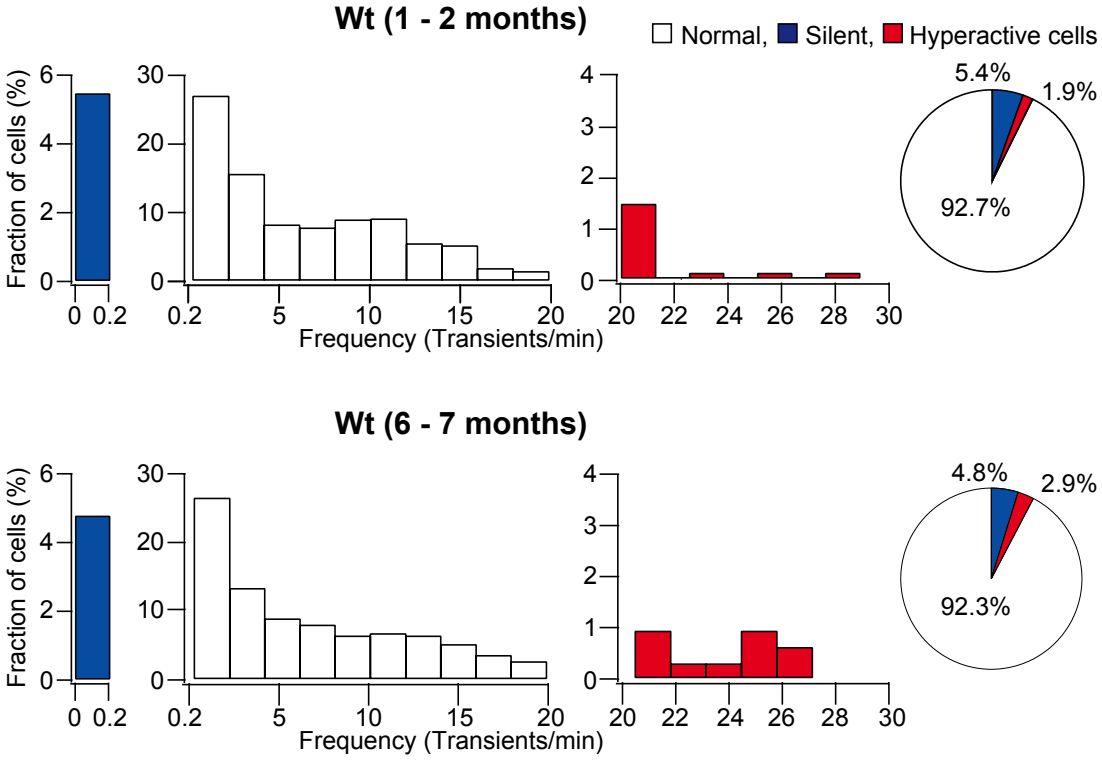

Figure 23: Histograms showing the frequency distribution of spontaneous calcium transients in 1- to 2-months-old (upper, n = 693 cells in 6 mice) and in 6- to 7-months-old (bottom, n = 312 cells in 5 mice) wild type (wt) mice. Pie charts showing the relative proportions of silent, normal and hyperactive neurons.

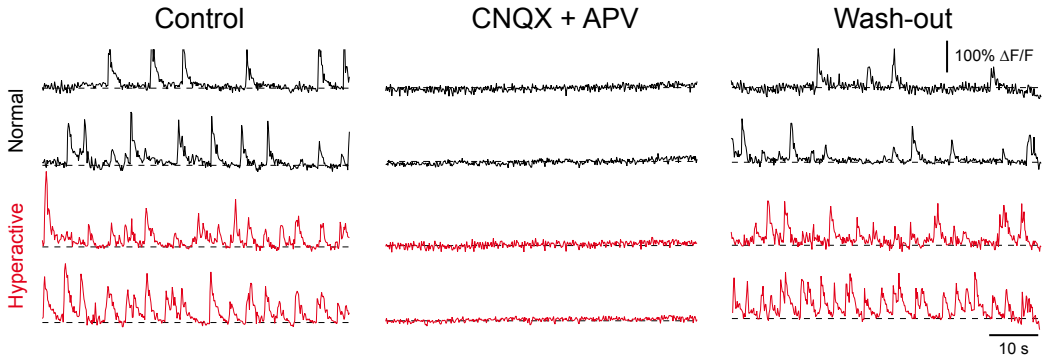

Figure 24: Spontaneous calcium transients in normal (black traces) and hyperactive (red traces) CA1 neurons of a transgenic mouse before, during, and after local application of CNQX and APV.

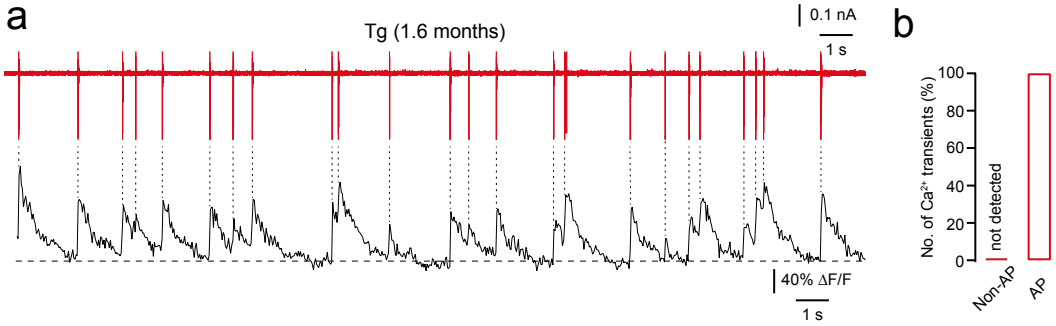

Figure 25: (**a**) Simultaneous *in vivo* recordings of spontaneous calcium transients (black trace) and underlying action potential (AP) firing (red trace, number of APs indicated) in cell-attached configuration from a CA1 neuron in a transgenic (tg) mouse. (**b**) Number of spontaneous calcium transients triggered (AP) and not triggered (Non-AP) by action potential firing in tg mice (n = 13 cells in 3 mice).

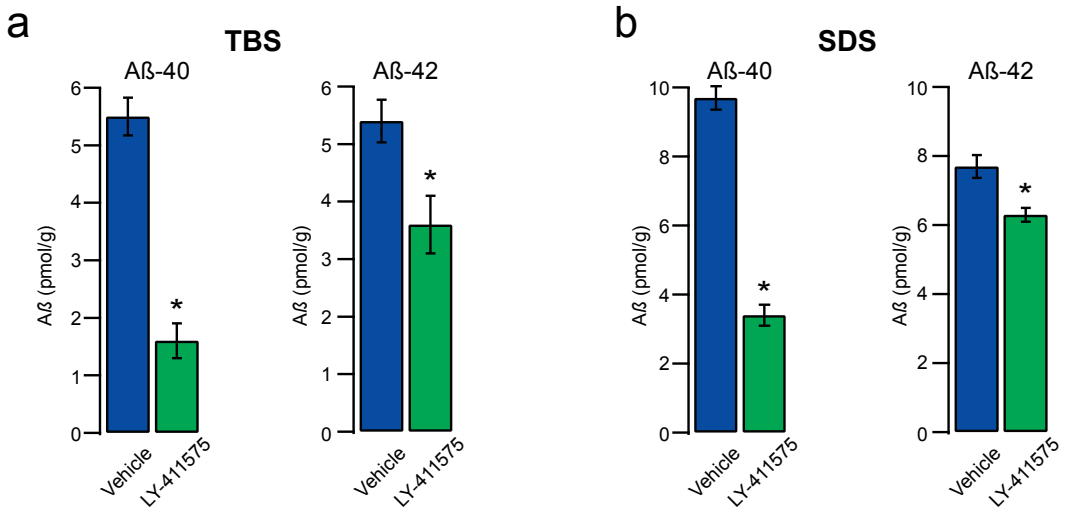

Figure 26: (**a and b**) Acute LY-411575 treatment significantly reduced TBS- and SDS-soluble Aß-40 and Aß-42 hippocampal levels in transgenic mice (n = 4-5 mice/group, $P < 0.001$ for Aß-40 and $P < 0.05$ for Aß-42, Student´s *t*-test). All error bars denote s.e.m.

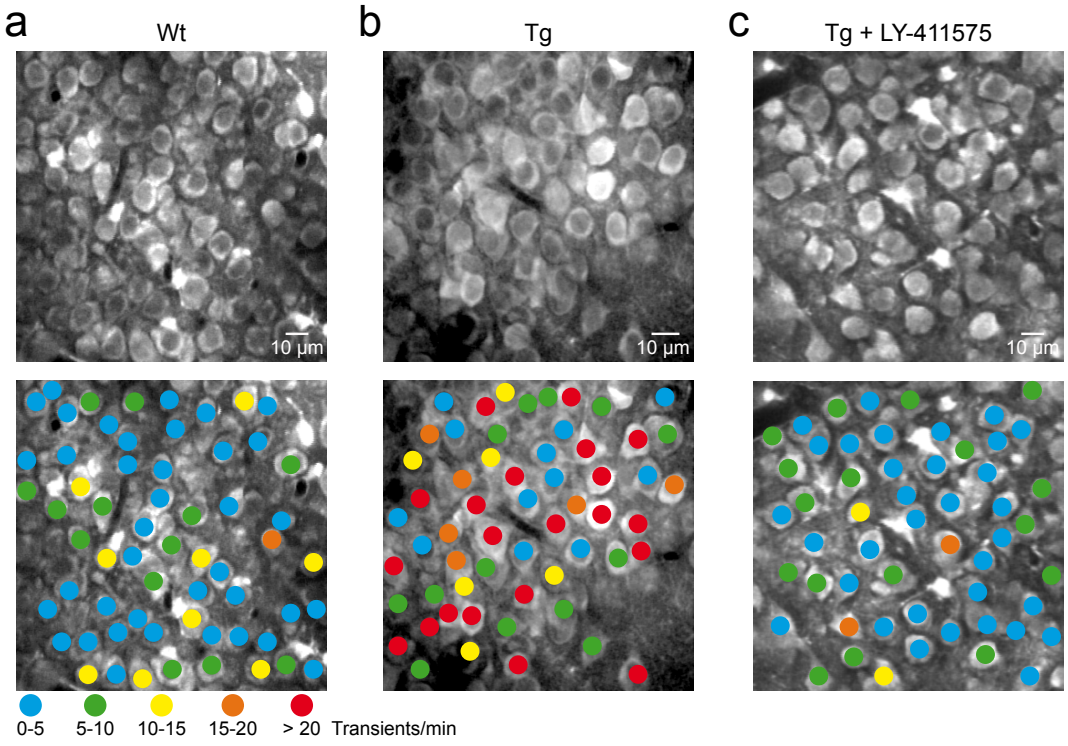

Figure 27: (**a - c**) Upper, CA1 neurons imaged *in vivo* in a wild type (wt), transgenic (tg) and LY-411575 treated tg mouse, respectively. Lower, activity maps in which hue is determined by the frequency of spontaneous calcium transients, overlaid with the anatomical image in upper panel.

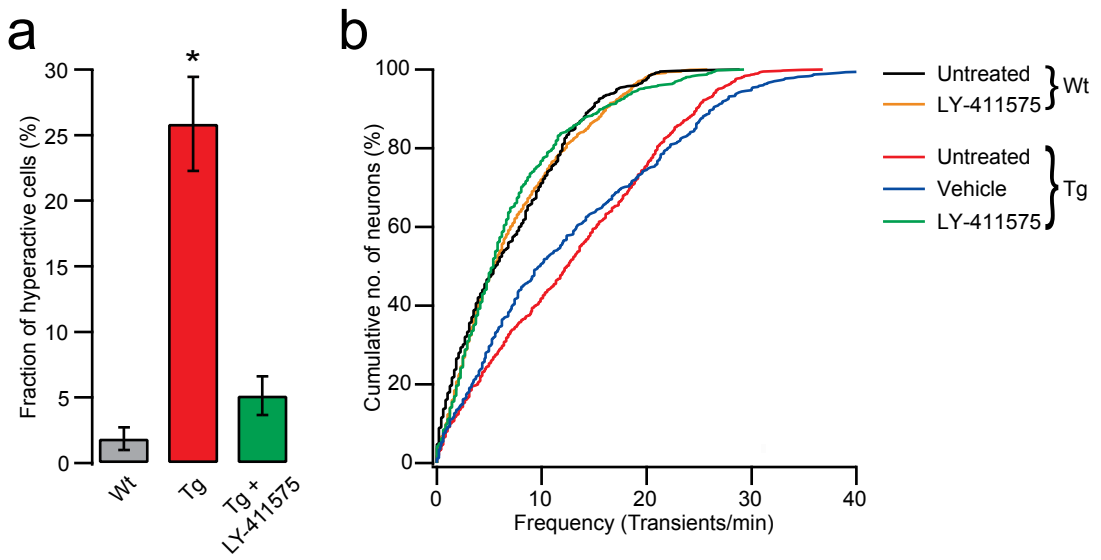

Figure 28: (**a**) The fraction of hyperactive neurons was significantly smaller in LY-411575 treated transgenic (tg) (5.13 ± 1.47 %, n = 5 mice) than in untreated tg mice (25.85 ± 3.59 %, n = 7 mice; $P < 0.001$, Student´s *t*-test) and not significantly different from untreated wild type (wt) mice (1.85 ± 0.86 %, n = 6 mice; $P > 0.05$, Student´s *t*-test). (**b**) Cumulative distribution of spontaneous calcium transients in LY-411575 treated tg mice (n = 709 cells) was not significantly different from untreated wt (n = 693 cells) and LY-411575 treated wt controls (n = 841 cells, $P > 0.05$, Kolmogorov-Smirnov test), but it was significantly different from vehicle-treated tg (n = 484 cells) and untreated tg mice (n = 818 cells, $P < 0.001$, Kolmogorov-Smirnov test). All error bars denote s.e.m.

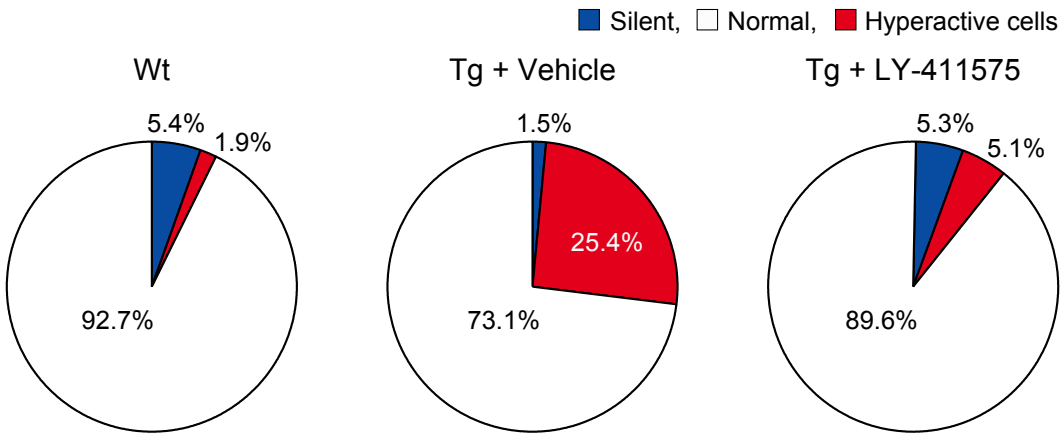

Figure 29: Pie charts showing the relative proportions of silent, normal and hyperactive neurons in wild type (left, wt), vehicle treated transgenic (middle) and LY-411575 treated tg mice (right).

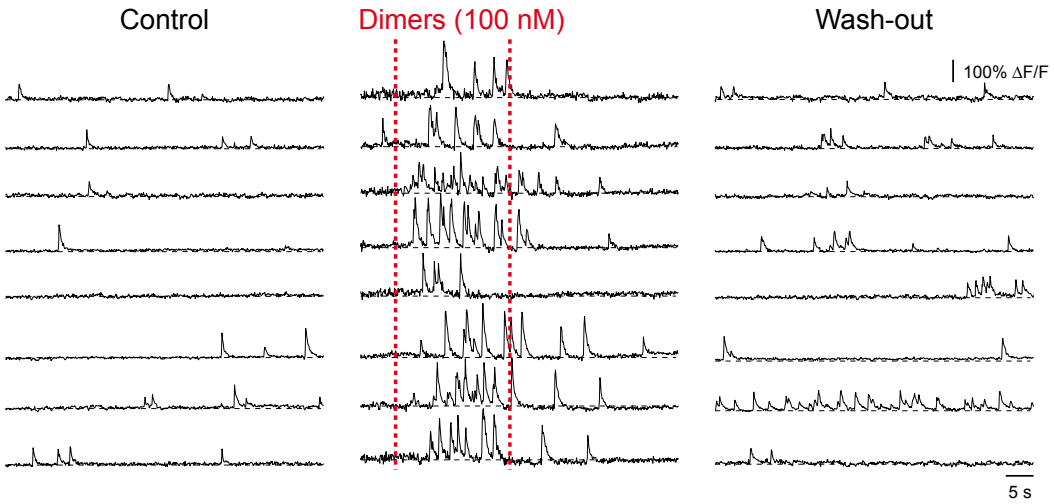

Figure 30: Calcium transients in CA1 neurons of a wild type mouse before, during and after local application of synthetic Aß-40 dimer solution (30 s, 100 nM in the application pipette).

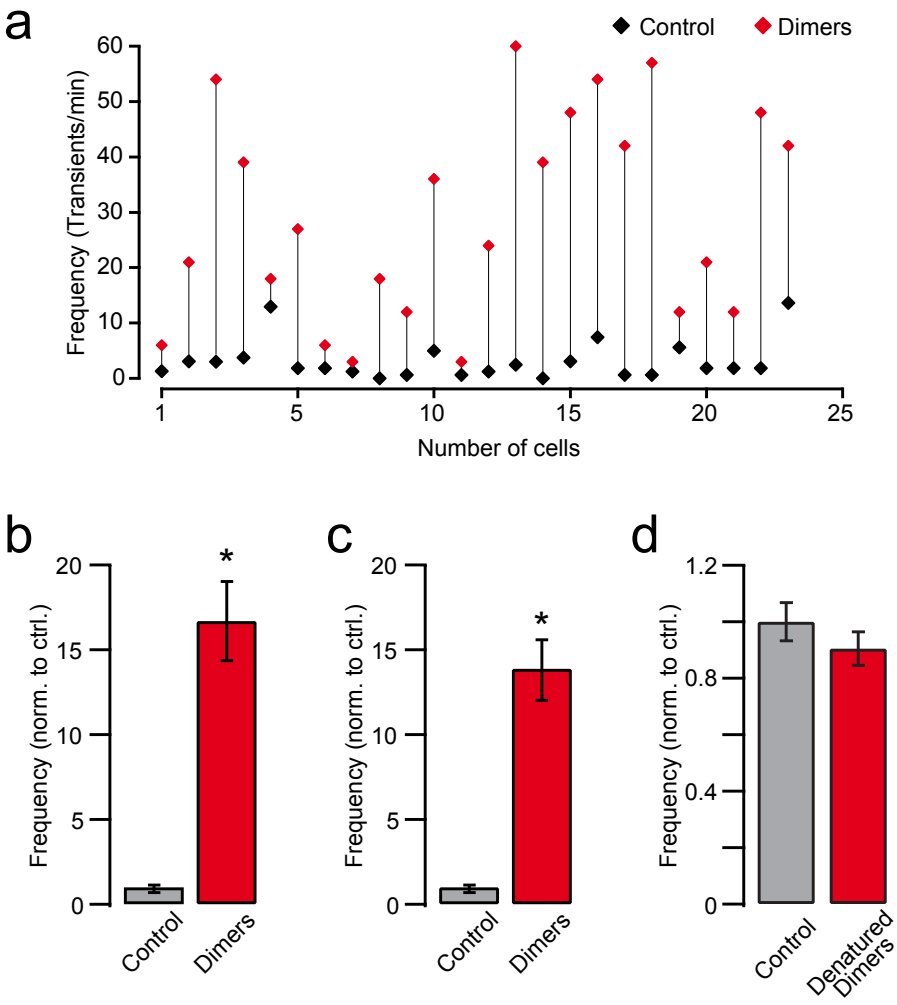

Figure 31: (**a**) Rates of calcium transients in all recorded neurons from experiment in (Figure 30) before (black) and during (red) dimer application. (**b**) Summary graph from experiment in (a) showing the effect of dimers on the frequency of calcium transients (normalized to control, n = 24 cells, $P < 0.001$, Student´s *t*-test). (**c**) Summary graph from all experiments illustrating the effect of dimers on the frequency of calcium transients (normalized to control, n = 83 cells in 3 mice, $P < 0.001$, Student´s *t*-test). (**d**) Summary graph showing that heat-denatured dimers had no significant effect on the frequency of calcium transients (normalized to control, n = 158 cells in 3 mice, $P > 0.05$, Student´s *t*-test). All error bars denote s.e.m.

4 Discussion

In this thesis, we have advanced two-photon microscopy towards high-resolution imaging of hippocampal neuronal activity patterns *in vivo* to study of hippocampal network funtion in AD transgenic mice. We developed a surgical preparation that permits visualization of neuronal activity in the CA1 region of the hippocampus in living mice using two-photon calcium imaging. In addition, the preparation allows electrode and chemical access to the hippocampus, thereby offering the opportunity to directly investigate the mechanisms that underlie hippocampal function in the healthy and the diseased brain.

We demonstrated that neuronal activity in the hippocampus was significantly altered in AD transgenic mice that were depositing plaques as compared to age-matched wild type mice. Specifically, the fractions of neurons that were silent and hyperactive increased significantly in the transgenic mice, and hyperactive neurons were exclusively found near plaques, similar to previous findings from cortex [Busche et al. 2008; Grienberger et al. 2012]. Surprisingly, we showed that there was a marked increase in hippocampal activity with an excess of hyperactive neurons already before the transgenic mice began to deposit plaques. We provided direct experimental evidence that this abnormal hyperactivity was causally related to the action of soluble Aß. First, we demonstrated that treatment with a γ-secretase inhibitor rapidly reduced soluble Aß levels and completely reversed neuronal hyperactivity. Second, we showed that local application of soluble Aß induced neuronal hyperactivity in wild type mice.

In conclusion, we developed a novel approach to use two-photon calcium imaging for studying the function of hippocampal neurons and networks *in vivo*. We revealed, for the first time, that neurons in the hippocampus of AD transgenic mice are abnormally hyperactive already in very

early disease stages and that this hyperactivity is directly promoted by soluble Aß.

4.1 *In vivo* imaging of hippocampal neurons

Most of our knowledge about hippocampal neurons is derived from experiments using single- and multi-unit electrical recording techniques. For instance, extracellular microelectrodes have been used to study neuronal responses in the hippocampus of awake freely moving rats [O'Keefe and Dostrovsky 1971; Henze et al. 2000; Andersen 2007], which resulted in the discovery of place cells. Today, four-channel recording electrodes (tetrodes) are most commonly used to record activity in ensembles of hippocampal place cells [Gray et al. 1995; Jog et al. 2002]. Individual tetrodes can resolve the activity of about five single hippocampal neurons with very high temporal resolution [Wilson and McNaughton 1993; Buzsáki 2004]. However, those recordings are limited by a low spatial resolution (> 100 µm) and a sparse sampling within the recording area. Furthermore, they may not identify silent neurons, which can make up a considerable fraction of the total neuronal population in AD transgenic mice [Busche et al. 2008; Grienberger et al. 2012]. Thus, all electrical recordings are so far unable to resolve the precise spatiotemporal dynamics of a population of nearby neurons *in vivo*.

Two-photon imaging offers several key advantages over electrical recordings. First, imaging permits to correlate the activity status of neurons with their precise spatial location. This advantage is of prime importance in the study of AD, because previous work has shown that alterations of neuronal activity can depend on the distance to plaques [Busche et al. 2008; Kuchibhotla et al. 2008]. Second, imaging allows to detect silent neurons, which have been found in increased numbers in AD transgenic mice [Busche et al. 2008; Grienberger et al. 2012]. Third, imaging allows to identify and record same neurons over longer periods of time [Mank et al. 2008; Tian et al. 2009; Andermann et al. 2010; Dombeck et al. 2010]. Fourth, imaging allows to investigate the function of subcellular structures such as signal transduction and structural plasticity [Dreosti et al. 2009; Shigetomi et al. 2010]. Those last two points require the use of genetically encoded indicators and were not the focus of this thesis.

In our work, we combined two-photon microscopy with bolus loading of small-molecule calcium indicators. Yet, in a recent study, the genetically encoded calcium indicator GCaMP3 was used together with two-photon microscopy to study the activity of hippocampal place cells in head-fixed mice navigating in a virtual environment [Dombeck et al. 2010]. The results of this study were largely consistent with a number of known properties of place fields, including the directionality in linear environments, the size of the fields relative to the environment, the proportion of cells that had a place field, and the general lack of a topographic organization of place fields. The major disadvantage of using GCaMP3 was that, in contrast to Fluo-8 that was used in this thesis, the detection of single APs was not achieved.

To image activity of CA1 hippocampal neurons *in vivo*, it is necessary to unilaterally remove parts of the overlying neocortex. This raises the concern that the hippocampal network may be disrupted by direct trauma to the hippocampus or by altering inputs to the hippocampus through the cortical removal. However, the ventral part of the neocortex is anatomically separated from the dorsal hippocampus by a sheet of myelinated fibers [Paxinos and Franklin 2001; Andersen 2007], so that the neocortex can be easily peeled away without touching or damaging the surface of the hippocampus. The removed cortical parts, including parts of parietal and visual cortices, do not provide strong direct projections to the hippocampus [Andersen 2007; Dombeck et al. 2010]. As described above, it was shown in rodents that there are massive commissural projections within the dentate gyrus, hippocampus and enthorinal cortex [Amaral et al. 1984; Demeter et al. 1985]. The functional implication of this is that each hippocampal region is not entirely dependent on the preceding input. This is for example consistent with electrophysiological findings demonstrating that CA1 fields are normal after pharmacological inactivation of the dentate gyrus [Andersen 2007]. Furthermore, recent work showed that the properties of CA1 place cells measured electrophysiologically and optically after cortical removal were similar to the same properties measured with electrophysiology in mice with intact cortex [Dombeck et al. 2010]. Also, in the same study no difference was found in the performance of a spatial behavior task before and after cortical removal. In another recent mouse

study, even bilateral cortical aspiration did not alter local field potentials in the hippocampus or cognitive function in the Morris water maze and contextual fear conditioning [Sakaguchi et al. 2012]. It is still possible that AD transgenic mice are more sensitive towards the cortical removal than wild type mice. However, in our work, alterations of neuronal activity were prominent already in very young transgenic mice without plaques or any other pathological lesions that can influence connectivity between brain areas. Moreover, we showed that a single dose of γ-secretase inhibitor acutely restores neuronal function.

In principle, our method can be used to address a wide range of questions regarding the pathogenic effects of AD on hippocampal function and it also opens new avenues for the investigation of other brain diseases that affect the hippocampus and deeper brain areas, such as temporal lobe epilepsy, depression or schizophrenia.

4.2 Neuronal hyperactivity

Our work demonstrates that neuronal hyperactivity in the hippocampus is an early pathophysiological feature in AD transgenic mice. It is interesting in this regard that humans with prodromal AD exhibited hippocampal hyperactivation during an associative memory task, as measured by fMRI [Dickerson et al. 2005]. Thus, hippocampal hyperactivity may play an important role not only in AD transgenic mice but also in humans with sporadic AD. It is likely that the alterations of hippocampal activity in transgenic mice represent the neuronal substrate for the changes in fMRI signal levels in humans, because recent work has provided strong evidence for a direct relationship between neuronal AP firing and fMRI responses [Lee et al. 2010]. However, it has been debated with respect to the neuroimaging studies in humans whether the abnormal increase in activity is compensatory or represents by itself a pathogenic mechanism. Our work provides direct evidence that neuronal hyperactivity is caused by soluble Aß indicating that hyperactivity is per se related to the pathophysiological process of AD. The downstream cellular targets that are involved in Aß-induced neuronal hyperactivity are not entirely clear yet, but may involve elevated levels of synaptic glutamate due to reductions of synaptic glutamate uptake, as

previously shown in hippocampal slices treated with Aß dimers [Li et al. 2009, 2010].

What may be the functional consequences of neuronal hyperactivity? First, hyperactivity may contribute to calcium overload in neurons [Kuchibhotla et al. 2008]. Through the activity-dependent elevation in intracellular calcium concentration and for example an associated activation of caspase-3 [D'Amelio et al. 2011], combined with a changed ratio of inhibition vs. excitation [Busche et al. 2008], it may be causally related to neuronal silencing. Also, calcium overload may result in calcineurin activation [Kuchibhotla et al. 2008], which may trigger dendritic structural degeneration and neuritic beading [Zeng et al. 2007]. Indeed, our work directly demonstrated that neuronal silencing occurs during later disease stages. Furthermore, humans in advanced stages of AD showed hippocampal hypoactivation compared to controls or humans with prodromal AD [O'Brien et al. 2010]. A second important consequence may be that hyperactive neurons may increase the risk for epileptiform activity. In line with this, long-term video-EEG monitoring in APP transgenic mice revealed spontaneous epileptiform activity in hippocampus and cortex [Palop et al. 2007; Minkeviciene et al. 2009]. Interestingly, some of the epileptiform discharges within hippocampal networks remained focal, with minimal spread to the cortex. AD patients are also known to have an increased incidence of epileptic seizures [Palop and Mucke 2009]. Third, several lines of evidence indicate that neuronal activity increases Aß levels in the interstitial fluid of the brain, which may lead to enhanced plaque formation [Kamenetz et al. 2003; Cirrito et al. 2005; Bero et al. 2011]. Increased Aß production is mediated, at least in part, by clathrin-dependent endocytosis of surface APP at presynaptic terminals, endosomal proteolytic cleavage of APP, and Aß release at synaptic terminals [Cirrito et al. 2005, 2008]. The activity–dependent regulation of Aß secretion has been observed during pathological events such as epileptiform activity induced by electrical stimulation [Nitsch et al. 1993], as well as during normal physiological processes, such as the sleep–wake cycle [Kang et al. 2009]. It is also supported by the earlier development of Aß plaques in patients with epilepsy [Mackenzie and Miller 1994; Gouras et al. 1997]. Those observations indicate that neuronal hyperactivity may result in enhanced Aß production and increased conversion of soluble Aß

into oligomers and plaques [Deshpande et al. 2009]. This process may sustain a vicious cycle by further increasing neuronal hyperactivity. However, it is important in this regard that high levels of Aß can reduce glutamatergic synaptic transmission and cause synaptic loss [Chapman et al. 1999; Kamenetz et al. 2003; Hsieh et al. 2006; Shankar et al. 2007]. This could contribute to synaptic depression and neuronal silencing that become more prominent in advanced disease stages, perhaps in combination with mechanisms related to calcium overload of the cells, as described above. Finally, the relative contributions of increased vs. reduced activity of neurons to the AD pathophysiology remain unknown, but it is likely that both hypo- and hyperactivity can lead to neuronal network imbalances and thus can negatively impact the disease process.

4.3 Regional functional vulnerability

Over the past few years, we have applied *in vivo* two-photon calcium imaging initially to cortex [Busche et al. 2008; Grienberger et al. 2012] and now to hippocampus in AD transgenic mice. When theses studies are examined together, a clearer picture emerges about the temporal sequences of neuronal dysfunction across different brain regions. Our work demonstrates that alterations of neuronal activity are first apparent in the hippocampus and with time progress to the cortex. The early manifestation of hippocampal dysfunction is consistent with the clinical course of AD, with hippocampus-dependant learning and memory impairments being among the first symptoms both in animal models and in humans [Budson and Solomon 2011]. In the cortex, hyperactive neurons were exclusively found near plaques, but in the hippocampus, they occur independent of plaque formation and are causally related to the action of soluble Aß. One possible explanation for this discrepancy between cortex and hippocampus relates to possible different local concentrations of soluble Aß in these brain regions. Soluble Aß may be initially higher in the hippocampus than in cortex, perhaps due to the substantially higher rates of spontaneous neuronal activity in hippocampal neurons. Indeed, previous *in vitro* and *in vivo* studies showed that Aß production and secretion into the extracellular space is tightly regulated by neuronal activity [Kamenetz et al. 2003; Cirrito et al. 2005]. In the cortex, toxic Aß levels

may be present only in the vicinity of plaques, since previous work showed that dimers and higher order oligomers are found both associated with plaque cores and locally enriched near plaques [Shankar et al. 2008; Koffie et al. 2009]. Another explanation may be that the difference reflects distinct mechanisms of action, namely soluble Aß versus plaques, for the two diverse neuronal populations in cortex and hippocampus. Thus, it seems that the overall effect of Aß on neurons and their networks depends critically on the abundance of Aß near neurons, their intrinsic vulnerability and the basic network anatomy of the brain area. It is also possible that differential effects of Aß on excitatory and inhibitory cells play a role.

4.4 Clinical implications

Today, there are no effective treatments available that delay or modify AD progression. Current drugs, including the acetylcholinesterase inhibitors and memantine, can improve symptoms, but work for only a limited time or offer no relief at all for some patients [Budson and Solomon 2011]. The development of disease-modifying therapies in AD focuses mainly on treatments that target the Aß peptide, however most of these agents have failed in the pivotal phase 3 therapeutic trials [Karran 2012]. Those recent failures have been explained by the fact that therapies were evaluated in patients with advanced disease, when irreversible degeneration had already occurred and removal of Aß was no longer beneficial [Selkoe 2011]. For instance, a recent study has shown that the biochemical pathways thought to lead to AD can precede symptoms by more than 20 years [Bateman et al. 2012]. In particular, the concentrations of Aß appear to decline in the cerebrospinal fluid 25 years before symptom onset in patients at risk for dominantly inherited AD. Moreover, Aß deposition as measured by PiB imaging was detected 15 years before expected symptom onset, as were increases in the tau protein in CSF, and brain atrophy detected on MRI scans. Abnormalities in cerebral glucose metabolism as well as impaired episodic memory were observed 10 years before predicted symptom onset. The first evidence of global cognitive impairment as measured using the mini-mental state examination and clinical dementia rating scale was detected five years before symptom onset. Thus, it has

been suggested that therapies need to be applied earlier when neuronal dysfunction has not already become irreversible [Sperling et al. 2011]. This is supported by preclinical studies using immunotherapy or secretase inhibition in AD transgenic mouse models. For instance, it has been shown that in a mouse model harboring mutated APP, PS1 and tau transgenes intrahippocampal injections of an anti-Aß antibody reduced extracellular Aß and ameliorated tau pathology when given at a young age, but not later on [Oddo et al. 2004]. Consistently, γ-secretase inhibition in APP/PS1 transgenic mice stopped plaque formation and growth at 6 months but not at 10 months of age [Yan et al. 2009]. This important concept has also resulted in new diagnostic guidelines by the National Institute of Aging and the Alzheimer´s Association that should guide earlier detection and treatment of AD [Sperling et al. 2011; Albert et al. 2011; McKhann et al. 2011]. It is important in this regard that most chronic diseases such as hypertension, atherosclerosis or diabetes exhibit early (sometimes asymptomatic) disease stages when treatment is more likely to be effective.

Our work identifies Aß-induced hippocampal hyperactivity as a very early neuronal dysfunction in AD transgenic mice. Interestingly, increased excitatory hippocampal activity has also been found in humans with prodromal AD and subjects with the highest neuronal activity levels at baseline showed the greatest clinical decline [Dickerson et al. 2005; O'Brien et al. 2010]. Those data indicate that hippocampal hyperactivity might be an early biomarker of AD pathology and might also be a promising target for disease-modifying treatments. Our work provides direct evidence that treatment with a γ-secretase inhibitor rapidly reverses neuronal hyperactivity in AD transgenic mice. Because hippocampal hyperactivity and rate of cognitive decline seems to be correlated, it is possible that disease-modifying treatment is most effective in a subgroup of patients with particularly high neuronal activity levels. It may be useful to include measures of hippocampal activity in future clinical treatment trials.

Most therapeutic development in AD focuses on anti-Aß treatment to decrease Aß production, aggregate formation or removal of preexisting plaques. However, anti-Aß treatments are most likely to show efficacy in the pre-symptomatic stage of AD and are likely to be much less

effective or even ineffective in advanced stages. Unfortunately, there have been identified only few other targets for disease-modifying treatments, among them tau-targeted and more general neuroprotective agents. We and others have begun to study the neuronal network-level abnormalities in AD, also with the aim to target these abnormalities with novel treatment approaches. Altered brain activity, such as neuronal silencing and hyperactivity or epileptiform activity, might be a promising target for therapy, perhaps even at later disease stages when anti-Aß drugs seem to fail. In line with this idea, recent work in humans with prodromal AD has shown that low doses of the antiepileptic drug levetiracetam reduced elevated hippocampal activity and improved performance during a cognitive task [Bakker et al. 2012]. Furthermore, evidence from an AD transgenic mouse model showed that levetiracetam reduced epileptiform activity detected by cortical EEG recording and reversed behavioral and cognitive deficits [Sanchez et al. 2012]. Importantly, while the hippocampal region is hyperactive and needs calming down, other brain regions could be hypoactive and require activation. For instance, a recent fMRI study has shown that the entorhinal cortex was hypoactive in humans with prodromal AD performing a pattern separation task [Yassa et al. 2010]. In addition, we have found that cortical and hippocampal neurons become hypoactive in advanced disease stages [Busche et al. 2008]. Thus, the development of drugs that benefit hypoactive brain circuits is also very important. The relative contributions of increased versus reduced neuronal activity to the AD disease process remain unknown, but it is likely that both hyperactive as well as hypoactive networks can negatively impact the AD disease process.

5 Publications in Peer Reviewed Journals

1. Busche MA, Chen X, Henning HA, Reichwald J, Staufenbiel M, Sakmann B, Konnerth A (2012) Critical role of soluble amyloid-ß for early hippocampal hyperactivity in a mouse model of Alzheimer's disease. *Proceedings of the National Academy of Sciences of the United States of America* 109:8740-8745.

2. Busche MA, Eichhoff G, Adelsberger H, Abramowski D, Wiederhold KH, Haass C, Staufenbiel M, Konnerth A, Garaschuk O (2008) Clusters of hyperactive neurons near amyloid plaques in a mouse model of Alzheimer's disease. *Science* 321:1686–89.

3. Eichhoff G, Busche MA, Garaschuk O (2008) In vivo calcium imaging of the aging and diseased brain. *European Journal of Nuclear Medicine and Molecular Imaging* 35 Suppl 1: 99-106.

Bibliography

Abramowski D, Wiederhold KH, Furrer U, Jaton AL, Neuenschwander A, Runser MJ, Danner S, Reichwald J, Ammaturo D, Staab D, Stoeckli M, Rueeger H, Neumann U, Staufenbiel M (2008) Dynamics of amyloid-ß turnover and deposition in different ß-amyloid precursor protein transgenic mouse models following gamma-secretase inhibition. *Journal of Pharmacology and Experimental Therapeutics* 327:411–24.

Adalsteinsson E, Sullivan EV, Kleinhans N, Spielman DM, Pfefferbaum A (2000) Longitudinal decline of the neuronal marker N-acetyl aspartate in Alzheimer's disease. *Lancet* 355:1696–7.

Alberdi E, Sanchez-Gomez MV, Cavaliere F, Perez-Samartin A, Zugaza JL, Trullas R, Domercq M, Matute C (2010) Amyloid-ß oligomers induce calcium dysregulation and neuronal death through activation of ionotropic glutamate receptors. *Cell Calcium* 47:264–72.

Albert MS, DeKosky ST, Dickson D, Dubois B, Feldman HH, Fox NC, Gamst A, Holtzman DM, Jagust WJ, Petersen RC, Snyder PJ, Carrillo MC, Thies B, Phelps CH (2011) The diagnosis of mild cognitive impairment due to Alzheimer's disease: recommendations from the National Institute on Aging and Alzheimer's Association workgroups on diagnostic guidelines for Alzheimer's disease. *Alzheimer's & Dementia* 7:270–9.

Allen G, Barnard H, McColl R, Hester AL, Fields JA, Weiner MF, Ringe WK, Lipton AM, Brooker M, McDonald E, Rubin CD, Cullum CM (2007) Reduced hippocampal functional connectivity in Alzheimer's disease. *Archives of Neurology* 64:1482–7.

Amaral DG, Insausti R, Cowan WM (1984) The commissural connections of the monkey hippocampal formation. *Journal of Comparative Neurology* 224:307–36.

Andermann ML, Kerlin AM, Reid RC (2010) Chronic cellular imaging of mouse visual cortex during operant behavior and passive viewing. *Frontiers in Cellular Neuroscience* 4:3.

Andersen P (2007) *The hippocampus book.* Oxford University Press, Oxford ; New York.

Bacskai BJ, Kajdasz ST, Christie RH, Carter C, Games D, Seubert P, Schenk D, Hyman BT (2001) Imaging of amyloid-ß deposits in brains of living mice permits direct observation of clearance of plaques with immunotherapy. *Nature Medicine* 7:369–72.

Bacskai BJ, Hickey GA, Skoch J, Kajdasz ST, Wang Y, Huang GF, Mathis CA, Klunk WE, Hyman BT (2003) Four-dimensional multiphoton imaging of brain entry, amyloid binding, and clearance of an amyloid-ß ligand in transgenic mice. *Proceedings of the National Academy of Sciences of the United States of America* 100:12462–7.

Bakker A, Krauss GL, Albert MS, Speck CL, Jones LR, Stark CE, Yassa MA, Bassett SS, Shelton AL, Gallagher M (2012) Reduction of hippocampal hyperactivity improves cognition in amnestic mild cognitive impairment. *Neuron* 74:467–74.

Bartsch T, Schönfeld R, Müller FJ, Alfke K, Leplow B, Aldenhoff J, Deuschl G, Koch JM (2010) Focal lesions of human hippocampal CA1 neurons in transient global amnesia impair place memory. *Science* 328:1412–5.

Bassett SS, Yousem DM, Cristinzio C, Kusevic I, Yassa MA, Caffo BS, Zeger SL (2006) Familial risk for Alzheimer's disease alters fMRI activation patterns. *Brain* 129:1229–39.

Bateman RJ, Xiong C, Benzinger TLS, Fagan AM, Goate A, Fox NC, Marcus DS, Cairns NJ, Xie X, Blazey TM, Holtzman DM, Santacruz A, Buckles V, Oliver A, Moulder K, Aisen PS, Ghetti B, Klunk WE, McDade E, Martins RN, Masters CL, Mayeux R, Ringman JM, Rossor MN, Schofield PR, Sperling RA, Salloway S, Morris JC, Dominantly Inherited Alzheimer

Network (2012) Clinical and biomarker changes in dominantly inherited Alzheimer's disease. *New England Journal of Medicine* 367:795–804.

Bero AW, Yan P, Roh JH, Cirrito JR, Stewart FR, Raichle ME, Lee JM, Holtzman DM (2011) Neuronal activity regulates the regional vulnerability to amyloid-ß deposition. *Nature Neuroscience* 14:750–6.

Berridge MJ, Lipp P, Bootman MD (2000) The versatility and universality of calcium signalling. *Nature Reviews Molecular Cell Biology* 1:11–21.

Bezprozvanny I, Mattson MP (2008) Neuronal calcium mishandling and the pathogenesis of Alzheimer's disease. *Trends in Neuroscience* 31:454–63.

Bird CM, Burgess N (2008) The hippocampus and memory: insights from spatial processing. *Nature Reviews Neuroscience* 9:182–94.

Bland BH (1986) The physiology and pharmacology of hippocampal formation theta rhythms. *Progress in Neurobiology* 26:1–54.

Bobinski M, de Leon MJ, Wegiel J, Desanti S, Convit A, Saint Louis LA, Rusinek H, Wisniewski HM (2000) The histological validation of post mortem magnetic resonance imaging-determined hippocampal volume in Alzheimer's disease. *Neuroscience* 95:721–5.

Bolmont T, Haiss F, Eicke D, Radde R, Mathis CA, Klunk WE, Kohsaka S, Jucker M, Calhoun ME (2008) Dynamics of the microglial/amyloid interaction indicate a role in plaque maintenance. *Journal of Neuroscience* 28:4283–92.

Bookheimer SY, Strojwas MH, Cohen MS, Saunders AM, Pericak-Vance MA, Mazziotta JC, Small GW (2000) Patterns of brain activation in people at risk for Alzheimer's disease. *New England Journal of Medicine* 343:450–6.

Braak H, Alafuzoff I, Arzberger T, Kretzschmar H, Del Tredici K (2006) Staging of Alzheimer's disease-associated neurofibrillary pathology using paraffin sections and immunocytochemistry. *Acta Neuropathologica* 112:389–404.

Brendza RP, Bacskai BJ, Cirrito JR, Simmons KA, Skoch JM, Klunk WE, Mathis CA, Bales KR, Paul SM, Hyman BT, Holtzman DM (2005) Anti-Aß antibody treatment promotes the rapid recovery of amyloid-associated neuritic dystrophy in PDAPP transgenic mice. *Journal of Clinical Investigation* 115:428–33.

Brendza RP, O'Brien C, Simmons K, McKeel DW, Bales KR, Paul SM, Olney JW, Sanes JR, Holtzman DM (2003) PDAPP;YFP double transgenic mice: a tool to study amyloid-ß associated changes in axonal, dendritic, and synaptic structures. *Journal of Comparative Neurology* 456:375–83.

Brorson JR, Bindokas VP, Iwama T, Marcuccilli CJ, Chisholm JC, Miller RJ (1995) The calcium influx induced by ß-amyloid peptide 25-35 in cultured hippocampal neurons results from network excitation. *Journal of Neurobiology* 26:325–38.

Buckner RL, Sepulcre J, Talukdar T, Krienen FM, Liu H, Hedden T, Andrews-Hanna JR, Sperling RA, Johnson KA (2009) Cortical hubs revealed by intrinsic functional connectivity: mapping, assessment of stability, and relation to Alzheimer's disease. *Journal of Neuroscience* 29:1860–73.

Budson AE, Solomon PR (2011) *Memory loss: a practical guide for clinicians.* Elsevier Saunders.

Busche MA, Eichhoff G, Adelsberger H, Abramowski D, Wiederhold KH, Haass C, Staufenbiel M, Konnerth A, Garaschuk O (2008) Clusters of hyperactive neurons near amyloid plaques in a mouse model of Alzheimer's disease. *Science* 321:1686–89.

Buzsáki G (1986) Hippocampal sharp waves: their origin and significance. *Brain Research* 398:242–52.

Buzsáki G, Horváth Z, Urioste R, Hetke J, Wise K (1992) High-frequency network oscillation in the hippocampus. *Science* 256:1025–7.

Buzsáki G (2002) Theta oscillations in the hippocampus. *Neuron* 33:325–40.

Buzsáki G (2004) Large-scale recording of neuronal ensembles. *Nature Neuroscience* 7:446–51.

Carmichael O, Xie J, Fletcher E, Singh B, DeCarli C, Alzheimer's Disease Neuroimaging Initiative (2012) Localized hippocampus measures are associated with Alzheimer pathology and cognition independent of total hippocampal volume. *Neurobiology of Aging* 33:1124.e31–41.

Chapman PF, White GL, Jones MW, Cooper-Blacketer D, Marshall VJ, Irizarry M, Younkin L, Good MA, Bliss TV, Hyman BT, Younkin SG, Hsiao KK (1999) Impaired synaptic plasticity and learning in aged amyloid precursor protein transgenic mice. *Nature Neuroscience* 2:271–6.

Chen LL, Lin LH, Green EJ, Barnes CA, McNaughton BL (1994) Head-direction cells in the rat posterior cortex. I. Anatomical distribution and behavioral modulation. *Experimental Brain Research* 101:8–23.

Cheng S, Frank LM (2008) New experiences enhance coordinated neural activity in the hippocampus. *Neuron* 57:303–13.

Chételat G, Landeau B, Eustache F, Mézenge F, Viader F, de la Sayette V, Desgranges B, Baron JC (2005) Using voxel-based morphometry to map the structural changes associated with rapid conversion in MCI: a longitudinal MRI study. *Neuroimage* 27:934–46.

Christie R, Bacskai B, Zipfel W, Williams R, Kajdasz S, Webb W, Hyman B (2001) Growth arrest of individual senile plaques in a model of Alzheimer's disease observed by in vivo multiphoton microscopy. *Journal of Neuroscience* 21:858–864.

Cirrito JR, Kang JE, Lee J, Stewart FR, Verges DK, Silverio LM, Bu G, Mennerick S, Holtzman DM (2008) Endocytosis is required for synaptic activity-dependent release of amyloid-ß in vivo. *Neuron* 58:42–51.

Cirrito JR, Yamada KA, Finn MB, Sloviter RS, Bales KR, May PC, Schoepp DD, Paul SM, Mennerick S, Holtzman DM (2005) Synaptic activity regulates interstitial fluid amyloid-ß levels in vivo. *Neuron* 48:913–22.

Cirrito JR, May PC, O'Dell MA, Taylor JW, Parsadanian M, Cramer JW, Audia JE, Nissen JS, Bales KR, Paul SM, DeMattos RB, Holtzman DM (2003) In vivo assessment of brain interstitial fluid with microdialysis reveals plaque-associated changes in amyloid-ß metabolism and half-life. *Journal of Neuroscience* 23:8844–53.

Collins DR, Lang EJ, Paré D (1999) Spontaneous activity of the perirhinal cortex in behaving cats. *Neuroscience* 89:1025–39.

Corkin S, Amaral DG, González RG, Johnson KA, Hyman BT (1997) H.M.'s medial temporal lobe lesion: findings from magnetic resonance imaging. *Journal of Neuroscience* 17:3964–79.

D'Amelio M, Cavallucci V, Middei S, Marchetti C, Pacioni S, Ferri A, Diamantini A, De Zio D, Carrara P, Battistini L, Moreno S, Bacci A, Ammassari-Teule M, Marie H, Cecconi F (2011) Caspase-3 triggers early synaptic dysfunction in a mouse model of Alzheimer's disease. *Nature Neuroscience* 14:69–76.

Davalos D, Grutzendler J, Yang G, Kim JV, Zuo Y, Jung S, Littman DR, Dustin ML, Gan WB (2005) ATP mediates rapid microglial response to local brain injury in vivo. *Nature Neuroscience* 8:752–8.

Demeter S, Rosene DL, Van Hoesen GW (1985) Interhemispheric pathways of the hippocampal formation, presubiculum, and entorhinal and posterior parahippocampal cortices in the rhesus monkey: the structure and organization of the hippocampal commissures. *Journal of Comparative Neurology* 233:30–47.

Denk W, Strickler JH, Webb WW (1990) Two-photon laser scanning fluorescence microscopy. *Science* 248:73–6.

Denk W, Svoboda K (1997) Photon upmanship: why multiphoton imaging is more than a gimmick. *Neuron* 18:351–7.

Deshpande A, Kawai H, Metherate R, Glabe CG, Busciglio J (2009) A role for synaptic zinc in

activity-dependent Aß oligomer formation and accumulation at excitatory synapses. *Journal of Neuroscience* 29:4004–15.

Dickerson BC, Salat DH, Greve DN, Chua EF, Rand-Giovannetti E, Rentz DM, Bertram L, Mullin K, Tanzi RE, Blacker D, Albert MS, Sperling RA (2005) Increased hippocampal activation in mild cognitive impairment compared to normal aging and AD. *Neurology* 65:404–11.

Dombeck DA, Harvey CD, Tian L, Looger LL, Tank DW (2010) Functional imaging of hippocampal place cells at cellular resolution during virtual navigation. *Nature Neuroscience* 13:1433–40.

Dreosti E, Odermatt B, Dorostkar MM, Lagnado L (2009) A genetically encoded reporter of synaptic activity in vivo. *Nature Methods* 6:883–9.

Eichhoff G, Busche MA, Garaschuk O (2008) In vivo calcium imaging of the aging and diseased brain. *European Journal of Nuclear Medicine and Molecular Imaging* 35 Suppl 1:S99–106.

Förstl H, Bickel H, Perneczky R, Hüll M, Daffertshofer M (2012) Demenzen. *Klinische Neurologie* pp. 925–953.

Freund TF, Buzsáki G (1996) Interneurons of the hippocampus. *Hippocampus* 6:347–470.

Frisoni GB, Fox NC, Jack J CR, Scheltens P, Thompson PM (2010) The clinical use of structural MRI in Alzheimer disease. *Nature Reviews Neurology* 6:67–77.

Garaschuk O, Milos RI, Konnerth A (2006) Targeted bulk-loading of fluorescent indicators for two-photon brain imaging in vivo. *Nature Protocols* 1:380–6.

Garaschuk O, Konnerth A (2010) In vivo two-photon calcium imaging using multicell bolus loading. *Cold Spring Harbor Protocols* 2010:pdb.prot5482.

Gilles C, Brucher JM, Khoubesserian P, Vanderhaeghen JJ (1984) Cerebral amyloid angiopathy as a cause of multiple intracerebral hemorrhages. *Neurology* 34:730–5.

Gosche KM, Mortimer JA, Smith CD, Markesbery WR, Snowdon DA (2002) Hippocampal volume as an index of Alzheimer neuropathology: findings from the Nun Study. *Neurology* 58:1476–82.

Gottlieb DI, Cowan WM (1973) Autoradiographic studies of the commissural and ipsilateral association connection of the hippocampus and detentate gyrus of the rat. I. The commissural connections. *Journal of Comparative Neurology* 149:393–422.

Gouras GK, Relkin NR, Sweeney D, Munoz DG, Mackenzie IR, Gandy S (1997) Increased apolipoprotein E epsilon 4 in epilepsy with senile plaques. *Annals of Neurology* 41:402–4.

Goussakov I, Miller MB, Stutzmann GE (2010) NMDA-mediated calcium influx drives aberrant ryanodine receptor activation in dendrites of young Alzheimer's disease mice. *Journal of Neuroscience* 30:12128–37.

Grady CL, McIntosh AR, Beig S, Keightley ML, Burian H, Black SE (2003) Evidence from functional neuroimaging of a compensatory prefrontal network in Alzheimer's disease. *Journal of Neuroscience* 23:986–93.

Gray CM, Maldonado PE, Wilson M, McNaughton B (1995) Tetrodes markedly improve the reliability and yield of multiple single-unit isolation from multi-unit recordings in cat striate cortex. *Journal of Neuroscience Methods* 63:43–54.

Green KN, LaFerla FM (2008) Linking calcium to Aß and Alzheimer's disease. *Neuron* 59:190–4.

Greenberg DS, Houweling AR, Kerr JND (2008) Population imaging of ongoing neuronal activity in the visual cortex of awake rats. *Nature Neuroscience* 11:749–51.

Greenberg SM (2002) Cerebral amyloid angiopathy and dementia: two amyloids are worse than one. *Neurology* 58:1587–8.

Greicius MD, Srivastava G, Reiss AL, Menon V (2004) Default-mode network activity distinguishes Alzheimer's disease from healthy aging: evidence from functional MRI. *Proceedings of the National Academy of Sciences of the United States of America* 101:4637–42.

Grienberger C, Konnerth A (2012) Imaging calcium in neurons. *Neuron* 73:862–85.

Grienberger C, Rochefort NL, Adelsberger H, Henning HA, Hill DN, Reichwald J, Staufenbiel M, Konnerth A (2012) Staged decline of neuronal function in vivo in an animal model of Alzheimer's disease. *Nature Communications* 3:774.

Haass C (2010) Initiation and propagation of neurodegeneration. *Nature Medicine* 16:1201–4.

Hafting T, Fyhn M, Molden S, Moser MB, Moser EI (2005) Microstructure of a spatial map in the entorhinal cortex. *Nature* 436:801–6.

Haier RJ, Alkire MT, White NS, Uncapher MR, Head E, Lott IT, Cotman CW (2003) Temporal cortex hypermetabolism in down syndrome prior to the onset of dementia. *Neurology* 61:1673–9.

Helmchen F, Denk W (2005) Deep tissue two-photon microscopy. *Nature Methods* 2:932–40.

Henze DA, Borhegyi Z, Csicsvari J, Mamiya A, Harris KD, Buzsaki G (2000) Intracellular features predicted by extracellular recordings in the hippocampus in vivo. *Journal of Neurophysiology* 84:390–400.

Herzig MC, Winkler DT, Burgermeister P, Pfeifer M, Kohler E, Schmidt SD, Danner S, Abramowski D, Sturchler-Pierrat C, Burki K, van Duinen SG, Maat-Schieman ML, Staufenbiel M, Mathews PM, Jucker M (2004) Aß is targeted to the vasculature in a mouse model of hereditary cerebral hemorrhage with amyloidosis. *Nature Neuroscience* 7:954–60.

Hires SA, Tian L, Looger LL (2008) Reporting neural activity with genetically encoded calcium indicators. *Brain Cell Biology* 36:69–86.

Ho A, Shen J (2011) Presenilins in synaptic function and disease. *Trends in Molecular Medicine* 17:617–24.

Holtmaat A, de Paola V, Wilbrecht L, Trachtenberg JT, Svoboda K, Portera-Cailliau C (2012) Imaging neocortical neurons through a chronic cranial window. *Cold Spring Harbor Protocols* 2012 Jun:694–701.

Holtmaat A, Svoboda K (2009) Experience-dependent structural synaptic plasticity in the mammalian brain. *Nature Reviews Neuroscience* 10:647–58.

Hsia AY, Masliah E, McConlogue L, Yu GQ, Tatsuno G, Hu K, Kholodenko D, Malenka RC, Nicoll RA, Mucke L (1999) Plaque-independent disruption of neural circuits in Alzheimer's disease mouse models. *Proceedings of the National Academy of Sciences of the United States of America* 96:3228–33.

Hsiao K, Chapman P, Nilsen S, Eckman C, Harigaya Y, Younkin S, Yang F, Cole G (1996) Correlative memory deficits, Aß elevation, and amyloid plaques in transgenic mice. *Science* 274:99–102.

Hsieh H, Boehm J, Sato C, Iwatsubo T, Tomita T, Sisodia S, Malinow R (2006) AMPAR removal underlies Aß-induced synaptic depression and dendritic spine loss. *Neuron* 52:831–43.

Hu NW, Smith IM, Walsh DM, Rowan MJ (2008) Soluble amyloid-ß peptides potently disrupt hippocampal synaptic plasticity in the absence of cerebrovascular dysfunction in vivo. *Brain* 131:2414–24.

Hyman BT, Van Hoesen GW, Damasio AR, Barnes CL (1984) Alzheimer's disease: cell-specific pathology isolates the hippocampal formation. *Science* 225:1168–70.

Hyman JM, Zilli EA, Paley AM, Hasselmo ME (2005) Medial prefrontal cortex cells show dynamic modulation with the hippocampal theta rhythm dependent on behavior. *Hippocampus* 15:739–49.

Ito E, Oka K, Etcheberrigaray R, Nelson TJ, McPhie DL, Tofel-Grehl B, Gibson GE, Alkon DL (1994) Internal calcium mobilization is altered in fibroblasts from patients with Alzheimer's disease. *Proceedings of the National Academy of Sciences of the United States of America* 91:534–8.

Jack J CR, Lowe VJ, Senjem ML, Weigand SD, Kemp BJ, Shiung MM, Knopman DS, Boeve BF, Klunk WE, Mathis CA, Petersen RC (2008) 11C PiB and structural MRI provide complementary information in imaging of Alzheimer's disease and amnestic mild cognitive impairment. *Brain* 131:665–80.

Jin M, Shepardson N, Yang T, Chen G, Walsh D, Selkoe DJ (2011) Soluble amyloid ß-protein dimers isolated from Alzheimer cortex directly induce tau hyperphosphorylation and neuritic degeneration. *Proceedings of the National Academy of Sciences of the United States of America* 108:5819–24.

Jog MS, Connolly CI, Kubota Y, Iyengar DR, Garrido L, Harlan R, Graybiel AM (2002) Tetrode technology: advances in implantable hardware, neuroimaging, and data analysis techniques. *Journal of Neuroscience Methods* 117:141–52.

Johnson K, Fox N, Sperling R, Klunk W (2012) Brain imaging in Alzheimer disease. *Cold Spring Harbor Perspectives in Medicine* 2:a006213.

Jones TLS, Mielke ML, Rozkalne A, Meyer-Luehmann M, de Calignon A, Bacskai BJ, Schenk D, Hyman BT (2009) Passive immunotherapy rapidly increases structural plasticity in a mouse model of Alzheimer disease. *Neurobiology of Disease* 33:213–220.

Jonsson T, Atwal JK, Steinberg S, Snaedal J, Jonsson PV, Bjornsson S, Stefansson H, Sulem P, Gudbjartsson D, Maloney J, Hoyte K, Gustafson A, Liu Y, Lu Y, Bhangale T, Graham RR, Huttenlocher J, Bjornsdottir G, Andreassen OA, Jönsson EG, Palotie A, Behrens TW, Magnusson OT, Kong A, Thorsteinsdottir U, Watts RJ, Stefansson K (2012) A mutation in APP protects against Alzheimer's disease and age-related cognitive decline. *Nature* 488:96–99.

Kalyan-Raman UP, Kalyan-Raman K (1984) Cerebral amyloid angiopathy causing intracranial hemorrhage. *Annals of Neurology* 16:321–9.

Kamenetz F, Tomita T, Hsieh H, Seabrook G, Borchelt D, Iwatsubo T, Sisodia S, Malinow R (2003) APP processing and synaptic function. *Neuron* 37:925–37.

Kandel ER, Spencer WA, Brinley FJ J (1961) Electrophysiology of hippocampal neurons. I. Sequential invasion and synaptic organization. *Journal of Neurophysiology* 24:225–42.

Kang JE, Lim MM, Bateman RJ, Lee JJ, Smyth LP, Cirrito JR, Fujiki N, Nishino S, Holtzman DM (2009) Amyloid-ß dynamics are regulated by orexin and the sleep-wake cycle. *Science* 326:1005–7.

Kantarci K, Petersen RC, Boeve BF, Knopman DS, Weigand SD, O'Brien PC, Shiung MM, Smith GE, Ivnik RJ, Tangalos EG, Jack J CR (2005) DWI predicts future progression to Alzheimer disease in amnestic mild cognitive impairment. *Neurology* 64:902–4.

Karran E (2012) Current status of vaccination therapies in Alzheimer's disease. *Journal of Neurochemistry* 123:647–51.

Kerr JN, Denk W (2008) Imaging in vivo: watching the brain in action. *Nature Reviews Neuroscience* 9:195–205.

Kerr JN, Greenberg D, Helmchen F (2005) Imaging input and output of neocortical networks in vivo. *Proceedings of the National Academy of Sciences of the United States of America* 102:14063–8.

Khachaturian ZS (1985) Diagnosis of Alzheimer's disease. *Archives of Neurology* 42:1097–105.

Kitamura K, Judkewitz B, Kano M, Denk W, Hausser M (2008) Targeted patch-clamp recordings and single-cell electroporation of unlabeled neurons in vivo. *Nature Methods* 5:61–7.

Klunk W, Bacskai B, Mathis C, Kajdasz S, McLellan M, Frosch M, Debnath M, Holt D, Wang Y, Hyman B (2002) Imaging Aß plaques in living transgenic mice with multiphoton

microscopy and methoxy-X04, a systemically administered Congo red derivative. *Journal of Neuropathology and Experimental Neurology* 61:797–805.

Klunk WE, Engler H, Nordberg A, Wang Y, Blomqvist G, Holt DP, Bergström M, Savitcheva I, Huang Gf, Estrada S, Ausén B, Debnath ML, Barletta J, Price JC, Sandell J, Lopresti BJ, Wall A, Koivisto P, Antoni G, Mathis CA, Långström B (2004) Imaging brain amyloid in Alzheimer's disease with Pittsburgh Compound-B. *Annals of Neurology* 55:306–19.

Kocsis B, Vertes RP (1994) Characterization of neurons of the supramammillary nucleus and mammillary body that discharge rhythmically with the hippocampal theta rhythm in the rat. *Journal of Neuroscience* 14:7040–52.

Koenigsknecht-Talboo J, Meyer-Luehmann M, Parsadanian M, Garcia-Alloza M, Finn MB, Hyman BT, Bacskai BJ, Holtzman DM (2008) Rapid microglial response around amyloid pathology after systemic anti-Aß antibody administration in PDAPP mice. *Journal of Neuroscience* 28:14156–64.

Koffie RM, Meyer-Luehmann M, Hashimoto T, Adams KW, Mielke ML, Garcia-Alloza M, Micheva KD, Smith SJ, Kim ML, Lee VM, Hyman BT, Spires-Jones TL (2009) Oligomeric amyloid-ß associates with postsynaptic densities and correlates with excitatory synapse loss near senile plaques. *Proceedings of the National Academy of Sciences of the United States of America* 106:4012–7.

Kuchibhotla KV, Goldman ST, Lattarulo CR, Wu HY, Hyman BT, Bacskai BJ (2008) Aß plaques lead to aberrant regulation of calcium homeostasis in vivo resulting in structural and functional disruption of neuronal networks. *Neuron* 59:214–25.

Kuchibhotla KV, Lattarulo CR, Hyman BT, Bacskai BJ (2009) Synchronous hyperactivity and intercellular calcium waves in astrocytes in Alzheimer mice. *Science* 323:1211–5.

Kuga N, Sasaki T, Takahara Y, Matsuki N, Ikegaya Y (2011) Large-scale calcium waves traveling through astrocytic networks in vivo. *Journal of Neuroscience* 31:2607–14.

Kurucz J, Charbonneau R, Kurucz A, Ramsey P (1981) Quantitative clinicopathologic study of senile dementia. *Journal of the American Geriatrics Society* 29:158–63.

Lanz TA, Hosley JD, Adams WJ, Merchant KM (2004) Studies of Aß pharmacodynamics in the brain, cerebrospinal fluid, and plasma in young (plaque-free) Tg2576 mice using the gamma-secretase inhibitor LY-411575. *Journal of Pharmacology and Experimental Therapeutics* 309:49–55.

Lee JH, Durand R, Gradinaru V, Zhang F, Goshen I, Kim DS, Fenno LE, Ramakrishnan C, Deisseroth K (2010) Global and local fMRI signals driven by neurons defined optogenetically by type and wiring. *Nature* 465:788–92.

Li S, Hong S, Shepardson NE, Walsh DM, Shankar GM, Selkoe D (2009) Soluble oligomers of amyloid-ß protein facilitate hippocampal long-term depression by disrupting neuronal glutamate uptake. *Neuron* 62:788–801.

Li S, Shankar GM, Selkoe DJ (2010) How do soluble oligomers of amyloid ß-protein impair hippocampal synaptic plasticity ? *Frontiers in Cellular Neuroscience* 4:5.

Li SJ, Li Z, Wu G, Zhang MJ, Franczak M, Antuono PG (2002) Alzheimer disease: evaluation of a functional MR imaging index as a marker. *Radiology* 225:253–9.

Lichtman JW, Denk W (2011) The big and the small: challenges of imaging the brain's circuits. *Science* 334:618–23.

Linden DEJ (2012) The challenges and promise of neuroimaging in psychiatry. *Neuron* 73:8–22.

Lütcke H, Murayama M, Hahn T, Margolis DJ, Astori S, Zum Alten Borgloh SM, Göbel W, Yang Y, Tang W, Kügler S, Sprengel R, Nagai T, Miyawaki A, Larkum ME, Helmchen F, Hasan MT (2010) Optical recording of neuronal activity with a genetically-encoded calcium indicator in anesthetized and freely moving mice. *Frontiers in Neural Circuits* 4:9.

Mackenzie IR, Miller LA (1994) Senile plaques in temporal lobe epilepsy. *Acta Neuropathologica* 87:504–10.

Mandybur TI (1975) The incidence of cerebral amyloid angiopathy in Alzheimer's disease. *Neurology* 25:120–6.

Mank M, Santos AF, Direnberger S, Mrsic-Flogel TD, Hofer SB, Stein V, Hendel T, Reiff DF, Levelt C, Borst A, Bonhoeffer T, Hubener M, Griesbeck O (2008) A genetically encoded calcium indicator for chronic in vivo two-photon imaging. *Nature Methods* 5:805–11.

Mank M, Griesbeck O (2008) Genetically encoded calcium indicators. *Chemical Reviews* 108:1550–64.

Manook A, Yousefi BH, Willuweit A, Platzer S, Reder S, Voss A, Huisman M, Settles M, Neff F, Velden J, Schoor M, von der Kammer H, Wester HJ, Schwaiger M, Henriksen G, Drzezga A (2012) Small-animal PET imaging of amyloid-beta plaques with [11C]PiB and its multi-modal validation in an APP/PS1 mouse model of Alzheimer's disease. *PLoS One* 7:e31310.

Markram H, Helm PJ, Sakmann B (1995) Dendritic calcium transients evoked by single back-propagating action potentials in rat neocortical pyramidal neurons. *Journal of Physiology* 485 (Pt 1):1–20.

Mattson MP (2004) Pathways towards and away from Alzheimer's disease. *Nature* 430:631–9.

Mayeux R, Stern Y (2012) Epidemiology of Alzheimer disease. *Cold Spring Harbor Perspectives in Medicine* 2.

Mc Donald JM, Savva GM, Brayne C, Welzel AT, Forster G, Shankar GM, Selkoe DJ, Ince PG, Walsh DM (2010) The presence of sodium dodecyl sulphate-stable Aß dimers is strongly associated with Alzheimer-type dementia. *Brain* 133:1328–41.

McFarland WL, Teitelbaum H, Hedges EK (1975) Relationship between hippocampal theta activity and running speed in the rat. *Journal of Comparative Physiological Psychology* 88:324–8.

McKhann GM, Knopman DS, Chertkow H, Hyman BT, Jack J CR, Kawas CH, Klunk WE, Koroshetz WJ, Manly JJ, Mayeux R, Mohs RC, Morris JC, Rossor MN, Scheltens P, Carrillo MC, Thies B, Weintraub S, Phelps CH (2011) The diagnosis of dementia due to Alzheimer's disease: recommendations from the National Institute on Aging and Alzheimer's Association workgroups on diagnostic guidelines for Alzheimer's disease. *Alzheimer's & Dementia* 7:263–9.

Meyer-Luehmann M, Spires-Jones TL, Prada C, Garcia-Alloza M, de Calignon A, Rozkalne A, Koenigsknecht-Talboo J, Holtzman DM, Bacskai BJ, Hyman BT (2008) Rapid appearance and local toxicity of amyloid-ß plaques in a mouse model of Alzheimer's disease. *Nature* 451:720–4.

Minkeviciene R, Rheims S, Dobszay MB, Zilberter M, Hartikainen J, Fulop L, Penke B, Zilberter Y, Harkany T, Pitkanen A, Tanila H (2009) Amyloid ß-induced neuronal hyperexcitability triggers progressive epilepsy. *Journal of Neuroscience* 29:3453–62.

Mizrahi A, Crowley JC, Shtoyerman E, Katz LC (2004) High-resolution in vivo imaging of hippocampal dendrites and spines. *Journal of Neuroscience* 24:3147–51.

Moechars D, Dewachter I, Lorent K, Reverse D, Baekelandt V, Naidu A, Tesseur I, Spittaels K, Haute CV, Checler F, Godaux E, Cordell B, Van Leuven F (1999) Early phenotypic changes in transgenic mice that overexpress different mutants of amyloid precursor protein in brain. *Journal of Biology and Chemistry* 274:6483–92.

Mondadori CRA, Buchmann A, Mustovic H, Schmidt CF, Boesiger P, Nitsch RM, Hock C, Streffer J, Henke K (2006) Enhanced brain activity may precede the diagnosis of Alzheimer's disease by 30 years. *Brain* 129:2908–22.

Moran PM, Higgins LS, Cordell B, Moser PC (1995) Age-related learning deficits in transgenic mice expressing the 751-amino acid isoform of human ß-amyloid precursor protein. *Proceedings of the National Academy of Sciences of the United States of America* 92:5341–5.

Mott RT, Hulette CM (2005) Neuropathology of Alzheimer's disease. *Neuroimaging Clinics of North America* 15:755–65.

Mucke L, Masliah E, Yu GQ, Mallory M, Rockenstein EM, Tatsuno G, Hu K, Kholodenko D, Johnson-Wood K, McConlogue L (2000) High-level neuronal expression of Aß 1-42 in wild-type human amyloid protein precursor transgenic mice: synaptotoxicity without plaque formation. *Journal of Neuroscience* 20:4050–8.

Nádasdy Z, Hirase H, Czurkó A, Csicsvari J, Buzsáki G (1999) Replay and time compression of recurring spike sequences in the hippocampus. *Journal of Neuroscience* 19:9497–507.

Nelson O, Tu H, Lei T, Bentahir M, de Strooper B, Bezprozvanny I (2007) Familial Alzheimer disease-linked mutations specifically disrupt calcium leak function of presenilin 1. *Journal of Clinical Investigation* 117:1230–9.

Nimmerjahn A, Helmchen F (2012) In vivo labeling of cortical astrocytes with sulforhodamine 101 (SR101). *Cold Spring Harbor Protocols* 2012:326–334.

Nimmerjahn A, Kirchhoff F, Kerr JND, Helmchen F (2004) Sulforhodamine 101 as a specific marker of astroglia in the neocortex in vivo. *Nature Methods* 1:31–7.

Nitsch RM, Farber SA, Growdon JH, Wurtman RJ (1993) Release of amyloid ß-protein precursor derivatives by electrical depolarization of rat hippocampal slices. *Proceedings of the National Academy of Sciences of the United States of America* 90:5191–3.

O'Brien JL, O'Keefe KM, LaViolette PS, DeLuca AN, Blacker D, Dickerson BC, Sperling RA (2010) Longitudinal fMRI in elderly reveals loss of hippocampal activation with clinical decline. *Neurology* 74:1969–76.

Oddo S, Billings L, Kesslak JP, Cribbs DH, LaFerla FM (2004) Aß immunotherapy leads to clearance of early, but not late, hyperphosphorylated tau aggregates via the proteasome. *Neuron* 43:321–32.

Ohki K, Chung S, Kara P, Hübener M, Bonhoeffer T, Reid RC (2006) Highly ordered arrangement of single neurons in orientation pinwheels. *Nature* 442:925–8.

O'Keefe J (1976) Place units in the hippocampus of the freely moving rat. *Experimental Neurology* 51:78–109.

O'Keefe J, Dostrovsky J (1971) The hippocampus as a spatial map. preliminary evidence from unit activity in the freely-moving rat. *Brain Research* 34:171–5.

O'Keefe J, Burgess N (2005) Dual phase and rate coding in hippocampal place cells: theoretical significance and relationship to entorhinal grid cells. *Hippocampus* 15:853–66.

O'Keefe J, Nadel L (1978) *The hippocampus as a cognitive map.* Clarendon Press, Oxford.

O'Nuallain B, Freir DB, Nicoll AJ, Risse E, Ferguson N, Herron CE, Collinge J, Walsh DM (2010) Amyloid ß-protein dimers rapidly form stable synaptotoxic protofibrils. *Journal of Neuroscience* 30:14411–9.

Palop JJ, Chin J, Roberson ED, Wang J, Thwin MT, Bien-Ly N, Yoo J, Ho KO, Yu GQ, Kreitzer A, Finkbeiner S, Noebels JL, Mucke L (2007) Aberrant excitatory neuronal activity and compensatory remodeling of inhibitory hippocampal circuits in mouse models of Alzheimer's disease. *Neuron* 55:697–711.

Palop JJ, Mucke L (2009) Epilepsy and cognitive impairments in Alzheimer's disease. *Archives of Neurology* 66:435–40.

Palop JJ, Mucke L (2010) Amyloid-ß-induced neuronal dysfunction in Alzheimer's disease: from synapses toward neural networks. *Nature Neuroscience* 13:812–8.

Pavlides C, Winson J (1989) Influences of hippocampal place cell firing in the awake state on the activity of these cells during subsequent sleep episodes. *Journal of Neuroscience* 9:2907–18.

Paxinos G, Franklin K (2001) *The mouse brain in stereotaxic coordinates.* Academic Press, 2 edition.

Perrin RJ, Fagan AM, Holtzman DM (2009) Multimodal techniques for diagnosis and prognosis of Alzheimer's disease. *Nature* 461:916–22.

Prince M, Jackson J, International AD (2009) *World Alzheimer Report 2009.* Alzheimer's Disease International.

Prvulovic D, Van de Ven V, Sack AT, Maurer K, Linden DE (2005) Functional activation imaging in aging and dementia. *Psychiatry Research* 140:97–113.

Ranck J JB (1973) Studies on single neurons in dorsal hippocampal formation and septum in unrestrained rats. I. Behavioral correlates and firing repertoires. *Experimental Neurology* 41:461–531.

Rasch B, Born J (2007) Maintaining memories by reactivation. *Current Opinion in Neurobiology* 17:698–703.

Reitz C, Brayne C, Mayeux R (2011) Epidemiology of Alzheimer's disease. *Nature Reviews Neurology* 7:137–52.

Ridha BH, Symms MR, Tozer DJ, Stockton KC, Frost C, Siddique MM, Lewis EB, MacManus DG, Boulby PA, Barker GJ, Rossor MN, Fox NC, Tofts PS (2007) Magnetization transfer ratio in Alzheimer disease: comparison with volumetric measurements. *American Journal of Radiology* 28:965–70.

Robbins E, Betensky R, Domnitz S, Purcell S, Garcia-Alloza M, Greenberg C, Rebeck G, Hyman B, Greenberg S, Frosch M, Bacskai B (2006) Kinetics of cerebral amyloid angiopathy progression in a transgenic mouse model of Alzheimer disease. *Journal of Neuroscience* 26:365–371.

Rochefort NL, Garaschuk O, Milos RI, Narushima M, Marandi N, Pichler B, Kovalchuk Y, Konnerth A (2009) Sparsification of neuronal activity in the visual cortex at eye-opening. *Proceedings of the National Academy of Sciences of the United States of America* 106:15049–54.

Rochefort NL, Jia H, Konnerth A (2008) Calcium imaging in the living brain: prospects for molecular medicine. *Trends in Molecular Medicine* 14:389–99.

Rozkalne A, Spires-Jones TL, Stern EA, Hyman BT (2009) A single dose of passive immunotherapy has extended benefits on synapses and neurites in an Alzheimer's disease mouse model. *Brain Research* 1280:178–85.

Sakaguchi T, Ishikawa D, Nomura H, Matsuki N, Ikegaya Y (2012) Normal learning ability of mice with a surgically exposed hippocampus. *Neuroreport* 23:457–461.

Sanchez PE, Zhu L, Verret L, Vossel KA, Orr AG, Cirrito JR, Devidze N, Ho K, Yu GQ, Palop JJ, Mucke L (2012) Levetiracetam suppresses neuronal network dysfunction and reverses synaptic and cognitive deficits in an Alzheimer's disease model. *Proceedings of the National Academy of Sciences of the United States of America* 109:E2895–903.

Sanchez-Mejia RO, Newman JW, Toh S, Yu GQ, Zhou Y, Halabisky B, Cisse M, Scearce-Levie K, Cheng IH, Gan L, Palop JJ, Bonventre JV, Mucke L (2008) Phospholipase A2 reduction ameliorates cognitive deficits in a mouse model of Alzheimer's disease. *Nature Neuroscience* 11:1311–8.

Sanderson MJ, Parker I (2003) Video-rate confocal microscopy. *Methods in Enzymology* 360:447–81.

Sasaki T, Kuga N, Namiki S, Matsuki N, Ikegaya Y (2011) Locally synchronized astrocytes. *Cerebral Cortex* 21:1889–900.

Sato TR, Gray NW, Mainen ZF, Svoboda K (2007) The functional microarchitecture of the mouse barrel cortex. *PLoS Biology* 5:e189.

Scheuss V, Yasuda R, Sobczyk A, Svoboda K (2006) Nonlinear calcium signaling in dendrites and spines caused by activity-dependent depression of calcium extrusion. *Journal of Neuroscience* 26:8183–94.

Scoville W, Milner B (1957) Loss of recent memory after bilateral hippocampal lesions. *Journal of Neurology, Neurosurgery and Psychiatry* 20:11–21.

Selkoe DJ (2002) Alzheimer's disease is a synaptic failure. *Science* 298:789–91.

Selkoe DJ (2011) Resolving controversies on the path to Alzheimer's therapeutics. *Nature Medicine* 17:1060–5.

Serrano-Pozo A, Frosch M, Masliah E, Hyman B (2011) Neuropathological alterations in Alzheimer disease. *Cold Spring Harbor Perspectives in Medicine* 1:a006189.

Shankar GM, Bloodgood BL, Townsend M, Walsh DM, Selkoe DJ, Sabatini BL (2007) Natural oligomers of the Alzheimer amyloid-ß protein induce reversible synapse loss by modulating an NMDA-type glutamate receptor-dependent signaling pathway. *Journal of Neuroscience* 27:2866–75.

Shankar GM, Li S, Mehta TH, Garcia-Munoz A, Shepardson NE, Smith I, Brett FM, Farrell MA, Rowan MJ, Lemere CA, Regan CM, Walsh DM, Sabatini BL, Selkoe DJ (2008) Amyloid-ß protein dimers isolated directly from Alzheimer's brains impair synaptic plasticity and memory. *Nature Medicine* 14:837–42.

Shepherd GM (2004) *The synaptic organization of the brain.* Oxford University Press, Oxford, 5th ed edition.

Shigetomi E, Kracun S, Sofroniew MV, Khakh BS (2010) A genetically targeted optical sensor to monitor calcium signals in astrocyte processes. *Nature Neuroscience* 13:759–66.

Silverman DH, Small GW, Chang CY, Lu CS, Kung De Aburto MA, Chen W, Czernin J, Rapoport SI, Pietrini P, Alexander GE, Schapiro MB, Jagust WJ, Hoffman JM, Welsh-Bohmer KA, Alavi A, Clark CM, Salmon E, de Leon MJ, Mielke R, Cummings JL, Kowell AP, Gambhir SS, Hoh CK, Phelps ME (2001) Positron emission tomography in evaluation of dementia: Regional brain metabolism and long-term outcome. *Journal of the American Medical Association* 286:2120–7.

Small S, Schobel S, Buxton R, Witter M, Barnes C (2011) A pathophysiological framework of hippocampal dysfunction in ageing and disease. *Nature Reviews Neuroscience* 12:585–601.

Smith CD, Chebrolu H, Wekstein DR, Schmitt FA, Jicha GA, Cooper G, Markesbery WR (2007) Brain structural alterations before mild cognitive impairment. *Neurology* 68:1268–73.

Snyder EM, Nong Y, Almeida CG, Paul S, Moran T, Choi EY, Nairn AC, Salter MW, Lombroso PJ, Gouras GK, Greengard P (2005) Regulation of NMDA receptor trafficking by amyloid-ß. *Nature Neuroscience* 8:1051–8.

Sohya K, Kameyama K, Yanagawa Y, Obata K, Tsumoto T (2007) GABAergic neurons are less selective to stimulus orientation than excitatory neurons in layer II/III of visual cortex, as revealed by in vivo functional calcium imaging in transgenic mice. *Journal of Neuroscience* 27:2145–9.

Sperling RA, Bates JF, Chua EF, Cocchiarella AJ, Rentz DM, Rosen BR, Schacter DL, Albert MS (2003) fMRI studies of associative encoding in young and elderly controls and mild Alzheimer's disease. *Journal of Neurology, Neurosurgery and Psychiatry* 74:44–50.

Sperling RA, Laviolette PS, O'Keefe K, O'Brien J, Rentz DM, Pihlajamaki M, Marshall G, Hyman BT, Selkoe DJ, Hedden T, Buckner RL, Becker JA, Johnson KA (2009) Amyloid deposition is associated with impaired default network function in older persons without dementia. *Neuron* 63:178–88.

Sperling RA, Aisen PS, Beckett LA, Bennett DA, Craft S, Fagan AM, Iwatsubo T, Jack J CR, Kaye J, Montine TJ, Park DC, Reiman EM, Rowe CC, Siemers E, Stern Y, Yaffe K, Carrillo MC, Thies B, Morrison-Bogorad M, Wagster MV, Phelps CH (2011) Toward defining the preclinical stages of Alzheimer's disease: recommendations from the National Institute on Aging and Alzheimer's Association workgroups on diagnostic guidelines for Alzheimer's disease. *Alzheimer's & Dementia* 7:280–92.

Sperling RA, Dickerson BC, Pihlajamaki M, Vannini P, LaViolette PS, Vitolo OV, Hedden T, Becker JA, Rentz DM, Selkoe DJ, Johnson KA (2010) Functional alterations in memory networks in early Alzheimer's disease. *Neuromolecular Medicine* 12:27–43.

Spires TL, Meyer-Luehmann M, Stern EA, McLean PJ, Skoch J, Nguyen PT, Bacskai BJ, Hyman BT (2005) Dendritic spine abnormalities in amyloid precursor protein transgenic mice demonstrated by gene transfer and intravital multiphoton microscopy. *Journal of Neuroscience* 25:7278–87.

Squire LR, Zola-Morgan S (1991) The medial temporal lobe memory system. *Science* 253:1380–6.

Stosiek C, Garaschuk O, Holthoff K, Konnerth A (2003) In vivo two-photon calcium imaging of neuronal networks. *Proceedings of the National Academy of Sciences of the United States of America* 100:7319–24.

Sturchler-Pierrat C, Abramowski D, Duke M, Wiederhold KH, Mistl C, Rothacher S, Ledermann B, Burki K, Frey P, Paganetti PA, Waridel C, Calhoun ME, Jucker M, Probst A, Staufenbiel M, Sommer B (1997) Two amyloid precursor protein transgenic mouse models with Alzheimer disease-like pathology. *Proceedings of the National Academy of Sciences of the United States of America* 94:13287–92.

Sun A, Nguyen XV, Bing G (2002) Comparative analysis of an improved thioflavin-S stain, Gallyas silver stain, and immunohistochemistry for neurofibrillary tangle demonstration on the same sections. *Journal of Histochemistry and Cytochemistry* 50:463–72.

Sutherland GR, McNaughton B (2000) Memory trace reactivation in hippocampal and neocortical neuronal ensembles. *Current Opinion in Neurobiology* 10:180–6.

Svoboda K, Yasuda R (2006) Principles of two-photon excitation microscopy and its applications to neuroscience. *Neuron* 50:823–39.

Taoka T, Iwasaki S, Sakamoto M, Nakagawa H, Fukusumi A, Myochin K, Hirohashi S, Hoshida T, Kichikawa K (2006) Diffusion anisotropy and diffusivity of white matter tracts within the temporal stem in Alzheimer disease: evaluation of the "tract of interest" by diffusion tensor tractography. *American Journal of Neuroradiology* 27:1040–5.

Tarawneh R, Holtzman D (2012) The clinical problem of symptomatic Alzheimer disease and mild cognitive impairment. *Cold Spring Harbor Perspectives in Medicine* 2:a006148.

Taube JS, Muller RU, Ranck J JB (1990) Head-direction cells recorded from the postsubiculum in freely moving rats. I. Description and quantitative analysis. *Journal of Neuroscience* 10:420–35.

Thal DR, Rüb U, Orantes M, Braak H (2002) Phases of Aß-deposition in the human brain and its relevance for the development of AD. *Neurology* 58:1791–800.

Thomas D, Tovey SC, Collins TJ, Bootman MD, Berridge MJ, Lipp P (2000) A comparison of fluorescent calcium indicator properties and their use in measuring elementary and global calcium signals. *Cell Calcium* 28:213–23.

Tian L, Hires SA, Mao T, Huber D, Chiappe ME, Chalasani SH, Petreanu L, Akerboom J, McKinney SA, Schreiter ER, Bargmann CI, Jayaraman V, Svoboda K, Looger LL (2009) Imaging neural activity in worms, flies and mice with improved GCaMP calcium indicators. *Nature Methods* 6:875–81.

Tsai J, Grutzendler J, Duff K, Gan WB (2004) Fibrillar amyloid deposition leads to local synaptic abnormalities and breakage of neuronal branches. *Nature Neuroscience* 7:1181–3.

Tsien RY (1989) Fluorescent indicators of ion concentrations. *Methods in Cell Biology* 30:127–56.

Vanderwolf CH (1969) Hippocampal electrical activity and voluntary movement in the rat. *Electroencephalography and Clinical Neurophysiology* 26:407–18.

Vinters HV (1987) Cerebral amyloid angiopathy. a critical review. *Stroke* 18:311–24.

Wang L, Zang Y, He Y, Liang M, Zhang X, Tian L, Wu T, Jiang T, Li K (2006) Changes in hippocampal connectivity in the early stages of Alzheimer's disease: evidence from resting state fMRI. *Neuroimage* 31:496–504.

Weintraub S, Wicklund A, Salmon D (2012) The neuropsychological profile of Alzheimer disease. *Cold Spring Harbor Perspectives in Medicine* 2:a006171.

Whitwell JL, Przybelski SA, Weigand SD, Knopman DS, Boeve BF, Petersen RC, Jack J CR (2007) 3D maps from multiple MRI illustrate changing atrophy patterns as subjects progress from mild cognitive impairment to Alzheimer's disease. *Brain* 130:1777–86.

Wilson MA, McNaughton BL (1993) Dynamics of the hippocampal ensemble code for space. *Science* 261:1055–8.

Wilson MA, McNaughton BL (1994) Reactivation of hippocampal ensemble memories during sleep. *Science* 265:676–9.

Wimo A, Prince M, International AD (2010) *World Alzheimer Report 2010: the global economic impact of dementia.* Alzheimer's Disease International.

Wisniewski HM, Wen GY, Kim KS (1989) Comparison of four staining methods on the detection of neuritic plaques. *Acta Neuropathologica* 78:22–7.

Yan P, Bero AW, Cirrito JR, Xiao Q, Hu X, Wang Y, Gonzales E, Holtzman DM, Lee JM (2009) Characterizing the appearance and growth of amyloid plaques in APP/PS1 mice. *Journal of Neuroscience* 29:10706–14.

Yassa MA, Stark SM, Bakker A, Albert MS, Gallagher M, Stark CEL (2010) High-resolution structural and functional mri of hippocampal CA3 and dentate gyrus in patients with amnestic mild cognitive impairment. *Neuroimage* 51:1242–52.

Yasuda R, Nimchinsky EA, Scheuss V, Pologruto TA, Oertner TG, Sabatini BL, Svoboda K (2004) Imaging calcium concentration dynamics in small neuronal compartments. *Science Signaling* 2004:pl5.

Yuste R, MacLean J, Vogelstein J, Paninski L (2011) Imaging action potentials with calcium indicators. *Cold Spring Harbor Protocols* 2011:985–9.

Zeng LH, Xu L, Rensing NR, Sinatra PM, Rothman SM, Wong M (2007) Kainate seizures cause acute dendritic injury and actin depolymerization in vivo. *Journal of Neuroscience* 27:11604–13.

I WOULD LIKE TO THANK

Prof. Dr. Arthur Konnerth for his exceptional support, supervision and mentorship.

Prof. Dr. Olga Garaschuk for her scientific support and mentorship.

Dr. Iulia Milos and Dr. Nima Marandi for their scientific and personal support.

Dr. Xiaowei Chen, Dr. Horst Henning and Dr. Matthias Staufenbiel for their scientific collaboration.

Prof. Dr. Helmuth Adelsberger and Prof. Dr. Thomas Misgeld for joining the dissertation committee.

Maja, my parents, and my friends.